# IDENTIFICATION SCHEMES FOR MODELLING OF DEAD TIME PROCESSES: A LIMIT CYCLE APPROACH




***SAURABH PANDEY***

# IDENTIFICATION SCHEMES FOR MODELLING OF DEAD TIME PROCESSES: A LIMIT CYCLE APPROACH

*A*

*Thesis Submitted*

*in Partial Fulfilment of the Requirements*

*for the Degree of*

**DOCTOR OF PHILOSOPHY**

**By**

**SAURABH PANDEY**


Department of Electronics and Electrical Engineering

Indian Institute of Technology Guwahati

Guwahati - 781039, Assam, INDIA

January, 2018

# Declaration

I hereby declare that the thesis entitled "**Identification Schemes for Modelling of Dead Time Processes: A Limit Cycle Approach**", submitted in the *Department of Electronics and Electrical Engineering, Indian Institute of Technology Guwahati, Assam, India*, for the award of the degree of **Doctor of Philosophy**, has been carried out by me under the supervision and guidance of Prof. Somanath Majhi. The results embodied in this thesis are original and have not been submitted to any other University or Institute for the award of any degree or diploma.

Dated:

Place: Guwahati

Saurabh Pandey,
Research Scholar,
Dept. of Electronics and Electrical Engineering,
Indian Institute of Technology Guwahati,
Guwahati - 781039, Assam, India.

# Certificate

This is to certify that the thesis entitled "**Identification Schemes for Modelling of Dead Time Processes: A Limit Cycle Approach**", submitted by **SAURABH PANDEY** (11610240), a research scholar in the *Department of Electronics and Electrical Engineering, Indian Institute of Technology Guwahati, Assam, India*, for the award of the degree of **Doctor of Philosophy**, has been carried out by him under my supervision and guidance. The thesis has fulfilled all requirements as per the regulations of the institute and in my opinion has reached the standard needed for submission. The results embodied in this thesis have not been submitted to any other University or Institute for the award of any degree or diploma.

Dated:

Place: Guwahati

Prof. Somanath Majhi,
Dept. of Electronics and Electrical Engineering,
Indian Institute of Technology Guwahati,
Guwahati - 781039, Assam, India.

*Dedicated to*

*My beloved grand parents, parents and sisters*

*for their love, support and encouragement*

# Acknowledgements

First and foremost, I am highly thankful to Prof. Somanath Majhi and his committee members for selecting me in interview and have given a chance to pursue doctoral research in this Institute. It is my bounden duty to thank Government of India, for establishing IIT Guwahati and for providing all facilities, web resources and scholarship to do the research. Then I knot my arms and express my whole hearted and sincere gratitude to my thesis supervisor Prof. Somanath Majhi, for his excellent guidance and support throughout my research work. I found my supervisor has some uniqueness in his guidance. I thank my supervisor, for guiding me to choose all my courses in my first year. I am grateful that he has helped me to complete all my academic requirements on time throughout my research period. I acknowledge that he has spent enough time in discussing my research problems, teaching me related basics and used to work my simulations during my initial days in PhD. In my second and third year, he taught me the importance to think of a particular problem. He has also trained me how to structure the ideas in form of article. I acknowledge him gratefully that all chapters in this thesis are his ideas and that was worked out and elaborated in each pages. I believe over the past years, I have absorbed some of his tactics in doing research. Under his guidance, I got acquainted with many software tools and learned many technical issues especially about process modelling and identification. Along with my supervisor, I would like to thank my doctoral committee members Prof. Chitralekha Mahanta, Dr. Praveen Kumar and Dr. Sisir Kumar Nayak for sparing their precious time to evaluate the progress of my work. Their suggestions are valuable and they have asked questions, which helped me to widen my knowledge and research work.

I would also like to thank Prof. Anup Kumar Gogoi, Prof. Kshetrimayum Rakhesh Singh, Dr. Indrani Kar, Dr. Srinivasan Krishnaswamy, Dr. Hanumant Singh Shekhawat and other faculty members for their kind help during my academic studies. My special thanks to Mr. Sidananda Sonowal, Mr. Sanjib Das, Mr. Pranab Jyoti Goswami, Mr. Syed Samimul Mazid and all the members of the Control and Instrumentation Laboratory for maintaining an excellent computing facility and providing various resources useful for the research work. I would like to thank the Department of Electronics and Electrical Engineering, Indian Institute of Technology Guwahati, Assam, India and Department of Electronics and Instrumentation Engineering, National Institute of Technology Agartala, Tripura, India for providing the state of art laboratory facilities to carry out the experimental work in the laboratory set-ups

of coupled tanks system by FEEDBACK Instruments and the YOKOGAWA level control system. I had a great time with my many friends at IIT Guwahati and NIT Agartala, including but not limited to Dr. Sanjoy Mondal, Dr. Raghunath Bajarangbali, Dr. Ezhil Reena Joy, Akhilesh Pal, Pawan Kumar, Mridul Kanti Malakar, Yanumula Venkata Karteek, Tousif Khan Nizami, Arghya Chakravarty, Nagaraj Adiga, Satyabrata Dash, Kashyap Kumar Prabhakar, Gautam Rituraj and Prasenjit Ghorai. I thank them for their support and encouragement.

If words can express my thoughts and love then, with all my heart and with all my love I express my thanks to my grand parents, parents, sisters for their love, encouragement and prayers throughout my research. Finally, I would like to thank the Maa Kamakhya for granting me grace, time, health and essential wisdom to complete my research work. Last but not the least, I thank all the readers who read my thesis. The chapters of this thesis are carefully done and I hope all the readers would surely gain knowledge on relay based modelling and identification of dead time processes. Many relevant references are cited at the last pages of the thesis, which will also help you to understand and learn more about the system identification techniques. I thank one and all.

Thank you

*(Saurabh Pandey)*

# Abstract

This thesis proposes various identification strategies in the framework of relay control systems followed by the development of explicit expressions for transfer function modelling of dead time processes using limit cycle information. Time delays (or dead times) appear in many processes associated with various industries such as process control, network control, biological control, etc. Using a relay feedback experiment, the characteristics of unknown processes are captured in the form of sustained oscillatory responses, known as limit cycle. Important information from limit cycle at the process output is measured and thereafter substituted in a deduced set of mathematical expressions for the identification of time delay processes.

Initially, attempts have been made to represent the industrial process dynamics in terms of linear transfer function models with time delay using frequency domain methods. However, due to the involvement of approximation in the equivalent gain of relay, such frequency domain based mathematical expressions yield erroneous industrial plant transfer function models and may lead to an inefficient controller design, which is not desirable. Therefore, to obtain better accuracy in the estimation of process model parameters, a state space approach is adopted and an explicit set of mathematical expressions are derived for identification of time delay processes using limit cycle information. Thereafter, the proposed approach is extended for modelling and identification of non-minimum phase processes with time delay. From the identified models of stable, unstable and integrating processes, the model based controllers are designed. Tuning rules for choice of proportional and integral gains have been presented which are aimed at maintaining a balance between either of them to achieve improved output transient performance.

In addition, the conventional relay feedback experiment has been modified to meet practical requirements and the obtained limit cycle information is further substituted in the modified set of mathematical expressions for the identification of a class of industrial plants. The proposed relay

feedback configuration helps in the generation of sustained oscillations around the setpoint. Benchmark examples from literature are considered for simulation and experimental results from laboratory prototypes of the level control system and coupled tanks system are included to show the validation of the proposed relay based identification methods. Finally, comparisons of identified and actual plant models are made to demonstrate the superiority of the proposed identification algorithms.

# Contents

# List of Figures

# List of Tables

# Nomenclature

| | |
|---|---|
| FOPTD | First order plus time delay process model |
| PIPTD | Pure integrating plus time delay process model |
| IFOPTD | Integrating first order plus time delay process model |
| UFOPTD | Unstable first order plus time delay process model |
| SOPTD | Second order plus time delay process model |
| USOPTD | Unstable second order plus time delay process model |
| FOPTDZ | First order plus time delay process model with zero |
| SOPTDZ | Second order plus time delay process model with repeated poles and zero |
| ISE | Integral of squared error |
| IAE | Integral of absolute error |
| ITAE | Integral of time weighted absolute error |
| ITADE | Integral of time weighted absolute derivative error |
| TV | Total variation |
| PI | Proportional integral controller |
| PI-P | Feedforward proportional integral - feedback proportional controllers |
| SNR | Signal to noise ratio |
| NSR | Noise to signal ratio |
| SISO | Single-Input Single-Output |
| DCS | Distributed control system |
| FCS | Field control station |
| MV | Manual valve |
| OV | Outlet valve |
| HIS | Human interface station |
| PSUPA | Power supply unit and power amplifier |

# Mathematical Notations

| | |
|---|---|
| $G(s)$ | Transfer function of a process |
| $G_{CL}(s)$ | Closed loop transfer function of a process |
| $G_c(s)$ | Transfer function of a controller |
| $k$ | Steady state gain of a process |
| $\theta$ | Time delay of a process |
| $\theta_n$ | Normalized time delay or dead time |
| $\alpha_3$ | Coefficient of numerator polynomial |
| $\alpha_0, \alpha_1, \alpha_2$ | Coefficients of denominator polynomial |
| $\lambda_1, \lambda_2, \lambda_3$ | Eigen values of a process model |
| $h, h_1, h_2$ | Amplitudes of a relay |
| $\varepsilon, \varepsilon_1, \varepsilon_2$ | Hysteresis width or band of a relay |
| $A_p, A_v$ | Upper and lower peak amplitudes of process output |
| $N(A_m, B_m)$ | Describing function based equivalent gain of a relay |
| $A_m$ | Average value of peak amplitudes in process output |
| $B_m$ | Bias value in process output |
| $\omega, \phi$ | Process oscillation frequency |
| $T$ | Period for which the process output remains greater than setpoint |
| $T_p$ | Time period of process output or limit cycle |
| $t_0, t_2, t_4$ | Time at which relay switching occurs |
| $t_1$ | Time at which peak amplitude of limit cycle occurs in upper direction |
| $t_3$ | Time at which peak amplitude of limit cycle occurs in lower direction |
| $a_u$ | Area under process input signal over a time period |
| $a_y$ | Area under process output signal over a time period |
| $y(t)$ | Output signal |

| | |
|---|---|
| $\dot{y}(t)$ | First time derivative of process output |
| $\ddot{y}(t)$ | Second time derivative of process output |
| $u(t)$ | Control input |
| $r(t)$ | Setpoint or reference input |
| $e(t)$ | Error signal |
| $d$ | Static load disturbance at the input of a process |
| $t$ | Time |
| $K_p$ | Proportional gain |
| $K_i$ | Integral gain |
| $K_f$ | Feedback proportional gain |
| $T_i$ | Integral time constant |
| $T_d$ | Derivative time constant |
| $a_1, a_2$ | Outlet area of Tank 1 and Tank 2 in coupled tanks system |
| $A$ | Cross-sectional areas of Tank 1 and Tank 2 in coupled tanks system |
| $\eta$ | Pump control voltage constant of coupled tanks system |
| $h_1^l, h_2^l$ | Water level in Tank 1 and Tank 2 of coupled tanks system |
| $g$ | Gravitational constant |
| $h^l$ | Water level in process tank of level control system |
| $A_l$ | Cross-sectional area of process tank in level control system |

# List of Publications

**Journal Publications**

1. **Pandey S.**, Majhi S., Ghorai P., "A New Modelling and Identification Scheme for Time Delay Systems with Experimental Investigation: A Relay Feedback Approach," *International Journal of Systems Science (Taylor & Francis)*, vol. 48(9), pp. 1932-1940, 2017.

2. **Pandey S.**, Majhi S., "Identification and Control of Unstable FOPTD Processes with Improved Transients," *Electronics Letters (IET)*, vol. 53(5), pp. 312-314, 2017.

3. **Pandey S.**, Majhi S., "Limit Cycle-Based Exact Estimation of FOPDT Process Parameters Under Input/Output Disturbances: A State-Space Approach, " *International Journal of Systems Science (Taylor & Francis)*, vol. 48(1), pp. 118-127, 2017.

4. Ghorai P., Majhi S., **Pandey S.**, "Modelling and Identification of Real Time Processes Based on Non-Zero Setpoint Autotuning Test," *Journal of Dynamics, Measurement and Control (Transactions of ASME)*, vol. 139, pp. 02010-1-02010-8, 2017.

5. Ghorai P., Majhi S., **Pandey S.**, "Dynamic Model Identification of a Real Time Simple Level Control System," *Journal of Control and Decision (Taylor & Francis)*, vol. 3(4), pp. 248-266, 2016.

6. Bajarangbali R., Majhi S., **Pandey S.**, "Identification of FOPDT and SOPDT Process Dynamics using Closed Loop Test," *ISA Transactions (Elsevier)*, vol. 53(4), pp. 1223-1231, 2014.

7. **Pandey S.**, Majhi S., "Relay Based Identification Scheme for Processes with Non-minimum Phase and Time Delay," under review in *Control Theory & Applications (IET).*

8. **Pandey S.**, Majhi S., Ghorai P., "Limit Cycle Based Identification of Time Delay SISO Processes," under review in *IFAC Journal of Systems and Control (Elsevier).*

9. **Pandey S.**, Majhi S., "Parameter Estimation and Control of Stable FOPTD Systems," under review in *Electronics Letters (IET).*

10. **Pandey S.**, Majhi S., "Frequency Domain Based Identification of Time Delay SISO Processes: A Relay Feedback Approach," under review in *International Journal of Systems Science (Taylor & Francis).*

**Conference Publications**

1. Ghorai P., **Pandey S.**, Majhi S., "A New Relay Feedback Scheme for Identification of Non-minimum Phase Processes with Time Delay," *in Proc. of the 55th IEEE Conference on Decision and Control (CDC), Las Vegas, USA*, December 12-14, 2016, pp. 2033-2038.

2. **Pandey S.**, Majhi S., "Limit Cycle Based Identification of Second Order Processes with Time Delay," *in Proc. of the 2nd IEEE Indian Control Conference (ICC), IIT Hyderabad, India*, January 4-6, 2016, pp. 1-6.

3. **Pandey S.**, Majhi S., "Frequency Domain Based Identification of Processes Using Limit Cycle Information," *in Proc. of the 1st IEEE International Conference on Industrial Instrumentation and Control (ICIC), COEP Pune, India*, May 28-30, 2015, pp. 1-6.

4. **Pandey S.**, Majhi S., "Feedback Test for Identification of a Class of SISO Processes Using Process Reaction Curve," *in Proc. of the 3rd National Symposium on Advances in Control and Instrumentation (SACI), BARC Bombay, India*, November 24-26, 2014, pp. 1-8.

5. **Pandey S.**, Majhi S., "Estimation of Process Dynamics using Biased Relay Feedback," *in Proc. of the 3rd IFAC International Conference on Advances in Control and Optimization of Dynamical Systems (ACODS), IIT Kanpur, India*, March 13-15, 2014, pp. 913-916.

6. **Pandey S.**, Majhi S., "Relay Based Identification of Process Dynamics under Noisy Environment," *in Proc. of the 1st IEEE International Conference on Control, Automation, Robotics and Embedded Systems (CARE), IIITDM Jabalpur, India*, December 16-18, 2013, pp. 1-6.

7. **Pandey S.**, Majhi S., "Identification of System Dynamics in Presence of Measurement Noise," *in Proc. of the 10th IEEE Annual India Conference (INDICON), IIT Bombay, India*, December 13 - 15, 2013, pp. 1-6.

# 1

# Introduction

Contents

## 1.1 System Identification

Process (or system) identification is a broad field and has been explored since the late 1950s. It is defined as a method of developing a mathematical relationship between process inputs and outputs based on observed or measured information. The primary objective of system identification is to acquire sufficient amount of useful knowledge from the unknown plants for improved design of controllers rendering satisfactory performance. Therefore, an efficient process identification technique is necessary for exploration of plant properties before indulging into the problem of appropriate controller designs. Moreover, it is worth mentioning that process identification is ubiquitous and hence not limited to engineering problems. It has been extensively employed in the field of biology, economy, environment, psychology, biomedical research, hydrology and many more. Therefore, it is necessary to explore accurate identification algorithms which would help in the design of efficient controllers achieving the desired output in applications pertaining to various fields of engineering and science.

In recent decades, considerable research in the development of identification methods for linear time-invariant processes has been reported in literature. The study of such identification problems in automatic control has gradually gained momentum, owing to the facts that: (i) it is possible to derive plant information while performing suitable experiments to obtain the accurate model for the unknown process (ii) the need for the design of efficient control strategies for the unknown process dynamics based on the estimated plant parameters. The identification problems are generally designed on the choice of three important factors: (i) a class of process models (ii) a class of process input signals (iii) a process identification method. Depending on these three factors, the identification problem is also affected by a priori knowledge of plant dynamics and the goal of identification. Many identification problems are formulated as an optimization problem, establishing a close relationship between the theory of identification and approximation. Furthermore, researchers have formulated the identification problem in a probabilistic framework which is eventually solved using the concepts from theory of estimation and detection. To acquire better identification accuracy, researchers have utilized the Bayes' method and maximum likelihood estimation (MLE). Further, the conditions under which the process is identifiable are also addressed in literature and the concept of identifiability has gradually evolved from estimation theory. A system is said to be identifiable if the estimates of the process remain consistent and the information matrix is positive definite. Using the concept of identifiability, identified models for the unknown processes are categorized in two classes such as: (i) non-parametric

models (impulse responses, transfer functions, volterra series, etc.) (ii) parametric models (state space models), where the non-parametric representations do not require any explicit representation of order of the process model. The algorithms commonly used for modelling and identification of linear time-invariant processes are least squares, repeated least squares, generalized least squares, maximum likelihood, instrumental variable, Levin's method, tally principle which can be seen from [11, 12] and the references therein. These algorithms need a discrete-time structure of the process model with a priori knowledge of the sampling period. However, implementation of such algorithms are challenging in view of the unknown process time constants. These algorithms are time-consuming and require signals for excitation of processes in the open loop during the experimental tests. Moreover, most of the identification methods reported in literature are usually open-loop tests and are incompetent in identifying unstable and integrating processes. Therefore, in the light of relay control systems, a closed-loop test is proposed for process identification purposes, circumventing the drawbacks of open loop methods without bringing any drift from the operating point of the plant.

## 1.2 Relay Control Systems and System Identification

In the later half of the $20th$ century, electromechanical relays were used as amplifiers in power and communication systems. However, with the rapid progress of technology and science, such applications have now become obsolete due to the availability of modern low losses, high power amplifying devices, for example, insulated gate bipolar transistors (IGBTs). It has been firstly applied in the field of adaptive control where a self-oscillating adaptive controller was designed to achieve the desired amplitude margin for applications in flight control systems and missiles. In 1987, the relay was firstly implemented for modelling and identification of highly nonlinear distillation columns by Luyben [13].

In literature, based on input and output characteristics, the relays are categorized as symmetrical, symmetrical with hysteresis, asymmetrical and asymmetrical with hysteresis as shown in Figure 1.1 where $u(t)$ describes relay output, $e(t)$ represents relay input or error signal, $h, h_1, h_2$ denote symmetrical and asymmetrical relay amplitudes and $\varepsilon, \varepsilon_1, \varepsilon_2$ signify hysteresis band, respectively. Process responses under such relay configurations are controlled by varying relay settings which, however are sensitive to measurement noise. Therefore, the incurred multiple switching in relay output due to the presence of erroneous sensors at the process output are minimized by considering the relay with hysteresis. It helps in shifting the switching point to a user defined value and thus measurement noise

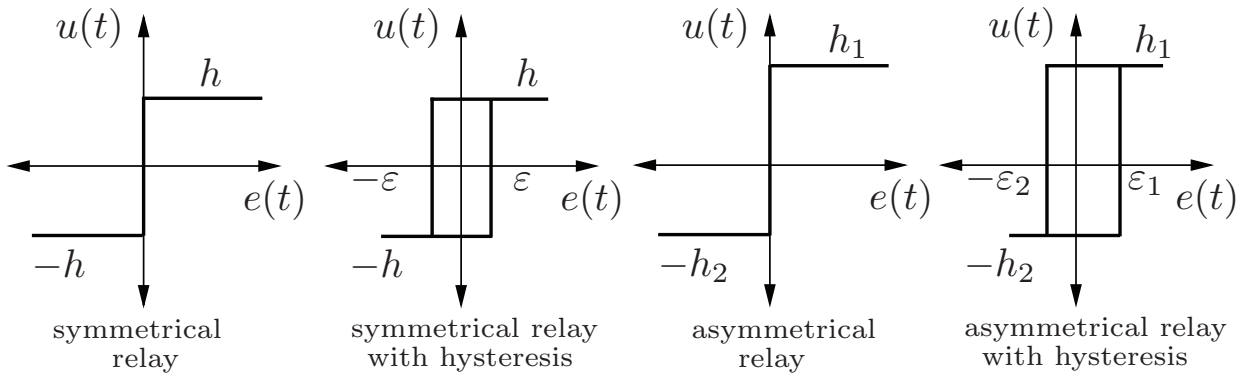


**Figure 1.1:** Various characteristics of relay

present in zero crossings can easily be avoided. Other variants of relay include saturation, relay with dead zone, backlash which have been considered rarely in literature for modelling and identification of various time delay processes. The mathematical contributions toward the investigation of sustained oscillations or limit cycle in relay control systems are primarily reported in literature by Tsypkin [14] and Hamel. Considering the on-off positions of relay, they suggested the conditions for existence of limit cycle under squared relay output waveform using the Fourier series and time domain analyses. From the symmetrical and asymmetrical relay feedback configurations, the authors proposed a set of nonlinear equations for the estimation of limit cycle frequency and on-off ratios. Furthermore, their analyses have been studied and extended for investigations of existence, uniqueness and stability of sustained oscillations by Chung and Atherton [15], Balasubramanian [16], Majhi and Atherton [17]. Initially, the conditions for existence of limit cycle were investigated using the describing function (DF) method by many researchers in the 1940s which involves the method of harmonic balance. Using Poincaré maps, the improved conditions for existence of sustained oscillations and its stability analysis were investigated by Gonclaves [18] and Lin *et al.* [19]. In literature, identification of linear time-invariant processes using a relay feedback approach is a celebrated research area which came into existence in late 80s with Hawkins [20] who first noticed the oscillation tendency of a temperature control system under discontinuous control. Since then, the study of relay feedback approach has stimulated its applications in various fields of research. Process identification is one such area wherein this ideology helps in the generation of sustained oscillations for the study of various industrial processes. In view of its implementation, simplicity and reduced computational intensity, relay based identification method has attracted the attention of a large number of researchers as evident from the

works presented by Luyben [13], Shen *et al.* [21], Atherton and Majhi [22], Thyagarajan and Yu [23], Panda and Yu [24]. The automatization property of the relay feedback approach helps the user to control the amplitudes of the process output by varying relay settings. Many identification methodologies for modelling of industrial plants in terms of lower order time delay models were proposed by practitioners and researchers as seen in [25–29]. A Fast Fourier Transform (FFT) technique was first investigated by Wang *et al.* [30, 31] for carrying out relay based identification tests in the presence of input and output disturbances. The frequency domain based identification algorithms require more number of relay feedback experiments for the identification of various processes. Vivek and Chidambaram [3, 10] have used a Laplace transform method for the identification of unknown parameters of the first order plus time delay (FOPTD) model with a considerable amount of ISE. However, their method requires an appropriate selection of an extra parameter $\gamma$ (displacement in relay settings) for the accurate estimation of process gain and ultimate frequency. Panda and Yu [32] detailed the identification of second order plus time delay (SOPTD) process dynamics using waveform analysis, exhibiting more accurate model structure and corresponding model parameters. Tan *et al.* [27] have proposed a modified relay feedback method for accurate estimation of the critical point. Atherton [33] has given an overview regarding the use of relay produced limit cycles and importance of a critical point for the selection of fixed controller parameters. Using a single relay feedback experiment, Atherton and Majhi [22] proposed a state space approach for modelling of a class of linear time-invariant processes with time delay. Their proposed set of mathematical expressions bring better accuracy in the estimation of FOPTD and SOPTD process model parameters. Motivated by the pioneering works of Atherton and Majhi [22], Kaya and Atherton [34] have proposed a group of mathematical expressions for identification of linear time delay processes in the presence of static load disturbance using the A-locus method. From the Laplace transform, Ramakrishnan and Chidambaram have proposed a set of mathematical expressions for the estimation of unknown process model parameters. Due to use of frequency domain approach, models identified by their algorithm brings a significant amount of identification error. Padhy and Majhi [35, 36] have proposed an on-line identification scheme for stable and unstable FOPTD processes using the describing function (DF) technique and also identified higher order processes in terms of FOPTD transfer function models. Lee *et al.* [37] have utilized the integrals of relay feedback responses to achieve the process information which ultimately suppresses the effect of higher order harmonic terms while carrying out the identification test by an asymmet-

rical or symmetrical relay. Liu *et al.* [38] have proposed a method for identification of dead time processes in the presence of unknown initial conditions and disturbances using the step test. Majhi and Atherton [39], Majhi [40] proposed a set of analytical expressions for the identification of a variety of processes using state space approach with the proper guess of initial conditions. Liu *et al.* [2] have developed the exact set of mathematical expressions for the estimation of FOPTD process model parameters using symmetrical and asymmetrical relay feedback tests. Fedele [1] has suggested a step response technique for the identification of a FOPTD process model using a linear regression equation where the regressors are solved to obtain the unknown process model parameters. Kim *et al.* [41] have utilized a simple method by cascading an integrator at the process output for the minimization of multiple switching at the relay output meanwhile increasing the order of overall process dynamics. Their approach successfully mitigated the noise content in higher order dynamical processes which however were incompetent in identifying lower order process models. Panda *et al.* [42] have proposed a relay feedback test for the estimation of integrating and dead time process model parameters. When the process identification test is conducted under the noisy environment, authors have implemented a relay with hysteresis band for the mitigation of transient fluctuations at zero crossings in the relay output. Liu and Gao [43] have proposed a frequency domain based mathematical expressions for the identification of time delay processes while considering a damping factor in step responses. Jeon *et al.* [44] have used several sub-relays with different frequencies and amplitudes for minimization of the harmonics present in the relay feedback signal. Šekara and Mataušek [45] have proposed a closed loop structure for an accurate estimation of a critical point of a process in the presence of input and output disturbances. Therefore, they have considered a series of band-pass filters with a relay in the inner loop and a notch filter in the outer loop of the closed loop structure. With the help of DF method, the equivalent gain of relay with hysteresis was approximated for off-line and on-line identification of FOPTD process model parameters by Bajarangbali and Majhi [46]. Due to approximations intrinsic to the DF method, expressions for relay based modelling and identification yield erroneous process model parameters. Therefore, Bajarangbali *et al.* [8], Bajarangbali and Majhi [47] have deduced a set of state space based analytical expressions for identification of time delay processes in terms of non-minimum phase stable and unstable SOPTD, stable and unstable SOPTD, non-minimum phase stable and unstable FOPTD, stable and unstable FOPTD models. Due to consideration of relay with hysteresis width, their expressions are less sensitive to the measurement noise which however needs the

proper guess of initial conditions for unknown process model parameters. Recently, Ghorai *et al.* [48] have proposed a set of mathematical expressions for modelling and identification of a class of time delay processes using the modified relay feedback scheme with non-zero setpoint. The tutorial review on process identification using relay feedback experiment since last three decades is well presented and elaborated by Liu *et al.* [49].

One of the major contribution of process identification lies in the appropriate design and automatic tuning of controllers for such processes. Åström [50] and co-workers have implemented the relay feedback technique for automatic tuning (or auto-tuning) of classical controllers such as PI/PID controllers which witnessed high demand in various industrial applications in the late 80s. Many methods for autotuning of controller parameters are reported in literature by researchers and scientists till date. Despite all, there are several limitations which are discussed in a chronological manner. Firstly, the Cohen-Coon [51] method demands an open-loop test on the process which is not practically desirable, therefore it is not convenient for the application in many unstable and integrating processes. Secondly, the controller-tuning parameters suggested by Yuwana and Seborg [52] method, Bristol [53, 54] methods need a significant change in setpoint that may drive the operating point of the process far away. Thirdly, PID controllers can be configured using the self-tuning controllers based on minimum variance, pole placement or Linear-Quadratic-Gaussian (LQG) design methods [55, 56]. These controllers require a prior information about the time scale of the process dynamics for the determination of suitable sampling intervals and filtering. The relay auto-tuning scheme has overcome these shortcomings. The attractive features of the relay based identification scheme for industrial processes are discussed below as:

(i) Relay feedback scheme helps in modelling and identification of a class of industrial processes around the important frequency, the ultimate frequency (the frequency at which the phase angle becomes $-\pi$).

(ii) Being a closed loop experiment, the processes under the relay feedback test will not drift far away from the nominal operating point.

(iii) As compared to other identification methods reported in literature *i.e.* step tests, pulse tests, the relay feedback scheme has found to be more time efficient for the processes with a long time constants. The experimental time required for conduction of the relay feedback experiment is approximately equal to two to four times the ultimate period.

(iv) Relay settings can be varied to minimize the input and output disturbances incurred during the process identification.

## 1.3 Motivation

In view of the advantages discussed in the previous section, a relay feedback approach is reported to be a powerful tool for modelling and identification of a class of industrial processes in terms of linear time-invariant models with time delay. Moreover, identification tests using the various relay feedback configurations can be utilized for minimization of adverse effects of static load disturbance and to avoid the erroneous switchings of relay in the presence of sensor noise. It has an additional advantage over other identification tools reported in literature. This motivates us to study the relay feedback scheme for transfer function modelling and identification of a class of time delay processes. Secondly, lots of methods are explored in literature by researchers for the identification of various industrial processes using frequency and time domain approaches. The frequency domain method yields a simple set of mathematical expressions for modelling and identification of a class of time delay processes. In literature, different relay feedback configurations are investigated for the estimation of process model parameters. An asymmetrical relay based modelling of time delay processes is a general relay feedback technique from which the responses due to symmetrical relay can be easily derived. Also, it helps in the minimization of static load disturbance. Therefore, we have considered an asymmetrical relay for modelling and identification of processes with time delay. Using the asymmetrical relay feedback responses, the frequency and state space based mathematical expressions are derived for the identification of various processes in terms of FOPTD, SOPTD and integrating models. The identification accuracy using the frequency domain based identification methods are found to be poor due to consideration of approximated relay gains. To circumvent this issue, methods for parameter estimation reported in literature are least squares, recursive least squares, curve fitting method. These methods yield accurate estimates of each process model parameters. However, some limitations associated with these methods are as follows. The least squares method and the recursive least square method need time for computation of regressors and the convergence of parametric errors whereas the curve fitting method requires the simultaneous solution of a set of nonlinear equations for the identification of process models with the proper choice of initial guess for each unknown process model parameters. Therefore, in this thesis we have investigated the frequency and state space based meth-

ods for modelling and identification of relay feedback processes. Using limit cycle information, a set of explicit expressions for accurate identification of industrial processes in terms of linear time delay transfer function models are proposed. These explicit set of mathematical expressions are completely free from the solution of nonlinear expressions and the issue of parameter convergence as compared to earlier works of Bajarangbali [57].

## 1.4 Contributions of this Thesis

One of the process identification method, relay feedback has been widely accepted for process modelling and autotuning of controllers due to its ease of operation. The thesis aims in the development of a set of explicit expressions for the identification of a class of time delay processes followed by experimental validation of the proposed identification algorithms. In particular, the following areas are investigated in this thesis are:

**I. Frequency Domain Approach for Identification of Time Delay Processes**

During the relay based identification experiment, a nonlinear device (relay) is fedback to an unknown process for the generation of sustained oscillations known as limit cycle. Using the limit cycle information and the equivalent gain of relay derived from describing function method, a general set of mathematical expressions for the identification of industrial processes in terms of stable and unstable FOPTD, stable and unstable SOPTD, SOPTD with repeated poles, integrating FOPTD, pure integrating plus time delay (PIPTD), non-minimum phase stable and unstable FOPTD, non-minimum phase SOPTD with repeated poles, non-minimum phase integrating FOPTD models are derived. When the process output is subjected to measurement noise, multiple switching at the relay output brings a noisy limit cycle therefore, a Fourier series based curve fitting method is utilized to retrieve a clean limit cycle information for accurate estimation of process model parameters using the derived set of mathematical expressions.

**II. State Space Approach for Identification and Control of Time Delay Processes**

In frequency domain based identification, the equivalent gain of an asymmetrical relay is approximated through the describing function method which yields the erroneous process model parameters and hence in inaccurate design of controller parameters. Therefore, a state space approach is utilized

for modelling and identification of a class of time delay processes under relay feedback control. Using limit cycle information, a generalized set of mathematical expressions are derived for FOPTD and PIPTD process models. The effects of static load disturbance and measurement noise during the identification test are minimized using the relay settings and signal processing techniques. Moreover, to achieve the improved transient performances, model based controllers are designed in terms of the estimated process model parameters using the balanced tuning rules.

**III. State Space Approach for Identification of Non-minimum Phase Processes with Time Delay**

The state space based identification method yields the better accuracy in the estimation of process model parameters. Therefore, the relay feedback scheme has been extended for modelling and identification of non-minimum phase processes with time delay. From the obtained process output information, a generalized set of mathematical expressions are derived for identification of a class of time delay processes in terms of non-minimum phase stable and unstable SOPTD, non-minimum phase integrating FOPTD process models. Furthermore, a set of explicit expressions are derived for identification of stable and unstable SOPTD, integrating FOPTD processes. Finally, the effects of measurement noise are suppressed using the Fourier series based curve fitting method.

**IV. A Modified Relay Feedback Experiment for Identification of Time Delay Processes**

In this chapter, a modified relay feedback experiment for modelling and identification of a class of time delay processes is addressed. While keeping the non-zero setpoint, a biased relay is fedback for the excitation of unknown processes yielding sustained oscillatory responses at the process output around the setpoint. Furthermore, a generalized set of mathematical expressions for the identification of a class of time delay processes in terms of FOPTD, first order plus time delay process with zero (FOPTDZ), SOPTD with repeated poles, second order plus time delay process with repeated poles and zero (SOPTDZ) models. The adverse effects of measurement noise during the process identification are mitigated using the Fourier series based curve fitting method.

**V. Experimental Case Studies**

This chapter presents the hardware implementation of proposed identification algorithms in the

laboratory set-ups of the YOKOGAWA level control system and coupled tanks system by FEEDBACK Instruments. From the relay feedback experiment, the real time plant data is measured and substituted in the derived set of mathematical expressions for the estimation of plant models. Finally, identified models using the frequency domain and state space based methods are compared through the frequency response plots.

## 1.5 Thesis Organization

The brief description of each chapter is presented in this section.

- **Chapter 2**: In this chapter, a frequency domain approach for modelling and identification of linear time-invariant processes with time delay is presented. An asymmetrical relay is considered for excitation of unknown plants to yield sustained oscillatory responses or limit cycle at the process output. Thereafter, a set of explicit expressions are derived using the limit cycle information and the equivalent gain of relay. The effects of measurement noise are demonstrated through the addition of Gaussian distributed random numbers at the process output and a clean limit cycle is recovered using the Fourier series based curve fitting method. Typical examples are considered to show the accuracy of the proposed identification method.

- **Chapter 3**: In this chapter, a state space analysis for modelling and identification of industrial processes in terms of FOPTD and PIPTD process models is proposed. Thereafter, the effects of static load disturbance and measurement noise during the process identification are minimized through relay feedback settings and signal processing techniques. On the basis of identified process model parameters, model based controllers are designed using the balanced tuning rules to achieve the improved transient performances. Simulations of well-known examples are illustrated to show the validation of proposed identification and control schemes.

- **Chapter 4**: In this chapter, the proposed relay feedback scheme is extended for the state space based modelling and identification of time delay processes in terms of non-minimum phase stable/unstable SOPTD, non-minimum phase integrating FOPTD, stable/unstable SOPTD, integrating FOPTD process models. From limit cycle information, a set of explicit expressions for all unknown parameters of process models are derived. Thereafter, a clean limit cycle output is reconstructed using the Fourier series based curve fitting method. Comparisons between identified models and the models reported in literature are drawn through Nyquist plots.

- **Chapter 5**: In this chapter, a modified relay feedback experiment for modelling and identification of a class of time delay processes is addressed. While keeping the non-zero setpoint, an asymmetrical relay with hysteresis width is fedback to unknown process for the generation of sustained oscillations around the setpoint. Finally, the simulation results are included and compared with the models reported in literature for the validation of the proposed relay based identification algorithms.

- **Chapter 6**: In this chapter, attempts have been made to validate the frequency domain and state space based identification algorithms suggested in Chapters 2-5 through experimentally. Using the proposed relay feedback schemes, the experimental set-ups of the YOKOGAWA level control system and coupled tanks system by FEEDBACK Instruments are identified in terms of FOPTD, SOPTD, non-minimum phase FOPTD, non-minimum phase SOPTD transfer function models, respectively. Finally, the identified models are compared through frequency response plots.

- **Chapter 7**: In this chapter, the concluding remarks from the carried out research works and the perspective for future works are elaborated.

# 2

# Frequency Domain Approach for Identification of Time Delay Processes

Contents

## 2.1 Introduction

Process identification is widely practiced for automatic tuning of model based controllers. Such controllers require an accurate estimation of model parameters associated with different types of processes for instance FOPTD, SOPTD and higher orders. It is a widely accepted methodology for modelling and identification of linear time-invariant processes associated with servomechanism, biological, petrochemical and process control industries. The design of tuning rules for classical controllers using relay autotuning is one of the popular method. It is observed that many electrical systems, chemical and biological processes exhibit an unstable, integrating and time delay responses. Identification and controller tuning for such processes are a challenging job.

Atherton [58] derived the mathematical expressions for a class of nonlinear characteristics shown by electromechanical relays in terms of equivalent gain using the well known describing function (DF) method. In the late 80s after the invention of relay autotuners for the design of classical controller parameters by Åström and Hägglund [50], the relay feedback technique was investigated for the identification of various industrial processes. The authors also suggested a relay with hysteresis band to eradicate the adverse effects of measurement noise at the sensor output, presence of measurement noise in the output would bring differences in the relay switching frequency and the ultimate period of the plant dynamics. Thereafter, an auto-tune variation (ATV) technique for the study of nonlinear behavior shown by distillation columns was reported in literature by Luyben [13]. Shen *et al.* [21] proposed a dual-input describing function (DIDF) approach for the estimation of two points on Nyquist curve. The authors considered the biased value to mitigate the measurement noise effects on the parameter estimates of various process models. However, the DIDF approach addressed by them is limited to stable processes only. Many authors [7, 59–63] proposed methodologies for an accurate identification of industrial processes using various topologies of relay based identification tests. Wang *et al.* [64, 65] proposed a relay feedback test for the identification of FOPTD processes using the numerous points on Nyquist plots. Vivek and Chidambaram [3] estimated the unknown parameters of FOPTD model using a Laplace transform method with a significant amount of ISE between the identified and true process models. Padhy and Majhi [35] derived a mathematical set of expressions for modelling and identification of FOPTD, higher order processes using frequency domain method. Kim *et al.* [41] proposed a method which minimizes the multiple relay switching. However their method results in an increased order of the overall process dynamics. Thyagarajan and Yu [23] discussed the limit cycle

analysis for identification of time delay processes based on different time delay to time constant ratios. Ghorai *et al.* [66] proposed a modified hysteresis relay feedback approach for mathematical modelling and identification of time delay processes in terms of SOPTD and FOPTD models.

The main contribution of this chapter lies in the derivation of a set of explicit (independent) expressions for the identification of unknown plants using the frequency domain analysis. From the frequency domain approach, the equivalent gain of an asymmetrical relay is approximated using the describing function method. It helps in the derivation of simple mathematical expressions for modelling and identification of a class of time delay processes. During the relay feedback experiment, the important limit cycle information is collected and substituted in the deduced set of explicit expressions for the identification of a class of time delay processes in terms of stable and unstable FOPTD, stable and unstable SOPTD, SOPTD with repeated poles, integrating FOPTD, PIPTD, non-minimum phase stable/unstable FOPTD, non-minimum phase SOPTD with repeated poles and non-minimum phase integrating FOPTD models. Further, the robustness of proposed method is verified through the addition of measurement noise at the process output and the limit cycle information is recovered using the Fourier series based curve fitting method. The important parameters from recovered limit cycle are substituted in the derived set of mathematical expressions for the identification of unknown processes. Finally, the comparisons between the identified models with/without measurement noise and models reported in literature are demonstrated through Nyquist plots.

## 2.2 Proposed Identification Scheme

In this section, an identification scheme for modelling and identification of time delay processes are discussed with the following two assumptions as

**Assumption 2.1** *The plants models are assumed to exhibit linear time-invariant behavior.*

**Assumption 2.2** *The structure of plant models are assumed to be known.*

Figure 2.1 shows the block diagram of relay based identification method for the processes $G(s)$ associated with various industrial applications where variables $R, E, U, Y$ are considered for representation of setpoint, error signal, process input and process output, respectively. During the identification test, the setpoint ($R$) is kept zero and a relay is fedback to unknown process for the generation of sustained oscillatory responses as shown in Figure 2.3, Figure 2.4 and Figure 2.5 for FOPTD, SOPTD and non-minimum phase processes.

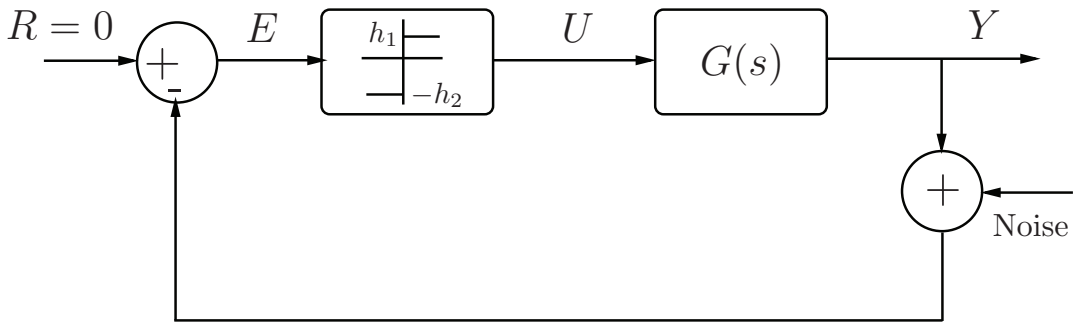


**Figure 2.1:** A schematic representation of relay feedback test

**Remark 2.1** *In the real time applications, electrical appliances, networked control and process industries commonly experiences a time delay in the form of current flow, data rate and liquid flow rate. Therefore, for a better identification accuracy, the real time dynamical processes are generally modelled as dead time process model. In relay feedback theory, the process dead time has played a key role in the generation of sustained oscillations/limit cycle especially for lower order dynamical systems. To ensure the sustained oscillatory behavior, the Nyquist curve of lower order dynamical processes with/without dead time should intersect with the negative real axis. The processes with dead time can easily be represented in second order transfer function using Taylor series or Padé approximations of dead time. The modified transfer function drives the process to reach the third quadrant and thereafter exhibits sustained oscillations as shown in Figure 2.2. In contrary, the processes without dead time*

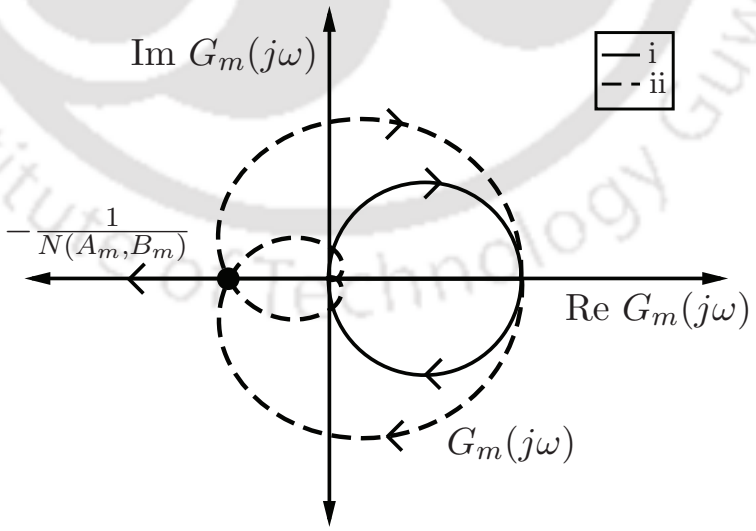


**Figure 2.2:** Nyquist plots for FOPTD process models: (i) without delay (ii) with delay

*lacks such a behavior, therefore fails in reaching the third quadrant and subsequent generation of sustained oscillations. The necessary and sufficient condition for generation of sustained oscillations for any class of plant with/without dead time can be written from [28] as*

$$G_m(j\omega) = -\frac{1}{N(A_m, B_m)} \tag{2.1}$$

*where, $N(A_m, B_m)$ represents gain of nonlinear element, $A_m, B_m$ are average of peak amplitudes and bias in input signal to nonlinear element.*

## 2.3 Frequency Domain Based Mathematical Expressions

In this section, a frequency domain analysis for modelling and identification of industrial processes in terms of FOPTD, SOPTD, SOPTD with repeated poles, integrating and non-minimum phase time delay models is addressed. Thereafter, a mathematical set of explicit expressions are derived using the limit cycle information and the relay settings for the estimation of unknown process model parameters. The information from the sustained oscillatory responses is collected in the form of peak amplitudes and time period.

### 2.3.1 FOPTD process model

A typical limit cycle for a FOPTD process is shown in Figure 2.3. The process output or limit

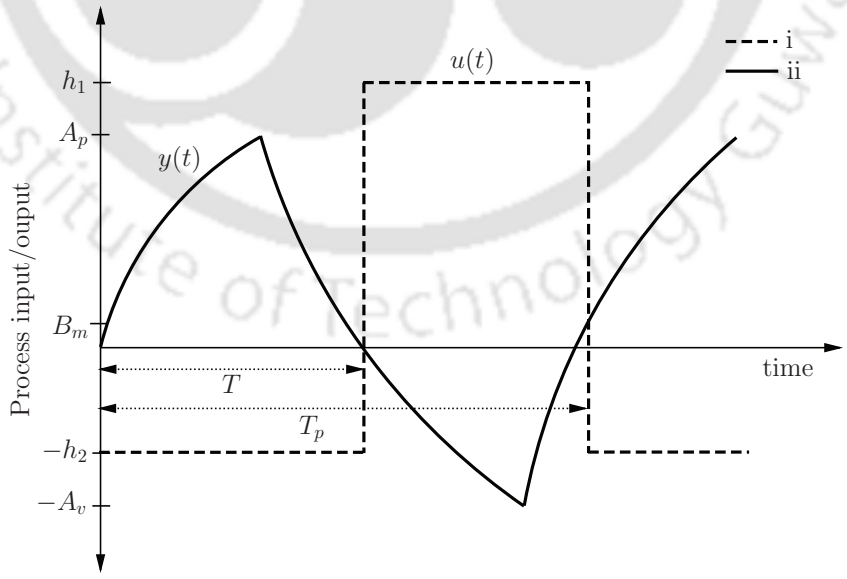


**Figure 2.3:** Plots for FOPTD process: (i) relay output (ii) process output

cycle is represented by $y(t)$, the relay output or process input is denoted by $u(t)$, $T$ represents the time for which the limit cycle remains greater than setpoint and $T_p$ describes the time period of limit cycle, the peak amplitudes of limit cycle in upper and lower directions are represented by $A_p$ and $A_v$ and the relay settings are denoted by $h_1$ and $-h_2$, respectively.

The general transfer function model for a FOPTD process is written as

$$G_m(s) = \frac{ke^{-\theta s}}{\alpha_1 s + \alpha_0} \tag{2.2}$$

where $k$, $\theta$, $\alpha_1$ and $\alpha_0$ are the process governing parameters, $\alpha_0 = 1$ for stable FOPTD process model and $\alpha_0 = -1$ for unstable FOPTD process model.

Now the expression for the equivalent gain of an asymmetrical relay is derived using describing function method (see A.1 for the detailed proof) as

$$N(A_m, B_m) = \frac{2(h_1 + h_2)}{\pi A_m} \sqrt{1 - \left(\frac{B_m}{A_m}\right)^2} \tag{2.3}$$

The condition for existence of sustained oscillations in a closed loop is written from [28] as

$$N(A_m, B_m) G_m(j\omega) = -1 \tag{2.4}$$

where, $N(A_m, B_m)$ is the equivalent gain of an asymmetrical relay, $A_m = \dfrac{A_p + A_v}{2}$ is the mean value of positive or upper $(A_p)$ and negative or lower $(A_v)$ peak amplitudes and $B_m = |A_m - A_p|$ or $|A_m - A_v|$ is a bias value in process output.

Substituting the expressions of $G_m(j\omega)$ and $N(A_m, B_m)$ from (2.2) and (2.3) in (2.4), we get

$$\frac{2(h_1 + h_2)}{\pi A_m} \sqrt{1 - \left(\frac{B_m}{A_m}\right)^2} \left(\frac{ke^{-j\theta\omega}}{\alpha_0 + j\omega\alpha_1}\right) = -1 \tag{2.5}$$

The expressions obtained from magnitude and phase conditions for (2.5) are written in explicit form as

$$\frac{2k(h_1 + h_2)\sqrt{A_m^2 - B_m^2}}{\pi A_m^2 \sqrt{\alpha_0^2 + (\omega\alpha_1)^2}} = 1 \tag{2.6}$$

$$-\theta\omega - \arctan\left(\frac{\omega\alpha_1}{\alpha_0}\right) = -\pi \tag{2.7}$$

Simplifying the magnitude and phase conditions, the unknown parameters of stable FOPTD model are derived as

$$\alpha_1 = \frac{\sqrt{4k^2(h_1+h_2)^2(A_m^2 - B_m^2) - \pi^2 A_m^4}}{\pi A_m^2 \omega} \tag{2.8}$$

$$\theta = \frac{\pi - \arctan(\omega\alpha_1)}{\omega} \tag{2.9}$$

Similarly, the magnitude and phase conditions yield the unknown parameters for unstable FOPTD process model as

$$\alpha_1 = \frac{\sqrt{4k^2(h_1+h_2)^2(A_m^2 - B_m^2) - \pi^2 A_m^4}}{\pi A_m^2 \omega} \tag{2.10}$$

$$\theta = \frac{\arctan(\omega\alpha_1)}{\omega} \tag{2.11}$$

The steady state gain ($k$) of stable and unstable FOPTD process models are derived from ratios of process output area to process input area over the time period as

$$k = \frac{\int_0^{T_p} y(t)dt}{\int_0^{T_p} u(t)dt} = \frac{a_y}{a_u} \tag{2.12}$$

### 2.3.2 SOPTD process model

Figure 2.4 represents the typical limit cycle for a general SOPTD process. The process output

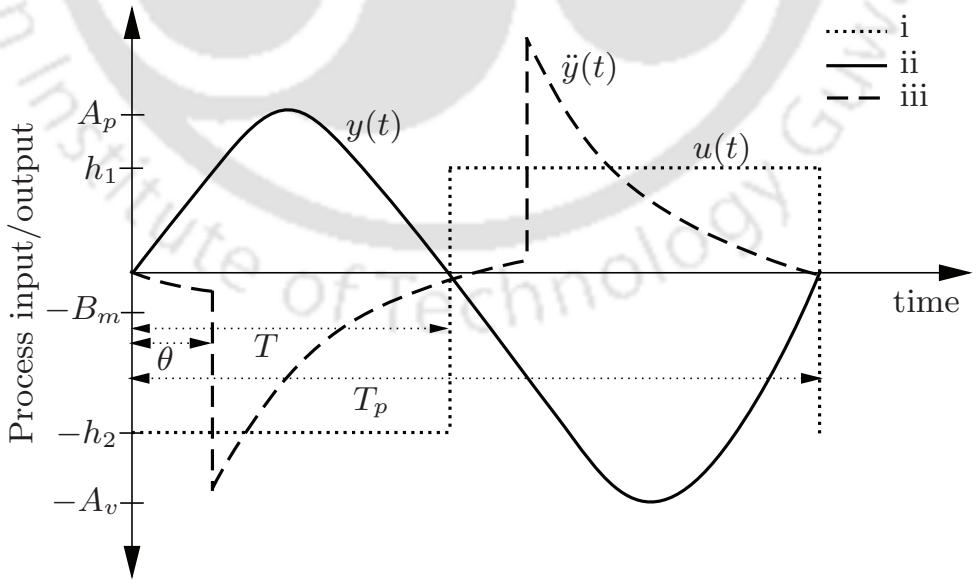


**Figure 2.4:** Plots for SOPTD process: (i) relay output (ii) process output (iii) second derivative of process output

and its second time derivative are represented by $y(t)$ and $\ddot{y}(t)$, the relay output or process input is denoted by $u(t)$, $T$ represents the time for which the limit cycle remains greater than setpoint and $T_p$ represents the time period of limit cycle, the peak amplitudes of limit cycle are represented by $A_p$ and $A_v$ and the relay settings are denoted by $h_1$ and $-h_2$, respectively.

Let us consider a general transfer function model for a SOPTD process as

$$G_m(s) = \frac{ke^{-\theta s}}{\alpha_2 s^2 + \alpha_1 s + \alpha_0} \tag{2.13}$$

where $k$, $\theta$, $\alpha_2$, $\alpha_1$ and $\alpha_0$ are the process governing parameters, $\alpha_0 = 1$ for stable SOPTD process model and $\alpha_0 = -1$ for unstable SOPTD process model.

Substituting the expressions of $G_m(j\omega)$ and $N(A_m, B_m)$ from (2.13) and (2.3) in (2.4), we get

$$\frac{2(h_1+h_2)}{\pi A_m}\sqrt{1-\left(\frac{B_m}{A_m}\right)^2}\left(\frac{ke^{-j\theta\omega}}{(\alpha_0-\alpha_2\omega^2)+j\omega\alpha_1}\right) = -1 \tag{2.14}$$

The explicit representations of magnitude and phase conditions for (2.14) are

$$\frac{2k(h_1+h_2)\sqrt{A_m^2-B_m^2}}{\pi A_m^2\sqrt{(\alpha_0-\alpha_2\omega^2)^2+(\omega\alpha_1)^2}} = 1 \tag{2.15}$$

$$-\theta\omega - \arctan\left(\frac{\omega\alpha_1}{\alpha_0-\alpha_2\omega^2}\right) = -\pi \tag{2.16}$$

Simplifying the magnitude condition for stable and unstable SOPTD process models, we get

$$(\pm 1-\alpha_2\omega^2)^2 + (\omega\alpha_1)^2 = \frac{4k^2(h_1+h_2)^2(A_m^2-B_m^2)}{\pi^2 A_m^4} \tag{2.17}$$

Similarly, the phase condition can be written in simplified form as

$$\omega\alpha_1 = (1-\alpha_2\omega^2)\tan(\pi-\theta\omega) \qquad \text{for stable model} \tag{2.18}$$

$$\omega\alpha_1 = (1+\alpha_2\omega^2)\tan(\theta\omega) \qquad \text{for unstable model} \tag{2.19}$$

Substituting the expression of $(\alpha_1)$ from (2.18) in (2.17), the two unknown parameters of stable SOPTD model are derived as

$$\alpha_2 = \frac{2k(h_1+h_2)\sqrt{A_m^2-B_m^2}\cos(\theta\omega)+\pi A_m^2}{\pi A_m^2\omega^2} \tag{2.20}$$

$$\alpha_1 = \frac{2k(h_1+h_2)\sqrt{A_m^2 - B_m^2}\sin(\theta\omega)}{\pi A_m^2 \omega} \tag{2.21}$$

Similarly, the expressions for two unknown parameters of unstable SOPTD model are derived from the simultaneous solution of (2.17) and (2.19) as

$$\alpha_2 = \frac{2k(h_1+h_2)\sqrt{A_m^2 - B_m^2}\cos(\theta\omega) - \pi A_m^2}{\pi A_m^2 \omega^2} \tag{2.22}$$

$$\alpha_1 = \frac{2k(h_1+h_2)\sqrt{A_m^2 - B_m^2}\sin(\theta\omega)}{\pi A_m^2 \omega} \tag{2.23}$$

For both stable and unstable SOPTD process models, the rest of the two unknown parameters are derived using the following procedures:

- Using (2.12), the steady state gain ($k$) is derived from ratios of process output area to process input area over the time period.
- The process time delay ($\theta$) is measured from distance between initial relay switching instant and the abrupt change shown by second derivative of process output as per the method suggested by Majhi [40] shown in Figure 2.4.

### 2.3.3 SOPTD process model with repeated poles

A general transfer function model for a SOPTD process with repeated poles is derived while substituting $\alpha_0 = 1$, $\alpha_1 = 2\sqrt{\alpha_2}$ in (2.13) as

$$G_m(s) = \frac{ke^{-\theta s}}{(\sqrt{\alpha_2}s^2 + 1)^2} \tag{2.24}$$

Substituting the expressions of $G_m(j\omega)$ and $N(A_m, B_m)$ from (2.24) and (2.3) in (2.4), we get the magnitude and phase conditions for SOPTD process model with repeated poles. Thereafter, one of the unknown parameter of assumed transfer function model is obtained from (2.15) with the substitution of $\alpha_0 = 1$, $\alpha_1 = 2\sqrt{\alpha_2}$ as

$$\sqrt{\alpha_2} = \frac{\sqrt{2k(h_1+h_2)\sqrt{A_m^2 - B_m^2} - \pi A_m^2}}{\sqrt{\pi} A_m \omega} \tag{2.25}$$

Further substituting $\alpha_0 = 1$ and $\alpha_1 = 2\sqrt{\alpha_2}$ in phase condition (2.16), the expression for process time delay is derived as

$$\theta = \frac{\pi - 2\arctan(\sqrt{\alpha_2}\omega)}{\omega} \tag{2.26}$$

Using (2.12), the steady state gain ($k$) is derived from ratios of process output area to process input area over the time period for SOPTD process model with repeated poles.

### 2.3.4 Integrating FOPTD process model

From (2.13), a general transfer function model is obtained for integrating FOPTD process with the substitution of $\alpha_1 = 1$, $\alpha_0 = 0$ as

$$G_m(s) = \frac{ke^{-\theta s}}{s(\alpha_2 s + 1)} \tag{2.27}$$

Substituting the expressions of $G_m(j\omega)$ and $N(A_m, B_m)$ from (2.27) and (2.3) in (2.4), we get the explicit representations of magnitude and phase conditions. The expressions for two unknown parameters for integrating FOPTD process model are derived using magnitude and phase conditions (2.15), (2.16) with the substitution of $\alpha_1 = 1$, $\alpha_0 = 0$ as

$$\alpha_2 = \frac{\sqrt{4k^2(h_1 + h_2)^2(A_m^2 - B_m^2) - \pi^2 A_m^4 \omega^2}}{\pi A_m^2 \omega^2} \tag{2.28}$$

$$\theta = \frac{0.5\pi - \arctan(\omega\alpha_2)}{\omega} \tag{2.29}$$

Using (2.12), the steady state gain ($k$) is derived for integrating FOPTD process model.

### 2.3.5 PIPTD process model

Again the general transfer function model for pure integrating plus time delay process is derived from (2.13) with the substitution of $\alpha_0 = 0$, $\alpha_1 = 1$ and $\alpha_2 = 0$ as

$$G_m(s) = \frac{ke^{-\theta s}}{s} \tag{2.30}$$

Substituting the expressions of $G_m(j\omega)$ and $N(A_m, B_m)$ from (2.30) and (2.3) in (2.4), the magnitude and phase conditions are obtained. Thereafter, the analytical expressions for two unknown parameters of PIPTD process model are derived from (2.15) and (2.16) with the substitution of $\alpha_0 = 0$, $\alpha_1 = 1$

and $\alpha_2 = 0$ as

$$k = \frac{\pi A_m^2 \omega}{2k(h_1 + h_2)\sqrt{A_m^2 - B_m^2}} \tag{2.31}$$

$$\theta = \frac{\pi}{2\omega} \tag{2.32}$$

### 2.3.6 Non-minimum phase FOPTD process model

A general transfer function model for a non-minimum phase FOPTD process is written as

$$G_m(s) = \frac{k(-\alpha_3 s + 1)e^{-\theta s}}{\alpha_1 s + \alpha_0} \tag{2.33}$$

where $k$, $\theta$, $\alpha_3$, $\alpha_1$ are the process governing parameters, $\alpha_0 = 1$ for non-minimum phase stable FOPTD process model and $\alpha_0 = -1$ for non-minimum phase unstable FOPTD process model. Substituting the expressions of $G_m(j\omega)$ and $N(A_m, B_m)$ from (2.33) and (2.3) in (2.4), we get

$$\frac{2(h_1 + h_2)}{\pi A_m}\sqrt{1 - \left(\frac{B_m}{A_m}\right)^2}\left(\frac{k(-j\alpha_3\omega + 1)e^{-j\theta\omega}}{\alpha_0 + j\omega\alpha_1}\right) = -1 \tag{2.34}$$

The explicit representations of magnitude and phase conditions for (2.34) are written as

$$\frac{2k(h_1 + h_2)\sqrt{A_m^2 - B_m^2}\sqrt{1 + (\alpha_3\omega)^2}}{\pi A_m^2\sqrt{\alpha_0^2 + (\omega\alpha_1)^2}} = 1 \tag{2.35}$$

$$-\theta\omega - \arctan\left(\frac{\omega\alpha_1}{\alpha_0}\right) - \arctan(\omega\alpha_3) = -\pi \tag{2.36}$$

Simplifying the magnitude condition (2.35) for non-minimum phase stable and unstable FOPTD processes, we get

$$4k^2(h_1 + h_2)^2(A_m^2 - B_m^2)(1 + (\alpha_3\omega)^2) = \pi^2 A_m^4(1 + (\omega\alpha_1)^2) \tag{2.37}$$

Similarly, the phase condition yields the following expressions for non-minimum phase stable and unstable FOPTD process models in simplified form as

$$-\theta\omega - \arctan(\omega\alpha_1) - \arctan(\omega\alpha_3) = -\pi \qquad \text{for stable model} \tag{2.38}$$

$$-\theta\omega + \arctan(\omega\alpha_1) - \arctan(\omega\alpha_3) = 0 \qquad \text{for unstable model} \tag{2.39}$$

From the expression of phase condition (2.38), one of the unknown parameter of non-minimum phase stable FOPTD process model is expressed in simplified form as

$$\alpha_3 = \frac{-\omega\,\alpha_1 - \tan(\omega\,\theta)}{\omega\,(-\alpha_1\omega\tan(\omega\,\theta)+1)} \tag{2.40}$$

Substituting the expression of $\alpha_3$ from (2.40) in (2.37), another unknown parameter of non-minimum phase stable FOPTD process model is derived as

$$\alpha_1 = \frac{2k(h_1+h_2)\sqrt{A_m^2 - B_m^2}\sec(\theta\omega) + \pi A_m^2}{\pi A_m^2 \omega\tan(\theta\omega)} \tag{2.41}$$

Similarly, the expression for one of the unknown parameter of non-minimum phase unstable FOPTD process model is derived using the phase condition (2.39) as

$$\alpha_3 = -\frac{-\omega\,\alpha_1 + \tan(\omega\,\theta)}{\omega\,(\alpha_1\omega\tan(\omega\,\theta)+1)} \tag{2.42}$$

Further the expression for $\alpha_3$ is substituted from (2.42) in (2.37) to yield the another unknown parameter ($\alpha_1$) for non-minimum phase unstable FOPTD process model as

$$\alpha_1 = \frac{2k(h_1+h_2)\sqrt{A_m^2 - B_m^2}\sec(\theta\omega) - \pi A_m^2}{\pi A_m^2 \omega\tan(\theta\omega)} \tag{2.43}$$

Finally, the rest of the two unknown parameters of non-minimum phase stable and unstable FOPTD process models are derived using the following methods as:

- Using (2.12), steady state gain ($k$) is derived from ratios of process output area to process input area over the time period for non-minimum phase stable and unstable FOPTD process models.
- The process time delay ($\theta$) is measured from distance between initial relay switching instant and the point of non-smoothness in the process output waveform.

### 2.3.7 Non-minimum phase SOPTD process model with repeated poles

Figure 2.5 shows the typical limit cycle for a general non-minimum phase SOPTD process. The general transfer function for a non-minimum phase SOPTD process model with repeated poles is written as

$$G_m(s) = \frac{k(-\alpha_3 s+1)e^{-\theta s}}{(\sqrt{\alpha_2}s+1)^2} \tag{2.44}$$

where $k$, $\theta$, $\alpha_3$, $\sqrt{\alpha_2}$ are the process governing parameters.

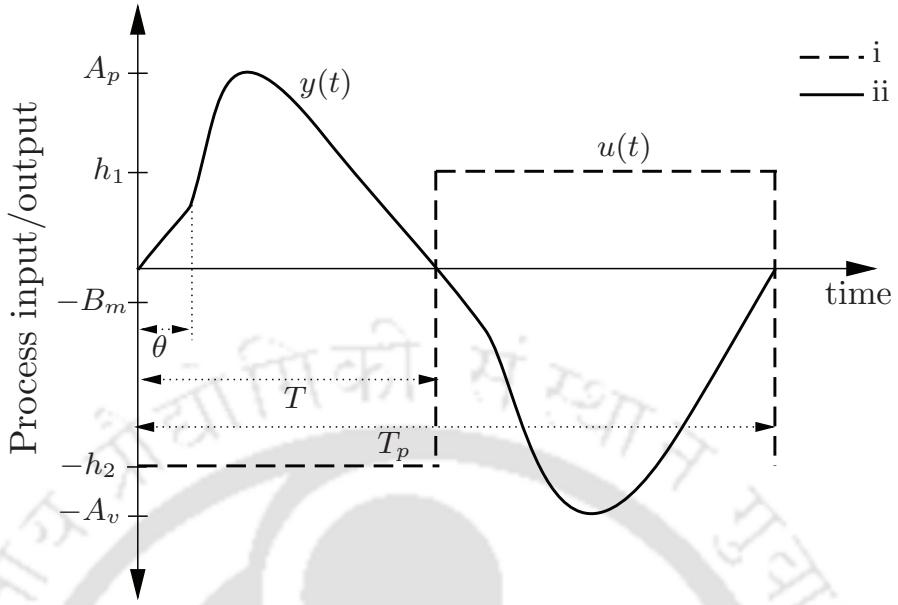


**Figure 2.5:** Plots for non-minimum phase SOPTD process: (i) relay output (ii) process output

Substituting the expressions of $G_m(j\omega)$ and $N(A_m, B_m)$ from (2.44) and (2.3) in (2.4), we get

$$\frac{2(h_1+h_2)}{\pi A_m}\sqrt{1-\left(\frac{B_m}{A_m}\right)^2}\left(\frac{k(-j\alpha_3\omega+1)e^{-j\theta\omega}}{(1+j\omega\sqrt{\alpha_2})^2}\right)=-1 \tag{2.45}$$

The expressions obtained from magnitude and phase conditions for (2.45) are written in explicit form as

$$\frac{2k(h_1+h_2)\sqrt{A_m^2-B_m^2}\sqrt{1+(\alpha_3\omega)^2}}{\pi A_m^2(1+(\omega\sqrt{\alpha_2})^2)}=1 \tag{2.46}$$

$$-\theta\omega-2\arctan(\omega\sqrt{\alpha_2})-\arctan(\omega\alpha_3)=-\pi \tag{2.47}$$

Simplifying the magnitude condition (2.46) for non-minimum phase SOPTD process with repeated poles, we get

$$4k^2(h_1+h_2)^2(A_m^2-B_m^2)\left(\omega^2{\alpha_3}^2+1\right)=\pi^2A_m^4\left((\omega\sqrt{\alpha_2})^2+1\right)^2 \tag{2.48}$$

Similarly, the phase condition (2.47) is written in simplified form as

$$2\sqrt{\alpha_2}\omega+\omega\,\alpha_3-\omega^3\alpha_2\alpha_3+\left(1-\alpha_2\omega^2-2\,\omega^2\sqrt{\alpha_2}\alpha_3\right)\tan(\omega\,\theta)=0 \tag{2.49}$$

Now the expression for one of the unknown parameter of SOPTD process model with repeated poles ($\alpha_3$) is derived from (2.49) as

$$\alpha_3 = -\frac{2\sqrt{\alpha_2}\omega + \tan(\omega\theta) - \tan(\omega\theta)\alpha_2\omega^2}{\omega\left(-\alpha_2\omega^2 - 2\omega\sqrt{\alpha_2}\tan(\omega\theta) + 1\right)} \tag{2.50}$$

Further the expression for another unknown parameter ($\sqrt{\alpha_2}$) of non-minimum phase SOPTD model with repeated roots is obtained from (2.48) with the substitution of ($\alpha_3$) from (2.50) as

$$\sqrt{\alpha_2} = \frac{\sqrt{\sec(\theta\omega)(2k(h_1+h_2)(\sqrt{A_m^2 - B_m^2}) + \pi A_m^2\sec(\theta\omega))} - \sqrt{\pi}A_m\tan(\theta\omega)}{\sqrt{\pi}A_m\omega} \tag{2.51}$$

Finally, the remaining two unknown parameters are derived using the following procedures as:

- Using (2.12), the steady state gain ($k$) of non-minimum phase SOPTD process model with repeated poles is derived.
- The process time delay ($\theta$) is measured from distance between initial relay switching instant and the point of non-smoothness in the process output as shown in Figure 2.5.

### 2.3.8 Non-minimum phase integrating FOPTD process model

A general transfer function model for a non-minimum phase integrating FOPTD process is written as

$$G_m(s) = \frac{k(-\alpha_3 s + 1)e^{-\theta s}}{s(\alpha_2 s + 1)} \tag{2.52}$$

where $k$, $\theta$, $\alpha_3$ and $\alpha_2$ are the process governing parameters.

Substituting the expressions of $G_m(j\omega)$ and $N(A_m, B_m)$ from (2.52) and (2.3) in (2.4), we get

$$\frac{2(h_1+h_2)}{\pi A_m}\sqrt{1 - \left(\frac{B_m}{A_m}\right)^2}\left(\frac{k(-j\alpha_3\omega + 1)e^{-j\theta\omega}}{j\omega(1 + j\omega\alpha_2)}\right) = -1 \tag{2.53}$$

The explicit expressions for magnitude and phase conditions using (2.53) are written as

$$\frac{2k(h_1+h_2)\sqrt{A_m^2 - B_m^2}\sqrt{1 + (\alpha_3\omega)^2}}{\pi A_m^2\omega\sqrt{1 + (\omega\alpha_2)^2}} = 1 \tag{2.54}$$

$$-\theta\omega - 0.5\pi - \arctan(\omega\alpha_2) - \arctan(\omega\alpha_3) = -\pi \tag{2.55}$$

Simplifying the magnitude condition (2.54) for non-minimum phase integrating FOPTD model, we get

$$\frac{4k^2(h_1+h_2)^2(A_m^2-B_m^2)\left(\omega^2{\alpha_3}^2+1\right)}{\pi^2 A_m^4\omega^2}-\omega^2{\alpha_2}^2-1=0 \tag{2.56}$$

Similarly, the phase condition (2.55) can be written in simplified form as

$$\omega\ (\alpha_2+\alpha_3)-\left(1-\omega^2\alpha_2\alpha_3\right)\cot\left(\omega\,\theta\right)=0 \tag{2.57}$$

Substituting the expression of $\alpha_3$ from (2.57) into (2.56), the two unknown parameters of non-minimum phase integrating FOPTD process model are derived as

$$\alpha_3=\frac{-\,\omega\,\alpha_2+\cot\left(\omega\,\theta\right)}{\omega\ \left(\alpha_2\cot\left(\omega\,\theta\right)\omega+1\right)} \tag{2.58}$$

$$\alpha_2=\frac{2k(h_1+h_2)\sqrt{A_m^2-B_m^2}\sec(\theta\omega)-\pi A_m^2\omega\tan\left(\omega\,\theta\right)}{\pi A_m^2\omega^2} \tag{2.59}$$

The rest of two unknown parameters are obtained from the following procedures as:

- The steady state gain ($k$) of non-minimum phase integrating FOPTD process model is derived using (2.12).
- The process time delay ($\theta$) is measured from distance between initial relay switching instant and the point of non-smoothness in the process output waveform.

## 2.4 Reconstruction of Limit Cycle in Presence of Noise

A Fourier series based curve fitting toolbox [67] with the options of nonlinear least squares method and trust-region algorithm is carried out for the reconstruction of original limit cycle output. Thereafter, the recovered limit cycle information is measured in the form of peak amplitude and time period for the estimation of process model parameters using the derived set of mathematical expressions. This technique basically searches the best matching function through the minimization of error between mean of limit cycle to its maximum and minimum value at each point. The equation that deals in fitting the noisy limit cycle is represented as

$$\hat{y}(t)=\psi_0+\sum_{j=1}^{N}\left[\psi_{1j}\cos(j\omega t)+\psi_{2j}\sin(j\omega t)\right] \tag{2.60}$$

where $\hat{y}(t)$, $\omega$, $T_p$ are respectively process output, oscillation frequency of the process, time period of the process output waveform and the Fourier series coefficients $\psi_0$, $\psi_{1j}$ and $\psi_{2j}$ are described as

$$\psi_0 = \frac{\int_{-T_p}^{T_p} \hat{y}(t) d(\omega t)}{2T_p} \tag{2.61}$$

$$\psi_{1j} = \frac{\int_{-T_p}^{T_p} \hat{y}(t) \cos(j\omega t) d(\omega t)}{T_p} \quad \forall\ j\ \geq\ 1 \tag{2.62}$$

$$\psi_{2j} = \frac{\int_{-T_p}^{T_p} \hat{y}(t) \sin(j\omega t) d(\omega t)}{T_p} \tag{2.63}$$

## 2.5 Results and Discussion

In this section, well-known examples from the literature are considered in order to validate the proposed frequency domain based analytical expressions for the identification of various processes in terms of stable and unstable FOPTD, SOPTD, integrating and non-minimum phase models. Simulation results are compared using identification error index values. The performance evaluation is examined here by calculating the estimation error index using the integral of absolute error criterion as

$$\text{IAE} = \int_0^{\omega_g} \left| \frac{G_m(j\omega) - G(j\omega)}{G(j\omega)} \right| d\omega \tag{2.64}$$

where $G_m(j\omega)$ is the identified process model, $G(j\omega)$ is the actual process and $\omega_g$ is the oscillation frequency of the process.

### 2.5.1 Example 1: Stable SOPTD process

Let us assume a stable SOPTD plant studied by Fedele [1] as $G_1(s) = \dfrac{e^{-4s}}{20s^2 + 12s + 1}$. When a relay with amplitudes ($h_1 = 1$ and $h_2 = -1.2$) is fedback to SOPTD plant, the sustained oscillations at the output are yielded. Further using the limit cycle information, measured parameters $A_m = 0.3718$, $B_m = 0.0328$ and $T_p = 19.34$ are substituted in (2.20), (2.21) for the estimation of SOPTD model parameters as $\alpha_1 = 11.1095$ and $\alpha_2 = 18.8448$ with a prior estimation of process steady state gain from (2.12) as $k = 1.0$ and time delay $\theta = 4.0$ from method discussed in Subsection 2.3.2. Further substituting the limit cycle information in (2.8) and (2.9), the two unknown parameters of FOPTD model are obtained as $\alpha_1 = 11.1320$ and $\theta = 5.6653$ with a prior estimation of process steady state gain using (2.12). To show the robustness of the proposed method, a white Gaussian noise is added

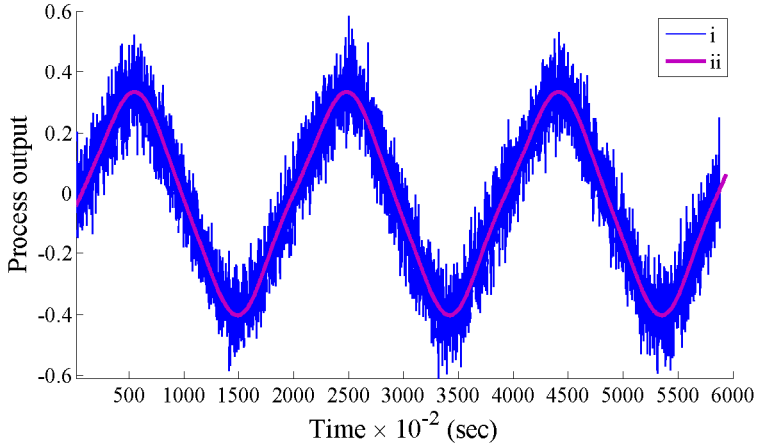


**Figure 2.6:** Plots for reconstruction of SOPTD process output using curve fitting method: (i) noisy data (ii) fitted data

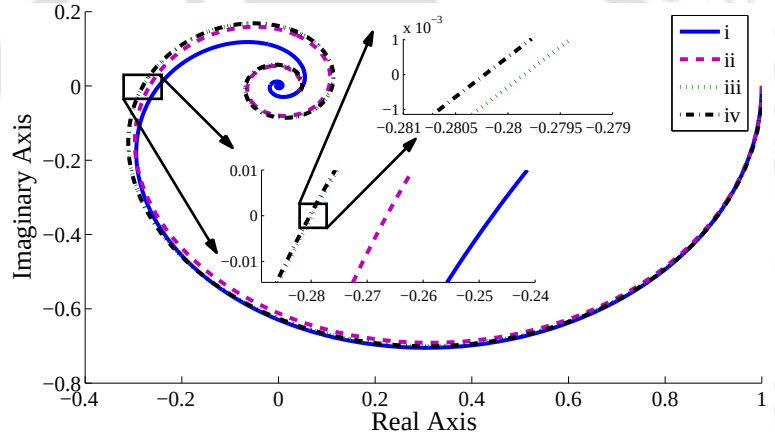


**Figure 2.7:** Nyquist plots for Example 1: (i) actual process (ii) proposed FOPTD model without noise (iii) proposed FOPTD model with 15 dB noise (iv) model suggested by Fedele [1] without noise

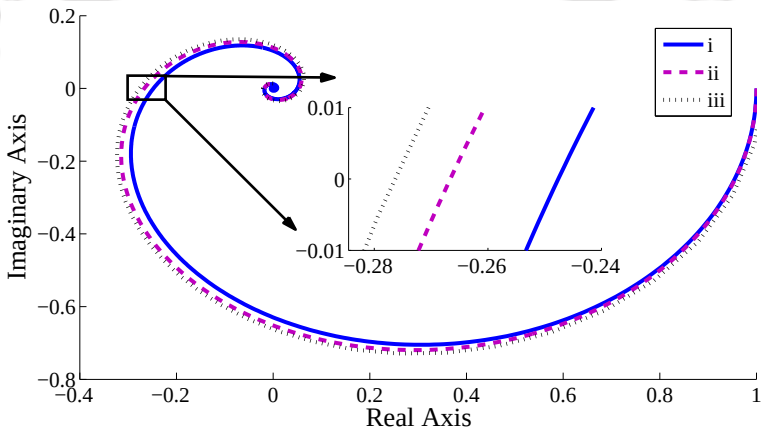


**Figure 2.8:** Nyquist plots for Example 1: (i) actual process (ii) proposed SOPTD model without noise (iii) proposed SOPTD model with 15 dB noise

at the process output resulting in a limit cycle with 15dB SNR. For the reconstruction of original limit cycle, a best fitted waveform is obtained using Fourier series based curve fitting technique as shown in Figure 2.6. The estimated process model parameters in the presence of measurement noise are detailed in Table 2.1 along with estimation error (IAE). The comparisons between the proposed model (with or without noise) and model suggested by Fedele [1] are drawn using Nyquist plots as shown in Figure 2.7 and Figure 2.8.

**Table 2.1:** Comparison of identified process models for Example 1

| Methods | Identified models | IAE |
|---|---|---|
| Proposed SOPTD model without noise | $\frac{1.0e^{-4.0s}}{18.8448s^2+11.1095s+1}$ | 0.0204 |
| Proposed SOPTD model with 15dB noise | $\frac{1.0120e^{-4.1201s}}{17.9520s^2+11.0105s+1}$ | 0.0247 |
| Proposed FOPTD model without noise | $\frac{1.0e^{-5.6653s}}{11.1320s+1}$ | 0.0103 |
| Proposed FOPTD model with 15dB noise | $\frac{1.0e^{-5.7127s}}{10.5683s+1}$ | 0.0112 |
| Fedele [1] FOPTD model without noise | $\frac{1.0015e^{-5.6474s}}{10.4495s+1}$ | 0.0141 |

### 2.5.2 Example 2: Unstable SOPTD process

Consider an unstable SOPTD process studied as $G_2(s) = \frac{e^{-0.5s}}{s^2+1.5s-1}$ by Majhi and Atherton [68]. An asymmetrical relay with amplitudes ($h_1 = 1.2$ and $h_2 = -0.9$) is fedback to unstable process for the generation of limit cycle at the process output as shown in Figure 2.9. The parameters obtained from

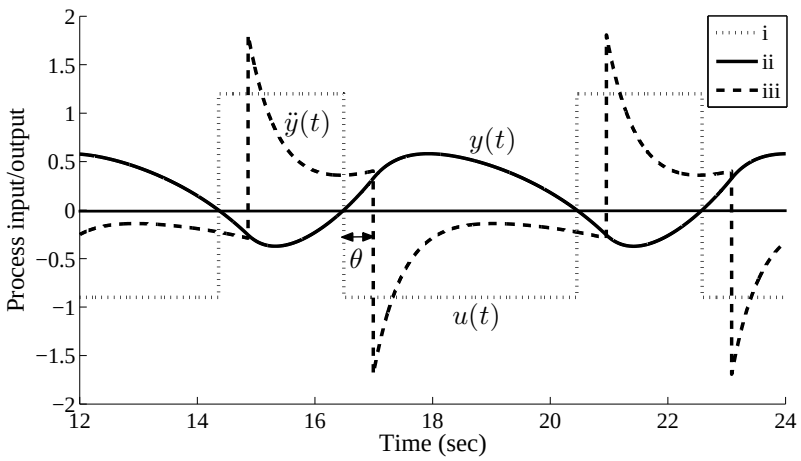


**Figure 2.9:** Plots for Example 2: (i) relay output (ii) process output (iii) second derivative of process output

limit cycle are $A_m = 0.4764$, $B_m = 0.1044$ and $T_p = 6.08$. Substituting the measured information in (2.22) and (2.23), the two unknown parameters of unstable SOPTD model are derived as $\alpha_1 = 1.3083$ and $\alpha_2 = 1.2918$ with a prior estimation of process steady state gain using (2.12) as $k = 1.0$ and time delay $\theta = 0.5$ from Figure 2.9. Again, the above process is modelled in terms of unstable FOPTD transfer function form and the process model parameters are obtained from (2.10) and (2.11) as $\alpha_1 = 2.4664$ and $\theta = 1.1582$ with a prior estimation of steady state gain parameter using (2.12) as $k = 1.0$. In the presence of measurement noise, a Fourier series based curve fitting technique is implemented to obtain a clean limit cycle. The proposed models with or without noise are compared with the model identified by Majhi and Atherton [68] using estimation error (IAE) index in Table 2.2.

**Table 2.2:** Comparison of identified process models for Example 2

| Methods | Identified models | IAE |
|---|---|---|
| Proposed SOPTD model without noise | $\frac{1.0e^{-0.5s}}{1.2918s^2 + 1.3083s - 1}$ | 0.1865 |
| Proposed SOPTD model with 15dB noise | $\frac{1.025e^{-0.4855s}}{1.2530s^2 + 1.2702s - 1}$ | 0.1937 |
| Proposed FOPTD model without noise | $\frac{1.0e^{-1.1582s}}{2.4664s - 1}$ | 0.1259 |
| Proposed FOPTD model with 15dB noise | $\frac{1.0e^{-1.1623s}}{2.5046s - 1}$ | 0.1358 |
| FOPTD model by Majhi and Atherton [68] without noise | $\frac{1.0e^{-1.061s}}{2.875s - 1}$ | 0.2558 |

### 2.5.3 Example 3: SOPTD process with repeated poles

Consider a SOPTD process with repeated poles studied by Vivek and Chidambaram [10] as $G_3(s) = \frac{e^{-0.5s}}{(20s+1)^2}$. For a fair comparison of results, relay settings ($h_1 = 1$ and $h_2 = -1.1$) are considered similarly as in [10] for the generation of sustained oscillations at the process output. The limit cycle parameters are obtained as $A_m = 0.0185$, $B_m = 9 \times 10^{-4}$, $T_p = 15.1077$ and the process steady state gain is derived using (2.12) as $k = 1.0$. Substituting all the measured information in (2.25) and (2.26) and solving these expressions one may obtain the process model parameters as $\sqrt{\alpha_2} = 20.2859$ and $\theta = 0.5673$, respectively. Using a Fourier series based curve fitting technique, a clean limit cycle is obtained and the recovered limit cycle information is substituted in the derived set of mathematical expressions for the estimation of process model parameters in presence of measurement

noise. Thereafter, the proposed models with or without noise are compared with the models identified by Vivek and Chidambaram [10], Thyagarajan and Yu [23] with estimation error indices in Table 2.3.

**Table 2.3:** Comparison of identified process models for Example 3

| Methods | Identified models | IAE |
|---|---|---|
| Proposed model without noise | $\frac{1.0e^{-0.5673s}}{(20.2859s+1)^2}$ | 0.0147 |
| Proposed model with 15dB noise | $\frac{1.0e^{-0.5664s}}{(20.3052s+1)^2}$ | 0.0153 |
| Vivek and Chidambaram model [10] without noise | $\frac{1.058e^{-0.551s}}{(20.81s+1)^2}$ | 0.0344 |
| Thyagarajan and Yu [23] model without noise | $\frac{3.03e^{-0.3259s}}{(35.4277s+1)^2}$ | 0.0996 |

### 2.5.4 Example 4: Integrating FOPTD process

Let us consider an integrating FOPTD process studied by Ho *et al.* [69] as $G_4(s) = \frac{e^{-10s}}{s(20s+1)}$. An asymmetrical relay with amplitudes ($h_1 = 1$ and $h_2 = -1.2$) is fedback to bring sustained oscillations at the process output. Subsequently, the limit cycle information in terms of measured parameters as $A_m = 13.9738$, $B_m = 1.3122$, $T_p = 100.4735$ and process gain $k = 1.0$ using (2.12) are substituted in (2.28) and (2.29) to derive the unknown parameters of integrating process model as $\alpha_2 = 19.8833$ and $\theta = 10.8308$, respectively. Furthermore, the robustness of the proposed relay based identification method in presence of sensor noise is demonstrated through the addition of Gaussian noise with 0.1% noise to signal ratio (NSR) at the process output. Under the real time environment, the limit cycle information is retrieved using the Fourier series based curve fitting method and hence the process model is derived using the explicit set of mathematical expressions. Table 2.4 shows the comparison

**Table 2.4:** Comparison of identified process models for Example 4

| Methods | Identified models | IAE |
|---|---|---|
| Proposed model without noise | $\frac{1.0e^{-10.8308s}}{s(19.8833s+1)}$ | 1.6693 |
| Ho *et al.* [62] model without noise | $\frac{1.0e^{-10.7347s}}{s(16.4684s+1)}$ | 1.9338 |
| Proposed model with 0.1% NSR | $\frac{1.0e^{-10.91203s}}{s(20.4658s+1)}$ | 1.8464 |

of identification errors between the true and estimated models using the IAE index.

### 2.5.5 Example 5: Non-minimum phase stable FOPTD process

Consider a non-minimum phase stable FOPTD process as $G_5(s) = \dfrac{(-s+1)e^{-s}}{2s+1}$. A relay with the parameters ($h_1 = 1$ and $h_2 = -1.2$) is adopted for excitation of above process to generate the sustained oscillatory responses as shown in Figure 2.10. The limit cycle parameters are measured as $A_m = 1.533$, $B_m = 0.0395$ and $T_p = 5.508$. The process steady state gain is calculated using (2.12) as $k = 1.0$ and the process time delay is obtained from the limit cycle as shown in Figure 2.10.

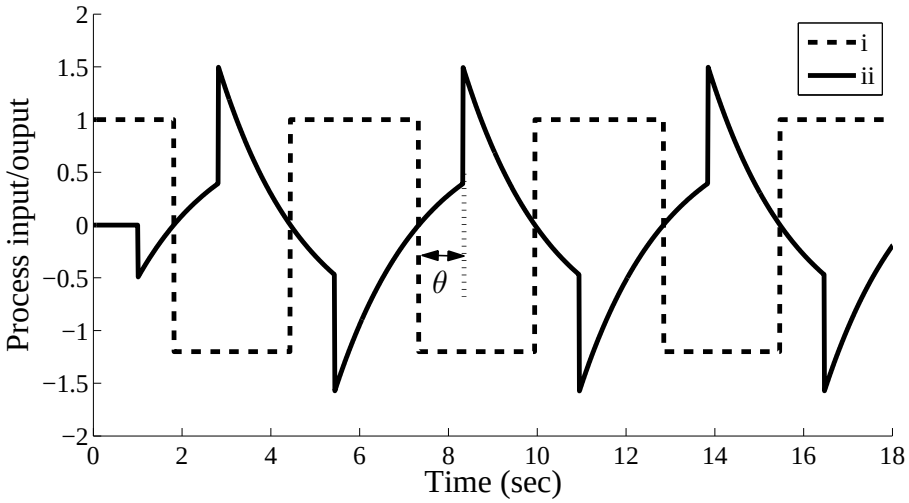


**Figure 2.10:** Plots for Example 5: (i) relay output (ii) process output

Substituting the limit cycle information in (2.40) and (2.41) and further solving these expressions, the

**Table 2.5:** Comparison of identified process models for Example 5

| Methods | Identified models | IAE |
|---|---|---|
| Proposed model without noise | $\dfrac{1.0(-1.4629s+1)e^{-1.0s}}{(1.2826s+1)}$ | 0.2883 |
| Proposed model with 10 dB noise | $\dfrac{1.051(-1.4556s+1)e^{-1.2510s}}{(1.2608s+1)}$ | 0.3333 |
| Proposed model with 15 dB noise | $\dfrac{1.012(-1.4513s+1)e^{-1.1012s}}{(1.2708s+1)}$ | 0.2995 |

model parameters of non-minimum phase stable FOPTD process are obtained as $\alpha_1 = 1.2826$ and $\alpha_3 = 1.4629$. When the process output is corrupted by sensor noise, a clean limit cycle is recovered

using Fourier series based curve fitting technique and the retrieved information is substituted in the derived set of mathematical expressions for the estimation of non-minimum phase stable FOPTD process model parameters in presence of measurement noise. Furthermore, the proposed models with or without noise are compared with the model identified in absence of measurement noise in Table 2.5 along with estimation error index (IAE).

### 2.5.6 Example 6: Non-minimum phase higher order process

A non-minimum phase higher order process $G_6(s) = \dfrac{(-s+1)}{(s+1)^5}$ is studied by Fedele [1] for parameter identification. When the relay feedback test is commissioned with relay amplitudes ($h_1 = 1$ and $h_2 = -1.2$), limit cycle parameters are obtained as $A_m = 0.8131$, $B_m = 0.0598$ and $T_p = 10.88$. The process steady state gain is derived using (2.12) as $k = 1.0$. For modelling of non-minimum phase higher order process in terms of stable FOPTD process model, the quantities measured from limit cycle are substituted in (2.8) and (2.9) to obtain the unknown process model parameters as $\alpha_1 = 2.4186$ and $\theta = 3.7959$. When a process output is subjected to measurement noise, a clean limit cycle is recovered using a Fourier series based curve fitting method. Subsequently, the recovered limit cycle information is substituted in the derived set of explicit expressions for stable FOPTD process model. Finally, the comparisons are drawn with the model suggested by Fedele [1] to show closeness between the identified models with or without noise and actual plant through IAE in Table 2.6.

**Table 2.6:** Comparison of identified process models for Example 6

| Methods | Identified models | IAE |
|---|---|---|
| Proposed model without noise | $\dfrac{1.0e^{-3.7959s}}{2.4186s+1}$ | 0.1347 |
| Proposed model with 15dB noise | $\dfrac{1.0e^{-3.8071s}}{2.3906s+1}$ | 0.1359 |
| Fedele [1] model without noise | $\dfrac{1.001e^{-3.9232s}}{2.1005s+1}$ | 0.1503 |

### 2.5.7 Example 7: Integrating higher order process

Consider an integrating higher order process $G_7(s) = \dfrac{e^{-0.5s}}{s(s+1)(0.5s+1)(0.2s+1)(0.1s+1)}$ studied by Kaya and Atherton [70]. When a biased relay with amplitudes ($h_1 = 1$ and $h_2 = -1.1$) is fedback to above process, sustained oscillations/limit cycle at the process output are observed. The

limit cycle parameters are measured as $A_m = 1.4346$, $B_m = 0.0796$, $T_p = 8.7606$ and further substituted in the derived set of explicit expressions for the identification of two unknown parameters of integrating FOPTD model wherein the process gain is obtained using (2.12) as $k = 1.0$. The behavior shown by higher order process dynamics is modelled in terms of integrating FOPTD model parameters with the substitution of measured limit cycle information and process steady gain in (2.28) and (2.29), respectively. In furtherance, the robustness of the proposed relay based identification approach is demonstrated through the addition of white Gaussian noise with noise to signal ratio (NSR) = 0.1% at the process output, respectively. The curve fitting method is utilized for the recovery of a clean limit cycle and the subsequent process models are derived in presence of measurement noise. Furthermore, the comparisons between identified models in absence/presence of noise with the models identified by Kaya and Atherton [70] are drawn through the estimation error index in Table 2.7.

**Table 2.7:** Comparison of identified process models for Example 7

| Methods | Identified models | IAE |
|---|---|---|
| Proposed model without noise | $\frac{1.0e^{-1.2271s}}{s(1.1523s+1)}$ | 0.0160 |
| Kaya and Atherton model [70] without noise | $\frac{1.0e^{-1.1230s}}{s(1.7560s+1)}$ | 0.1127 |
| Proposed model with 0.1% NSR | $\frac{1.0e^{-1.2096s}}{s(1.3560s+1)}$ | 0.0534 |

## 2.6 Summary

In this chapter, a frequency domain analysis for a class of time delay processes is investigated. Using a relay feedback experiment, a set of explicit expressions are deduced in terms of limit cycle information and relay settings for modelling and identification of industrial processes in terms of stable and unstable FOPTD, stable and unstable SOPTD, SOPTD with repeated poles, integrating FOPTD, PIPTD, non-minimum phase stable and unstable FOPTD, non-minimum phase SOPTD with repeated poles and non-minimum phase integrating FOPTD models. Due to consideration of approximated relay gains, the proposed set of mathematical expressions yield the erroneous process transfer function models. Moreover, the robustness of the proposed method is tested in presence of measurement noise where the Fourier series based curve fitting method is utilized for the reconstruction of original process output. Further, the recovered limit cycle information is substituted in the derived

set of mathematical expressions for the estimation of unknown process model parameters in presence of measurement noise. From frequency response plots, efficacy of the identified models with/without measurement noise using the proposed identification algorithms are verified and compared with the models reported in literature. It has been observed that the frequency domain based identification method yields inaccurate models and the explicit representation of only two unknown parameters in all the considered process models are possible. Therefore, attempts have been made to derive the explicit expressions for each unknown parameter of process models with an improved identification accuracy in the subsequent chapters.

# 3

# State Space Approach for Identification and Control of Time Delay Processes

Contents

## 3.1 Introduction

Identification of continuous processes with a time delay has been an active area of research in the last few decades because of its vital role in process analysis, control and optimization. A considerable amount of identification algorithms have been reported in the literature for modelling and identification of lower order time delay processes. Among them, the relay based modelling and identification of processes has gained momentum due to its ease of operation as compared to the methods reported in literature. In process control industries, many plants exhibit the first order plus time delay (FOPTD) and pure integrating plus time delay (PIPTD) characteristics therefore, many researchers have suggested various methods for identification of unknown parameters of such types of processes using frequency and time domain approaches. Using frequency domain analysis, a set of simpler expressions are yielded which however brings a significant amount of errors in process model parameters due to involvement of approximated gains of the relay. Therefore, researchers have investigated the time domain analysis to bring better accuracy in the estimation of process model parameters. Using state space approach, a set of mathematical equations for the identification of stable and unstable FOPTD, SOPTD process models under hysteresis relay control are derived by Bajarangbali *et al.* [8]. However, the derived equations are highly nonlinear and require the proper guess of initial conditions to be fed to the solver in order to evaluate the solutions of nonlinear equations. Furthermore, Liu *et al.* [49] have given a detailed review on relay and step tests based identification of various process models and highlighted the significance of DF based methodology.

In this chapter, attempts have been made to deduce a set of explicit expressions for the parameter estimation of general stable and unstable FOPTD, PIPTD process models. These exact expressions are advantageous in the sense that they can be utilized in the design of various controllers achieving high precision in the realization of their respective control objectives. The proposed set of mathematical expressions comprises limit cycle information which brings accuracy in the estimation of assumed transfer function model parameters. Thereafter, the explicit expressions are extended for the identification of higher order processes in terms of FOPTD process models. Both process input/output disturbances are easily eradicated by varying the relay amplitudes and Fast Fourier Transform (FFT) technique. Then a recovered limit cycle and its slope parameters are substituted in the derived set of explicit expressions for the estimation of original process model parameters, respectively. The proposed set of expressions are completely free from the solution of nonlinear equations and do not

require any prior knowledge of steady state gain. Added to that, feedforward and feedback controllers are designed using integral time weighted absolute error (ITAE) and integral time weighted absolute derivative error (ITADE) criterions to achieve an enhanced transient performance of output state. The robustness of the proposed methodology has been investigated by conducting extensive simulation studies under both static load disturbance and sensor inaccuracies manifested in the form of measurement noise.

## 3.2 Proposed Identification Scheme

The block diagram for a feedback compensation scheme utilized in the identification of various process dynamics is shown in Figure 3.1 which comprises of two separate blocks each for an asymmetrical relay and a process, a static load disturbance ($d$) at the process input which is not studied during process modelling in Figure 2.1. The setpoint ($R$) is made zero while carrying out the identifi-

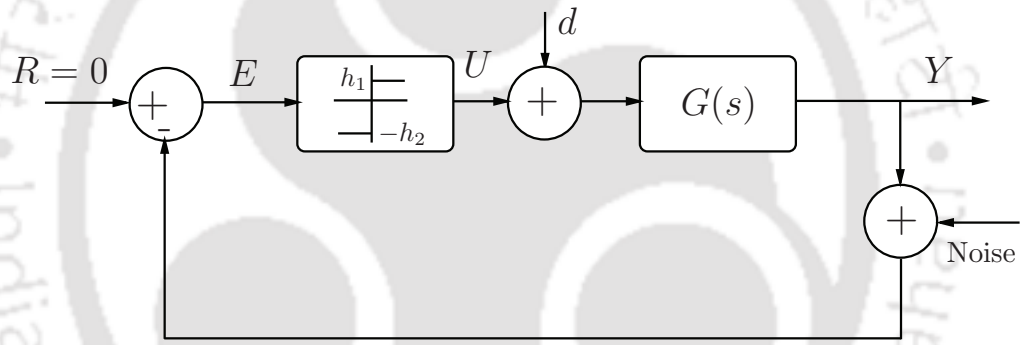


**Figure 3.1:** A schematic representation of relay feedback test

cation test where relay output serves as a process input to the unknown process. The valuable process information parameters, namely peak amplitude, ultimate period and slope are extracted from the obtained limit cycle and its derivatives. Thereafter, these parameters are substituted in the derived set of mathematical expressions for the estimation of unknown process model parameters. In practical scenarios, process output is generally corrupted by measurement noise due to the inherent inaccuracy of sensors. Therefore, while commissioning an identification test, the presence of such output disturbances result in limit cycle chattering and hence the test ends up in an erroneous system identification owing to the inaccuracy in the measurement of limit cycle parameters. In order to circumvent this problem, a signal processing technique has been augmented with the proposed method bearing the prime objective of maximal noise rejection with minimal limit cycle distortion. To illustrate the

robustness of the proposed methodology towards measurement noise, additive white Gaussian noise (AWGN) is added in the process output. Henceforth, the process identification is conducted using the proposed methodology yielding an exact estimation of plant parameters.

## 3.3 Reconstruction of Limit Cycle in Presence of Disturbances

This section presents techniques to deal with adverse effects of static load disturbance and measurement noise. The block diagram, shown in Figure 3.1, depicts the overview of an identification problem, where the occurrence of static load disturbance generally produces asymmetrical limit cycle and measurement noise leads to a corrupted system response.

### 3.3.1 Minimization of static load disturbance

A biased relay can overcome the effect of static load disturbance incurred during the identification test. Kaya and Atherton [71] have utilized an ideal relay for the generation of symmetrical process output. When static load disturbance occurs, the authors have suggested to vary the relay amplitude in order to achieve a symmetrical limit cycle at the process output. However, their method led to a change in the behavior of the relay from unbiased to biased. Using their approach, the magnitude of static load disturbance is measured from the variations in process input signal. Accordingly, magnitudes of the biased relay ($h_1$ and $-h_2$) are set to nullify the effect of static load disturbance. However, during the real time environment, it may be possible that process input is not available. Therefore, from the available process output we have attempted to extract the amount of static load disturbance present at the output. During an asymmetrical relay based identification test, the ratio of consecutive upper or lower peaks are to be estimated. If the ratio between both the peak estimates does not remain unity, an estimate of the incurred disturbance can be easily obtained using the derived mathematical expression (3.1) which ensures the process output is with or without load disturbance. The expression for static load disturbance estimation can be written as

$$\hat{d} = h_1 \left[ \frac{y_d(t_1) - y(t_1)}{y(t_1)} \right] \tag{3.1}$$

where, $y_d(t_1)$ and $y(t_1)$ are the upper or lower peak amplitude with and without disturbances. Further, in addition to constant input disturbance, the process output is also corrupted with measurement noise. Therefore, a process subjected to such disturbances, renders a reduced probability

in achieving an accurate process model. Hence, attempts have been made to recover the original limit cycle using a signal processing technique, Fast Fourier Transform (FFT). Several methods for the mitigation of sensor noise have been reported in literature and their limitations are detailed in succeeding section.

**Remark 3.1** *Generally in process industries, static load disturbance values are assumed to be smaller than relay settings. The relay settings ensure the overall system to yield limit cycle rather than forced oscillations. On the contrary, if such situation is incurred, the relay settings should be raised to yield sustained oscillatory output. A proportional-integral (PI) controller is utilized for on-line rejection of static load disturbance values incurred during the identification test. Moreover, due to the addition of PI controller, the modified closed loop transfer function changes the behavior of limit cycle oscillation. However, the proposed methodology reflects no change in limit cycle output. The proposed methodology can be implemented in real time plants in the presence of static load disturbance since the effect of such perturbations can be easily nullified and further can be estimated as well using the expression in (3.1). Thereafter, in accordance to amount of estimated disturbance, relay settings are varied in such a manner that it would compensate the effects of load disturbance over the entire process output.*

### 3.3.2 Mitigation of measurement noise

Noisy input to the biased relay results in spurious switching as shown in Figure 3.2. Numerous noise mitigation techniques have been reported in literature *viz.,* relay with hysteresis by Åström and Hägglund [50], curve fitting method by Majhi [40], Butterworth filter by Liu and Gao [2], averaging technique by Wang *et al.* [30], wavelet transform by Majhi [72] and the addition of an integrator at process output by Kim *et al.* [41]. In literature, FFT based techniques have been reported for the analysis of transient and steady state conditions while commissioning a relay feedback test. However, FFT techniques have not yet been proposed, in respect to the desired objective of mitigation of sensor noise at the process output. Using a relay with hysteresis, one can reduce the noise content up to a certain extent. Averaging limit cycle samples may bring deviation in the mean value due to noisy behavior. Further, curve fitting techniques may lead to erroneous calculation of peak values. Therefore, the proposed work attempts to obtain a clean limit cycle by the simple FFT method detailed in [73]. Mathematically, an FFT of a signal can be represented as a linear combination of signal samples or decomposition of a noisy signal into various frequency bands. Generally, all filter design methods always demand the frequency, the magnitude and phase of the signal such as pass band ripple, stop

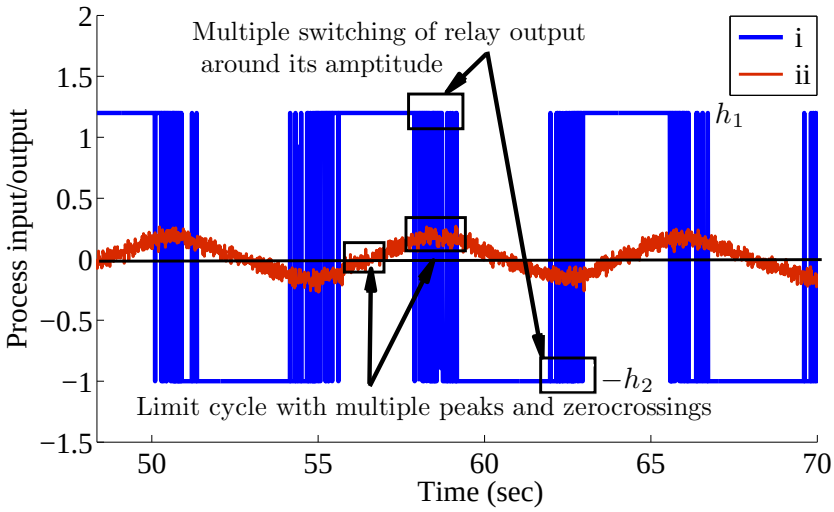


**Figure 3.2:** Plots for influence of measurement noise in FOPTD process: (i) relay output (ii) process output

band attenuation, transition width, and phase constraints for a successful noise suppression. The proposed filtering method utilizes MATLAB [67] based data processing of sampled points in limit cycle output. The assumption behind these design criteria is that, the signal is restricted to be in a certain frequency band and that the frequencies outside this specific band are treated as noise. Therefore, it is desirable to suppress these noisy coefficients by the selection of a suitable threshold. The N-point FFT, $Y_s(k)$ of a discrete time signal with a sampling period of 0.01 sec, $y_s(n)$ can be represented as

$$Y_s(k) = \sum_{n=0}^{N-1} y_s(n) \exp\left[-\frac{j2\pi kn}{N}\right] \tag{3.2}$$

where $k = 0, 1, ...(N-1)$ and $N$ = length of data samples and $N = 100$ data points are considered for the illustration of simulation examples in Section 3.6. For the selection of an appropriate threshold value, the absolute magnitude of coefficients are calculated and compared with their respective peak magnitudes. Further, the coefficients whose magnitude becomes less than 2% of peak magnitude are neglected. Thereafter, the threshold is chosen such that it replicates the original limit cycle behavior. Hence, a manual threshold parameter can be represented as

$$Y_{sth} = Z(:). * (abs(Y_s(:)) >= 0.02 * \nu) \tag{3.3}$$

where, $\nu$ is abs(max($Y_s$)) and $Y_{sth}$ is process output after thresholding. Subsequently, a clean limit cycle is derived from Inverse Fast Fourier Transform (IFFT) of thresholded signal which brings a little

smoothing around the peak magnitudes. Therefore, a reconstructed signal can be written as

$$\hat{y_s}(k) = \frac{1}{N}\sum_{k=0}^{N-1} Y_{sth}(k)\exp\left[\frac{j2\pi kn}{N}\right] \tag{3.4}$$

where $n = 0, 1, ...(N-1)$ and $\hat{y_s}(k)$ is a reconstructed process output.

**Remark 3.2** *In process control industries, accuracy in the estimation of process model parameters yields better tuning of controllers. When the process output is exposed to the real-time environment, an erroneous limit cycle output is obtained due to the presence of inaccuracy in sensor measurements. The proposed FFT method yields improved response for uniformly distributed noisy components such as Gaussian noise. In literature, Kim et al. [41] have introduced an on-line method by concatenating an integrator at the process output for the minimization of multiple switching at the relay output which increases the overall order of the assumed transfer function models. Their method successfully recover the noise at the peak amplitude while yielding an inaccurate ultimate period. Therefore, the proposed off-line methodology does not brings any modification on the limit cycle behavior of lower/higher order process models followed by negligible variations in peak and period of limit cycle. The proposed methodology successfully overcomes the challenges involved in the on-line method of noise mitigation in various process dynamics.*

## 3.4 State Space Based Mathematical Expressions

In this section, a stable and unstable FOPTD, PIPTD processes are modelled in their appropriate transfer function forms which would facilitate in the development of analytical expressions for the subsequent identification of unknown process dynamics. Therefore, let us consider a generalized transfer function model $G_m(s)$ of an FOPTD process as

$$G_m(s) = \frac{Y(s)}{U(s)} = \frac{ke^{-\theta s}}{\alpha_1 s + \alpha_0} = \frac{\tilde{k}e^{-\theta s}}{(s - \lambda_1)} \tag{3.5}$$

where $\lambda_1 = -\alpha_0/\alpha_1$, $\tilde{k} = k/\alpha_1$, $\alpha_0 = \pm 1$ depending upon stable or unstable process model and the model parameters $k$, $\theta$ and $\alpha_1$ are the steady state gain, time delay and time constant, respectively. Now a piecewise constant input $u(t)$ for the scheme shown in Figure 3.1 with noise free condition as

$$u(t) = \begin{cases} h_1 + \hat{d} & \text{if } y(t) < 0 \\ -h_2 + \hat{d} & \text{if } y(t) > 0 \end{cases} \tag{3.6}$$

Since the equation (3.5) is the frequency domain representation of assumed process dynamics, its time domain counterpart can easily be expressed as

$$\dot{y}(t) = \lambda_1 y(t) + \tilde{k}u(t-\theta) \tag{3.7}$$

Now, a general solution of the dynamical process (3.7) is given by,

$$y(t) = e^{\lambda_1(t-t_0)}y(t_0) + \int_{t_0}^{t} e^{\lambda_1(t-\zeta)}\tilde{k}u(\zeta-\theta)d\zeta \tag{3.8}$$

Without loss of generality, if $\alpha_1 \to \infty$ or $\lambda_1 \to 0$ such that $\tilde{k}$ remains finite, the transfer function model (3.5) of an FOPTD process reduces to a PIPTD process model dynamics represented by

$$G_m(s) = \frac{ke^{-\theta s}}{\alpha_1 s} = \frac{\tilde{k}e^{-\theta s}}{s} \tag{3.9}$$

Thereafter, the analytical expressions for the estimation of unknown parameters in stable, unstable and integrating process models have been elaborated in subsequent Sections 3.4.1 and 3.4.2.

### 3.4.1 FOPTD process model

Figure 3.3 shows typical waveforms obtained when a stable FOPTD process dynamics is excited by an asymmetrical relay output with corrected magnitude $(h_1 + \hat{d}, -h_2 + \hat{d})$ in order to overcome the effect of static load disturbance. The time instants $t_0$, $t_2$, $t_4$ refers to zero crossings, positive and

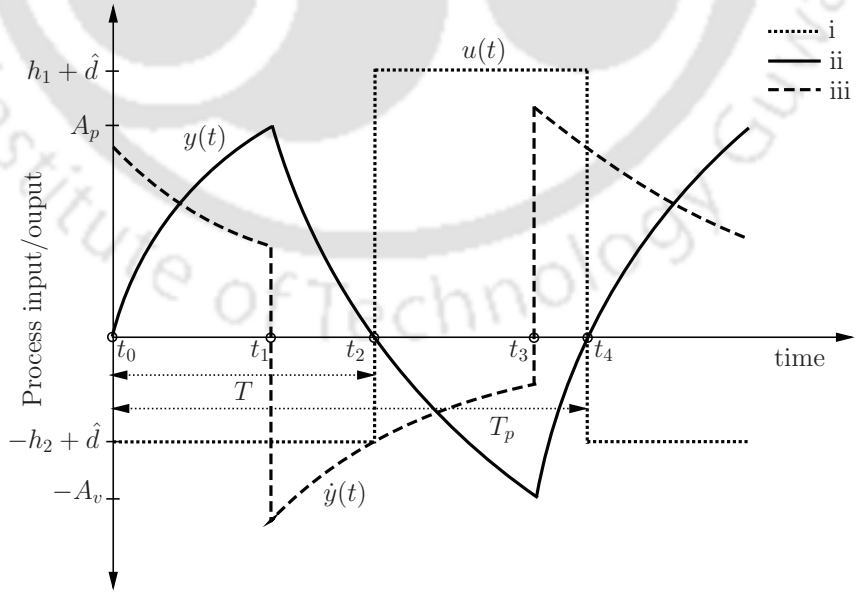


**Figure 3.3:** Plots for FOPTD process: (i) relay output (ii) process output (iii) first derivative of process output

negative peak instants are represented by $t_1$, $t_3$ and $T$ signifies the time for which $y(t)$ remains greater than setpoint and $T_p$ denotes the time period of limit cycle, respectively.

Attempts have been made in this section to derive explicit expressions for the unknown process model parameters in (3.5) using the state space method. Let us assume a process model subjected to an input from an asymmetrical relay with manipulated amplitudes in the presence of static load disturbance. The expressions for the process output during various time ranges can be obtained using the general solution given by (3.8). As shown in Figure 3.3, for the time range $t \in [t_0, t_1]$, using (3.8) limit cycle output (assuming the initial conditions $y(t_0) = 0$) can be represented as

$$y(t) = \frac{\tilde{k}}{\lambda_1}\left(e^{\lambda_1(t-t_0)} - 1\right)(h_1 + \hat{d}) \tag{3.10}$$

Substituting the expressions of $\lambda_1$ and $\tilde{k}$ in the first time derivative of (3.10), gives

$$\dot{y}(t) = \tilde{k}(h_1 + \hat{d})e^{\lambda_1(t-t_0)} \tag{3.11}$$

$$\dot{y}(t) = \frac{k(h_1 + \hat{d})}{\alpha_1}e^{\mp(t-t_0)/\alpha_1} \tag{3.12}$$

Calculating (3.12) at $t = t_0$ and $t = t_1$, respectively yields,

$$\dot{y}(t_0) = \frac{k(h_1 + \hat{d})}{\alpha_1} \tag{3.13}$$

$$\dot{y}(t_1) = \frac{k(h_1 + \hat{d})}{\alpha_1}e^{\mp\theta/\alpha_1} \tag{3.14}$$

Thus, the expression for the time delay parameter ($\theta$) of the FOPTD process model can be obtained from (3.13) and (3.14) as

$$\theta = \mp 2\alpha_1 \tanh^{-1}\left[\frac{\dot{y}(t_1) - \dot{y}(t_0)}{\dot{y}(t_1) + \dot{y}(t_0)}\right] \tag{3.15}$$

During the time span where $t \in (t_1, t_3]$, the typical expression for the process output using (3.8) can be written as

$$y(t) = \frac{\tilde{k}}{\lambda_1}\left((h_1 + \hat{d})e^{\lambda_1(t-t_0)} + (h_2 - \hat{d}) - (h_1 + h_2)e^{\lambda_1(t-t_1)}\right) \tag{3.16}$$

Considering the first time derivative of (3.16) and substituting the expressions of $\lambda_1$ and $\tilde{k}$ yields

$$\dot{y}(t) = \tilde{k}\left((h_1 + \hat{d})e^{\lambda_1(t-t_0)} - (h_1 + h_2)e^{\lambda_1(t-\theta)}\right) \tag{3.17}$$

$$\dot{y}(t) = \frac{k}{\alpha_1}\left((h_1 + \hat{d})e^{\mp(t-t_0)/\alpha_1} - (h_1 + h_2)e^{\mp(t-\theta)/\alpha_1}\right) \tag{3.18}$$

Subsequently, the expression of the first time derivative term at $t = t_2 = T$ can be written as

$$\dot{y}(t_2) = \frac{k}{\alpha_1}\left(h_1 + \hat{d} - (h_1 + h_2)\frac{\dot{y}(t_0)}{\dot{y}(t_1)}\right)e^{\mp T/\alpha_1} \tag{3.19}$$

While solving the above equation (3.19) for process time constant ($\alpha_1$), one can get the explicit representation of the process time constant ($\alpha_1$) as

$$\alpha_1 = \pm T\left[2\tanh^{-1}\left(\frac{\delta - 1}{\delta + 1}\right)\right]^{-1} \tag{3.20}$$

where, $\delta = \left[\dfrac{\dot{y}(t_0)\dot{y}(t_1)(h_1 + \hat{d}) - (h_1 + h_2)[\dot{y}(t_0)]^2}{\dot{y}(t_1)\dot{y}(t_2)(h_1 + \hat{d})}\right]$.

Further, the expression of the first time derivative term at $t = t_3$ can be written using (3.8) as

$$\dot{y}(t_3) = \frac{k}{\alpha_1}\left((h_1 + \hat{d})e^{\mp(T+\theta)/\alpha_1} - (h_1 + h_2)e^{\mp T/\alpha_1}\right) \tag{3.21}$$

Lastly, the steady state gain ($k$) of the unknown FOPTD process model is obtained from (3.21) as

$$k = \left[\frac{\delta\alpha_1\dot{y}(t_0)\dot{y}(t_3)}{(h_1 + \hat{d})\dot{y}(t_1) - (h_1 + h_2)\dot{y}(t_0)}\right] \tag{3.22}$$

### 3.4.2 PIPTD process model

From the solution of the state space equation given in (3.8), process output expressions are evaluated for PIPTD process model during various time intervals. Further, substituting the governing parameters $\lambda_1 = 0$ and $\tilde{k} = k/\alpha_1$ in (3.8), a limit cycle output can be presented in more simplified form. For a given time range $t \in [t_0, t_1]$ of the obtained limit cycle with the process input $u(t - \theta) = (h_1 + \hat{d})$ yields the expression for process output as

$$y(t) = y(t_0) + \tilde{k}(t - t_0)(h_1 + \hat{d}) \tag{3.23}$$

$$\dot{y}(t_0) = \tilde{k}(h_1 + \hat{d}) \tag{3.24}$$

While in a time range $t \in [t_1, t_2]$ the process input switches from $(h_1 + \hat{d})$ to $-(h_2 - \hat{d})$ and yields the process output as

$$y(t) = y(t_1) - \tilde{k}(t - t_1)(h_2 - \hat{d}) \tag{3.25}$$

$$y(t_1) = \tilde{k}\theta(h_1 + \hat{d}) \tag{3.26}$$

Further in a time range $t \in [t_2, t_3]$ where the process input is again $u(t - \theta) = -(h_2 - \hat{d})$, results in the process output given by

$$y(t) = y(t_2) - \tilde{k}(t - t_2)(h_2 - \hat{d}) \tag{3.27}$$

$$y(t_2) = \tilde{k}[(h_1 + h_2)\theta - (h_1 + \hat{d})t_0 - (h_2 - \hat{d})T] \tag{3.28}$$

Finally, for the time range $t \in [t_3, t_4]$, process input switching between $-(h_2 - \hat{d})$ to $(h_1 + \hat{d})$, gives the expression for process output as

$$y(t) = y(t_3) + \tilde{k}(t - t_3)(h_1 + \hat{d}) \tag{3.29}$$

$$y(t_3) = \tilde{k}[(h_1 + \hat{d})\theta - (h_2 - \hat{d})T] \tag{3.30}$$

Using (3.24) and (3.26), the time delay ($\theta$) parameter of PIPTD process dynamics is obtained as

$$\theta = \frac{y(t_1)}{\dot{y}(t_0)} \tag{3.31}$$

Simplifying (3.26) and (3.30), remaining parameter ($\tilde{k}$), the steady state gain of PIPTD process dynamics can be evaluated as

$$\tilde{k} = \left[\frac{y(t_1) - y(t_3)}{T(h_2 - \hat{d})}\right] \tag{3.32}$$

## 3.5 Design of Model Based Controllers

In this section, based on identified process transfer function models, feedforward and feedback controllers are designed. For stable processes, a proportional-integral (PI) controller is cascaded to unknown process in the feedforward path to achieve better transient performances. For unstable process, a feedback proportional (P) or proportional-derivative (PD) controller is required to stabilize the process dynamics through the reallocation of poles of the actual process and thereafter a feedforward controller is applied to achieve the better transient performances as shown in Figure 3.4. Most of the tuning rules reported in literature yield poor damping due to consideration of high proportional gain

for achieving better transient responses. It can make control action very aggressive which may cause serious damage to the actuators at the process input and sensors at the process output. Therefore balanced tuning rules [74] help in maintaining the balance between proportional and integral gains of the controller.

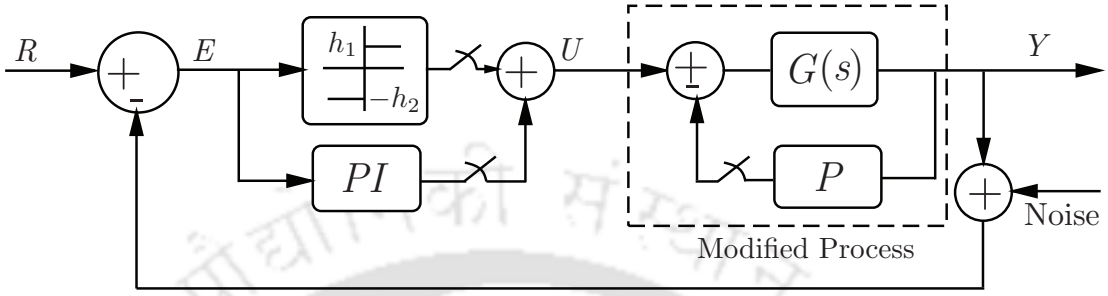


**Figure 3.4:** Proposed identification and control schemes for stable and unstable processes

### 3.5.1 PI tuning rules for stable FOPTD process model

The velocity form representation of a PI controller output is

$$\dot{u}(t) = K_p\dot{e}(t) + K_i e(t) \tag{3.33}$$

At steady state, $\dot{u}(t) = 0$, therefore, pre-multiplication of time followed by integration on both sides of (3.33) yields,

$$\frac{K_p}{K_i}\underbrace{\int_0^\infty t|\dot{e}(t)|dt}_{\text{ITADE}} = \underbrace{\int_0^\infty t|e(t)|dt}_{\text{ITAE}} \tag{3.34}$$

The closed loop errors for FOPTD process model from its step response is expressed as

$$e(t) = \begin{cases} k & \text{if } 0 \le t < \theta \\ ke^{\lambda_1(t-\theta)} & \text{if } t \ge \theta \end{cases} \tag{3.35}$$

Substituting error expressions from (3.35) in (3.34), a relationship between proportional and integral gains of the controller is obtained as

$$K_p = K_i\alpha_1\left(\frac{0.5\theta_n^2 + \theta_n + 1}{\theta_n + 1}\right) \tag{3.36}$$

where $\theta_n = \theta/\alpha_1$ represents the normalized time delay. The integral gain of controller $K_i$ is derived using sluggishness index [75] from the relationship between response time measure with open and

closed loop control. Hence, the average residence time for open loop process dynamics is derived as $\dot{G}(0)/G(0) = -(\theta + \alpha_1)$. Now, the overall closed-loop process transfer function is written as

$$G_{CL}(s) = \frac{ke^{-\theta s}(K_p s + K_i)}{s(\alpha_1 s + 1) + ke^{-\theta s}(K_p s + K_i)} \tag{3.37}$$

Similar to the inner loop, the closed loop system average residence time is calculated as $\dot{G}_{CL}(0)/G_{CL}(0) = -1/kK_i$. Finally, equating both the average residence time obtained from open and closed loop transfer functions to yield the integral gain $K_i$ as

$$K_i = \frac{1}{k\alpha_1(\theta_n + 1)} \tag{3.38}$$

### 3.5.2 PI-P tuning rules for unstable FOPTD process model

Replacing $s$ by $s/\alpha_1$, an unstable process $G(s) = \dfrac{ke^{-\theta_n s}}{s-1}$ is stabilized by a feedback proportional controller $(K_f)$. Thereafter, a PI controller $G_c(s) = K_p + \dfrac{K_i}{s}$ is cascaded to the modified process dynamics in feedforward path for improving the closed loop transient performances as shown in Figure 3.4. The inner closed loop transfer function using the feedback controller becomes

$$\tilde{G}(s) = \frac{ke^{-\theta_n s}}{(s - 1 + kK_f e^{-\theta_n s})} \tag{3.39}$$

For smaller dead time processes, the expression for $e^{-\theta_n s}$ can be written using Taylor series approximation as $e^{-\theta_n s} \approx (1 - \theta_n s)$, where $\theta_n = \theta/\alpha_1$. Now the stabilized transfer function model can be expressed as

$$\tilde{G}(s) = \frac{ke^{-\theta_n s}}{(1 - kK_f\theta_n)s + (kK_f - 1)} = \frac{\tilde{k}e^{-\theta_n s}}{\tilde{\alpha}_1 s + 1} \tag{3.40}$$

The range for which the unstable process can be stabilized by a feedback controller $(K_f)$ is derived as

$$\frac{1}{k} < K_f < \frac{1}{k\theta_n} \tag{3.41}$$

The closed-loop errors for a modified process (3.40) using a step response can be expressed as

$$e(t) = \begin{cases} \tilde{k} & \text{if } 0 \le t < \theta_n \\ \tilde{k}e^{-\frac{(t-\theta_n)}{\tilde{\alpha}_1}} & \text{if } t \ge \theta_n \end{cases} \tag{3.42}$$

While substituting the error expressions from (3.42) in (3.34), one of the controller parameter is derived in terms of normalized time delay ($\tilde{\theta}_n = \theta_n/\tilde{\alpha_1}$) as

$$K_p = K_i\tilde{\alpha}_1\left(\frac{0.5\tilde{\theta}_n^2 + \tilde{\theta}_n + 1}{\tilde{\theta}_n + 1}\right) \tag{3.43}$$

Furthermore, the closed loop transfer function model after replacing $s$ by $s/\tilde{\alpha_1}$ in (3.40), is written as

$$G_{CL}(s) = \frac{\tilde{k}e^{-\tilde{\theta}_n s}(K_p s + K_i)}{s(s+1) + \tilde{k}e^{-\tilde{\theta}_n s}(K_p s + K_i)} \tag{3.44}$$

Now, the remaining controller parameter, $K_i$ is derived explicitly using the relationship of average residence time [75] between the open loop system ($-\dot{G}_m(0)/\dot{G}_m(0)$) and closed loop system ($-\dot{G}_{CL}(0)/\dot{G}_{CL}(0)$) as

$$K_i = \frac{1}{\tilde{k}\tilde{\alpha}_1(1+\tilde{\theta}_n)} \tag{3.45}$$

### 3.5.3 PI-P tuning rules for PIPTD process model

Before the design of controller tuning rules, the pure integrating process $G(s) = \dfrac{ke^{-\theta s}}{s}$ is stabilized by a feedback proportional controller ($K_f$). Thereafter, a PI controller $G_c(s)$ is cascaded to the stabilized process dynamics in the feedforward path to achieve improved transient performances. Similar to unstable process, the inner closed loop transfer function model becomes

$$\tilde{G}(s) = \frac{ke^{-\theta s}}{(s + kK_f e^{-\theta s})} \tag{3.46}$$

For processes with small time delay, the expression for $e^{-\theta s}$ can be written using Taylor series approximation as $e^{-\theta s} \approx (1 - \theta s)$. Now the stabilized transfer function model can be expressed as

$$\tilde{G}(s) = \frac{ke^{-\theta s}}{(1 - kK_f\theta)s + kK_f} = \frac{\tilde{k}e^{-\theta s}}{\tilde{\alpha}_1 s + 1} \tag{3.47}$$

where $\tilde{k} = \dfrac{1}{K_f}$ and $\tilde{\alpha}_1 = \dfrac{1 - kk_f\theta}{kK_f}$.

The range for which the integrating process is stabilized by a feedback controller ($K_f$) is derived as

$$0 \; < \; K_f \; < \; \frac{1}{k\theta} \tag{3.48}$$

Now the tuning rules for the PIPTD process model are derived using the relationship of average residence time between open and closed loop systems as

$$K_p = K_i\tilde{\alpha}_1\left(\frac{0.5\tilde{\theta}_n^2 + \tilde{\theta}_n + 1}{\tilde{\theta}_n + 1}\right) \tag{3.49}$$

$$K_i = \frac{1}{\tilde{k}\tilde{\alpha}_1(1+\tilde{\theta}_n)} \tag{3.50}$$

where $\theta_n = \dfrac{kK_f\theta}{1 - kK_f\theta}$.

## 3.6 Results and Discussion

In this section, well known examples from literature are considered for validation of proposed identification and control schemes. A biased relay is considered for the generation of sustained oscillations in various processes. Extensive simulations are carried out for the estimation of stable and unstable FOPTD, PIPTD and higher order process model parameters using the deduced set of explicit expressions. The identification error between estimated models and actual process parameters is evaluated using integral of absolute error (IAE) and integral of squared error (ISE) criterions as

$$\text{IAE} = \int_0^{\omega_g} \left|\frac{G_m(j\omega) - G(j\omega)}{G(j\omega)}\right| d\omega \tag{3.51}$$

$$\text{ISE} = \int_0^{\omega_g} |G_m(j\omega) - G(j\omega)|^2 d\omega \tag{3.52}$$

where, $G_m(j\omega)$ is the identified process model, $G(j\omega)$ is the actual process and $\omega_g$ is the frequency of the process, respectively. Moreover, the controller performance index for $N$ data samples is described by total variation (TV) in [76] as

$$\text{TV} = \sum_{i=1}^{N} |u(i+1) - u(i)| \tag{3.53}$$

### 3.6.1 Example 1: Stable FOPTD process

Consider a stable FOPTD process widely studied in the literature by (Liu *et al.* [2], Vivek and Chidambaram [3], Srinivasan and Chidambaram [4]) as $G_1(s) = \dfrac{e^{-2s}}{10s+1}$. During the identification

test, a biased relay settings ($h_1 = 1.2$ and $h_2 = -1$) is fedback to yield an asymmetrical limit cycle at the process output. Meanwhile, a static load disturbance of magnitude ($d = 0.2$) at $t = 25$ sec is incurred at the process input yielding a transition in limit cycle by a magnitude of $d$ which can either be measured from (3.1) or from the difference in process input signal levels. Subsequently, at $t = 45$ sec, a biased relay with amplitudes ($h_1 = 1$ and $h_2 = -1.2$) is set in order to eliminate the effect of static load disturbance and reproduce the original sustained oscillations as shown in Figure 3.5. Measurements made on a single test of an asymmetrical relay yielding the limit cycle and its first time derivative parameters as $T = 3.9681$, $\dot{y}(t_0) = 0.12$, $\dot{y}(t_1) = 0.0983$, $\dot{y}(t_2) = -0.1$ and $\dot{y}(t_3) = -0.0819$. Subsequently, the explicit expressions given in (3.15), (3.20) and (3.22) are utilized to estimate the unknown process model parameters as $\alpha_1 = 10.0037$, $k = 1.0001$ and $\theta = 1.9954$, respectively with a minimal amount of IAE given in Table 3.1. To show the robustness of the proposed method under noisy environment, a Gaussian distributed white noise with variances of $1.3317 \times 10^{-3}$ and $4.2112 \times 10^{-4}$ equivalent to 10 dB and 15 dB SNR is added in the process output, respectively. In the adjoining Figure 3.6, noise at zero crossings and peak magnitudes are suppressed with a little smoothing around the peaks of the reconstructed limit cycle followed by a smoothed first derivative of the recovered limit cycle. The identification error in the actual and estimated process dynamics are compared with the literature in Table 3.1 for different SNR values. In Figure 3.7, a comparison between the estimated models and actual plant dynamics is drawn through Nyquist plots where the proposed method brings better accuracy in both identified models with/without noise as compared to available literature.

**Table 3.1:** Comparison of identified process models for Example 1

| **Methods** | **Identified models** | **IAE** |
|---|---|---|
| Proposed model without noise | $\frac{1.0001e^{-1.9954s}}{10.0037s+1}$ | 0.0016 |
| Model proposed by Liu and Gao [2] without noise | $\frac{1.0048e^{-2.0024s}}{10.049s+1}$ | 0.0022 |
| Model suggested by Vivek and Chidambaram [3] without noise | $\frac{0.9467e^{-2s}}{9.5028s+1}$ | 0.0160 |
| Model proposed by Srinivasan and Chidambaram [4] without noise | $\frac{1.03e^{-2.3s}}{10.3s+1}$ | 0.1155 |
| Proposed model with 10dB noise | $\frac{0.8819e^{-2.2741s}}{9.2493s+1}$ | 0.1071 |
| Proposed model with 15dB noise | $\frac{1.1264e^{-2.0196s}}{10.1682s+1}$ | 0.0952 |

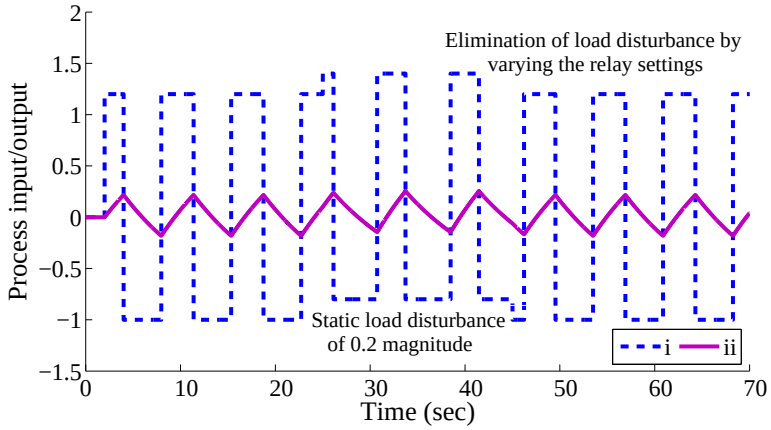


**Figure 3.5:** Plots for static load disturbance rejection in Example 1: (i) relay output (ii) process output

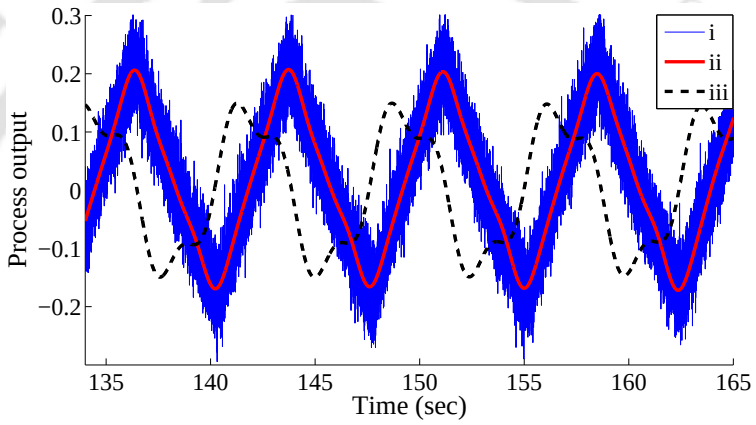


**Figure 3.6:** Plots for Example 1: (i) noisy data (ii) reconstruction of limit cycle data using FFT technique (iii) first derivative of reconstructed limit cycle data

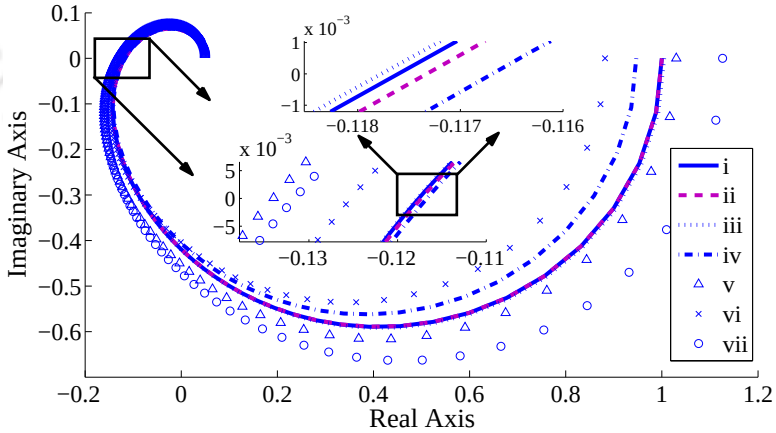


**Figure 3.7:** Nyquist plots for Example 1: (i) actual process (ii) proposed model without noise (iii) model proposed by Liu and Gao [2] without noise (iv) model suggested by Vivek and Chidambaram [3] without noise (v) model proposed by Srinivasan and Chidambaram [4] without noise (vi) proposed model with 10dB noise (vii) proposed model with 15dB noise

### 3.6.2 Example 2: Stable FOPTD process

Consider another stable FOPTD process as $G_2(s) = \dfrac{e^{-s}}{s+1}$. During identification, a biased relay yields an asymmetrical limit cycle at the process output. The process output and its slope information are measured as $T = 1.4235$, $\dot{y}(t_0) = 1.0005$, $\dot{y}(t_1) = 0.3679$, $\dot{y}(t_2) = -1.1982$ and $\dot{y}(t_3) = -0.4413$. Substituting the limit cycle information in (3.15), (3.20) and (3.22), three unknown process model parameters are estimated and parametric error between actual process and identified models with/without noise is elaborated in Table 3.2. The robustness of proposed identification technique towards measurement noise is demonstrated by considering additive white Gaussian noise with 10% and 20% NSR at the process output. Thereafter, utilizing the fast Fourier transform method, a clean process output and its slope information are retrieved. Based on the identified FOPTD process model parameters, a PI controller is designed whose parameters are derived using the (3.36) and (3.38) and the comparison with relevant designs in literature are drawn through IAE and ITAE performance indices in Table 3.3. The step responses show the enhanced transient performance of the proposed

**Table 3.2:** Comparison of identified process models for Example 2

| NSR(%) | $k$ | $\alpha_1$ | $\theta$ | IAE |
|---|---|---|---|---|
| 0 | 0.9998 | 0.9998 | 1.004 | 0.00053 |
| 10 | 1.0555 | 1.0683 | 0.9868 | 0.05524 |
| 20 | 0.9836 | 1.0808 | 0.9691 | 0.07014 |

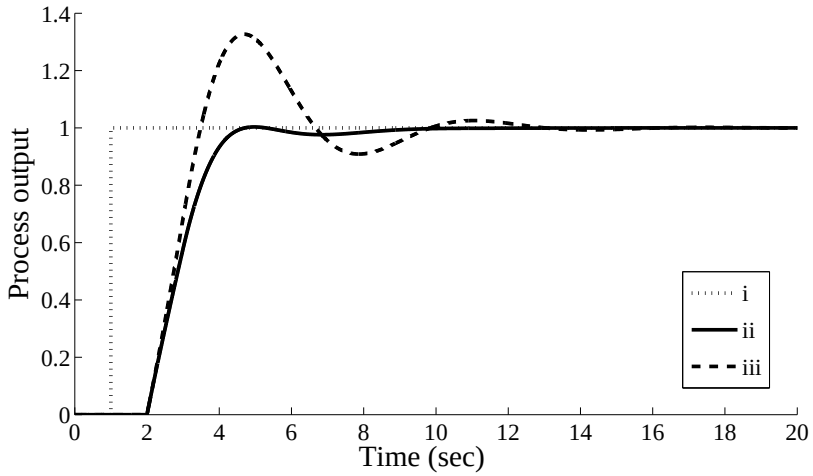


**Figure 3.8:** Step response plots for Example 2: (i) setpoint (ii) proposed PI controller (iii) PI controller proposed by Jeng *et al.* [5]

PI controller over the method reported in literature in Figure 3.8.

**Table 3.3:** Comparison of controller performances for Example 2

| Methods | $K_p$ | $K_i$ | ITAE | TV |
|---|---|---|---|---|
| Proposed PI controller | 0.6250 | 0.5000 | 4.5134 | 1.3720 |
| PI controller by Jeng *et al.* [5] | 0.6160 | 0.8052 | 8.7357 | 2.5791 |

### 3.6.3 Example 3: Unstable FOPTD process

Let us consider an unstable FOPTD process $G_3(s) = \dfrac{e^{-0.5s}}{s-1}$ studied by Vivek and Chidambaram [3]. During a relay based identification test, an ideal relay is fedback to the above process for the generation of sustained oscillations. Measured process output and its slope parameters $(T, y(t_1), \dot{y}(t_0), \dot{y}(t_1))$ are substituted in the derived set of explicit expressions for the exact evaluation of unknown process model parameters. Table 3.4 shows the identified transfer function models with/without measurement noise along with the respective model suggested in Vivek and Chidambaram [3]. The robustness of the proposed mathematical expressions towards sensor uncertainties is demonstrated by considering additive white Gaussian noise with zero mean and nonzero variance $(0, \sigma_n^2)$ at the process output generating noisy oscillations. To overcome the adverse effects of measurement noise due to the presence of erroneous sensors in the process output, a Fourier series based curve fitting method is utilized for the reconstruction of true process output. Subsequently, the recovered limit cycle information is substituted in the deduced set of explicit expressions (3.15), (3.20) and (3.22) for the evaluation of the unstable process model parameters. During the identification, a noise with 10 % NSR is injected at the process output and thereafter using the curve fitting method the original limit cycle is reconstructed. Further, the performance index of the proposed identification scheme is calculated using the integral of squared identification error *i.e.,* the ISE criterion. Using (3.41), (3.43) and (3.45), the feedforward and feedback controller parameters are evaluated as $K_p = 0.19534$, $T_i = 1.5614$, $K_f = 1.25$ and compared against the PI controller proposed by Vijayan and Panda [6] with setpoint filter ($K_p = 1.5353$, $T_i = 7.5753$, $T_f = 7.9248$) and PI controller suggested by Jung *et al.* [7] with setpoint filter ($K_p = 1.5353$, $T_i = 7.5753$, $T_f = 7.5753$) through step responses. The proposed controller tracking performance shows improved rise time $t_r = 2.07$, less settling time $t_s = 8.3098$ with negligible overshoot $M_p = 0.28\%$ as shown in Figure 3.9. Moreover, the proposed control strategy yields a minimum value of ITAE = 9.3743 and IAE = 6.0023 in contrast to the controllers proposed

by Vijayan and Panda [6] with ITAE = 24.3302 and IAE = 8.9649 and Jung *et al.* [7] with ITAE = 16.2467 and IAE = 8.3225.

**Table 3.4:** Comparison of identified process models for Example 3

| Methods | $k$ | $\alpha_1$ | $\theta$ | ISE ($10^{-3}$) |
|---|---|---|---|---|
| Proposed model† | 1.0019 | 1.0021 | 0.5003 | 0.0023 |
| Vivek and Chidambaram [3] model† | 1.0638 | 1.0832 | 0.5127 | 2.4954 |
| Proposed model‡ | 0.9795 | 1.0357 | 0.5168 | 1.2461 |

†:= without noise, ‡:= noise with 10% NSR

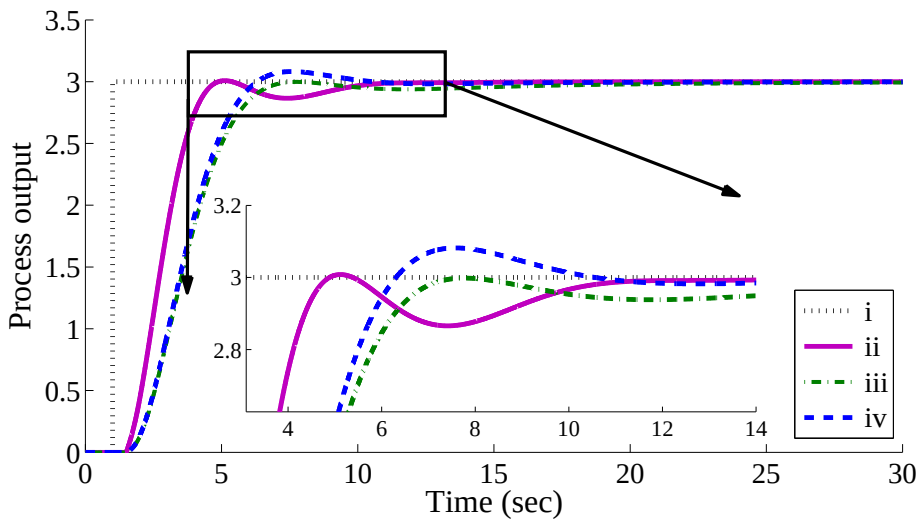


**Figure 3.9:** Step response plots for Example 3: (i) setpoint (ii) proposed PI-P controller (iii) PI controller proposed by Vijayan and Panda [6] (iv) Jung *et al.* [7] suggested PI controller

### 3.6.4 Example 4: Pure integrating process with large time delay

An integrating process studied by Panda *et al.* [42] is $G_4(s) = \dfrac{0.0506e^{-6s}}{s}$. A biased relay of magnitudes ($h_1 = 1.25$, $h_2 = -0.95$) induces asymmetrical limit cycle at the process output. Similar to Example 1, a static load disturbance of magnitude ($d = 0.25$) at $t = 50$ sec is added to bring a bias in the process input which can easily be evaluated from (3.1). Accordingly at $t = 70$ sec, relay settings ($h_1 = 1$ and $h_2 = -1.2$) is set to exploit the original asymmetrical limit cycle output. Thereafter, measured limit cycle and its derivative parameters $T = 13.895$, $y(t_1) = 0.3794$, $y(t_3) = -0.2883$ and $\dot{y}(t_0) = 0.0633$ are substituted in (3.31) and (3.32) to yield the process model parameters as $\theta =$

5.9936 and $\tilde{k} = 0.05058$, respectively with a small amount of IAE elaborated in Table 3.5. A Gaussian distributed noise with variances $3.6979 \times 10^{-3}$ and $1.1693 \times 10^{-3}$ is injected at the process output to obtain the noisy limit cycles of 10dB and 15dB SNR, respectively. Further noisy FFT coefficients are eliminated through a proper selection of threshold value in order to achieve a clean limit cycle output. Again, the explicit expressions obtained in (3.31) and (3.32) are used to estimate the unknown process model parameters. Table 3.5 shows the proposed process model parameters which are in the neighborhood of the parameters obtained in the absence of measurement noise.

**Table 3.5:** Comparison of identified process models for Example 4

| **Methods** | **Identified models** | **IAE($10^{-2}$)** |
|---|---|---|
| Proposed model without noise | $\frac{0.05058e^{-5.9936s}}{s}$ | 0.0243 |
| Model by Panda *et al.* [42] without noise | $\frac{0.0506e^{-6.5s}}{s}$ | 1.6493 |
| Proposed model with 10dB noise | $\frac{0.04593e^{-5.5940s}}{s}$ | 2.7708 |
| Proposed model with 15dB noise | $\frac{0.04743e^{-5.7175s}}{s}$ | 1.9013 |

### 3.6.5 Example 5: Pure integrating process with small time delay

Consider a pure integrating process studied by Majhi and Atherton [39] whose transfer function is given as $G_5(s) = \frac{e^{-s}}{5s}$. An asymmetrical relay with amplitudes ($h_1$ =1 and $h_2 = -1.2$) is fedback to an integrating process to induce the sustained asymmetrical limit cycle at the process output. Substituting the limit cycle information $T = 1.8352$, $y(t_1) = 0.2002$, $y(t_3) = -0.2402$ and $\dot{y}(t_0) = 0.2$, the two unknowns of process model are obtained from (3.31), (3.32) as $\tilde{k} = 0.2$ and $\theta = 0.9999$. Thereafter, the robustness of the proposed identification scheme is tested in the presence of measurement noise by adding the variances of $1.5825 \times 10^{-3}$, $5.0045 \times 10^{-4}$ and $1.5825 \times 10^{-4}$ to yield the limit cycles of 10dB, 15dB and 20dB SNR, respectively. A clean limit cycle is reconstructed using the Fourier series based curve fitting method and recovered limit cycle information is substituted in the derived set of mathematical expressions. Based on identified models, the feedforward and feedback controllers are designed from (3.48), (3.49) and (3.50) as $K_f = 2.2361$, $K_p = 1.4597$, $K_i = 1.00006$ to achieve the better transient performances with ITAE = 7.2892 and IAE = 2.5621 as shown in Figure 3.10.

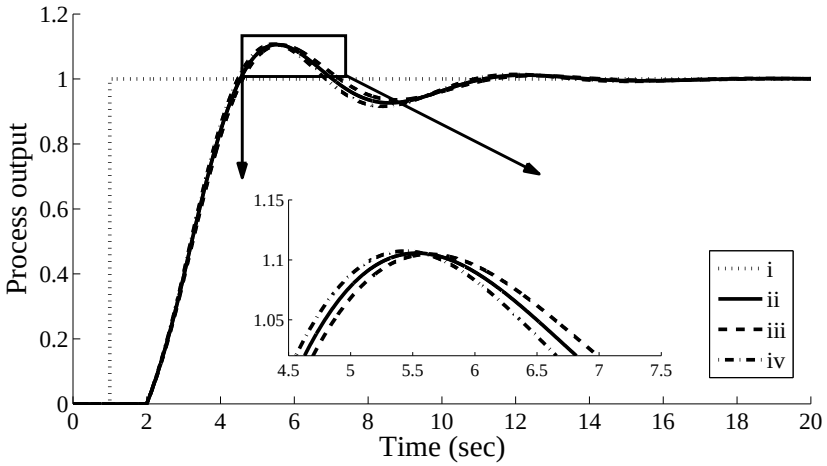


**Figure 3.10:** Step response plots for Example 5: (i) setpoint (ii) proposed PI-P controller (iii) proposed PI-P controller with 2% perturbation in model parameters (iv) proposed PI-P controller with −2% perturbation in models parameters

### 3.6.6 Example 6: Higher order process

Consider a higher order plant studied by Liu and Gao [2] as $G_6(s) = \dfrac{e^{-s}}{8(s+1)^3}$. The limit cycle at the process output is obtained using an asymmetrical relay settings ($h_1 = 1$ and $h_2 = -1.1$). A static load disturbance of magnitude ($d = 0.2$) at $t = 40$ sec shifts the asymmetrical process output. Subsequently, the magnitude of static load disturbance is obtained either from the difference in magnitude of original and shifted process input or from (3.1). Thereafter, the asymmetrical relay magnitudes ($h_1 = 0.8$ and $h_2 = -1.3$) is set at $t = 80$ sec to yield an original limit cycle at the process output, respectively. Substituting the recovered limit cycle and its slope parameters $T = 3.3295$, $\dot{y}(0) = 0.0551$, $\dot{y}(t_1) = 0.0422$, $\dot{y}(t_2) = -0.0574$ and $\dot{y}(t_3) = -0.046$ in (3.15), (3.20) and (3.22) to yield the approximated FOPTD process model parameters as $k = 0.1244$, $\alpha_1 = 2.15887$ and $\theta = 1.7275$ with a minimal amount of IAE detailed in Table 3.6. Further to show the effectiveness of the proposed method, a Gaussian distributed noise with variances $2.1799 \times 10^{-4}$ and $6.8936 \times 10^{-5}$ is added in process output to yield noisy limit cycles of 10dB and 15dB SNR, respectively. Similar to previous examples, limit cycle and its slope parameters are substituted in explicit expressions for the estimation of unknown process model parameters. Thereafter, comparisons between actual and identified process models are demonstrated through Nyquist plots as shown in Figure 3.11. Finally, a feedforward PI controller parameters are obtained from (3.36) and (3.38) using the identified FOPTD model as $K_p = 5.2594$ and $K_i = 2.0684$ which yields the improved transient performance as compared to ±2%

**Table 3.6:** Comparison of identified process models for Example 6

| Methods | Identified models | IAE |
|---|---|---|
| Proposed model without noise | $\frac{0.1244e^{-1.7275s}}{2.1588s+1}$ | 0.1848 |
| Model by Liu and Gao [2] without noise | $\frac{0.1369e^{-1.28s}}{2.6253s+1}$ | 0.3013 |
| Proposed model with 10dB noise | $\frac{0.1175e^{-1.6425s}}{2.5688s+1}$ | 0.2121 |
| Proposed model with 15dB noise | $\frac{0.1198e^{-1.6818s}}{2.3176s+1}$ | 0.1966 |

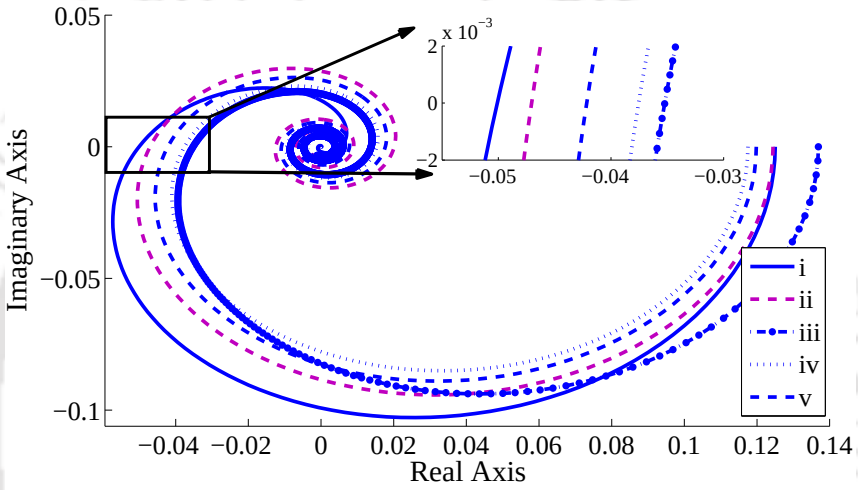


**Figure 3.11:** Nyquist plots for Example 6: (i) actual process (ii) proposed model without noise (iii) model proposed by Liu and Gao [2] without noise (iv) proposed model with 10dB noise (v) proposed model with 15dB noise

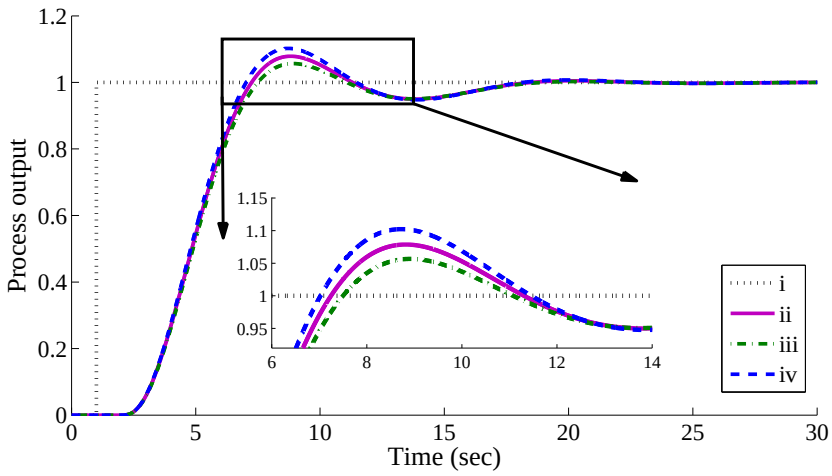


**Figure 3.12:** Step response plots for Example 6: (i) setpoint (ii) proposed PI controller (iii) proposed PI controller with 2% perturbation in model parameters (iv) proposed PI controller with −2% perturbation in model parameters

perturbation in the identified process model parameters with ITAE = 13.5179 and IAE = 4.0318 as shown in Figure 3.12.

## 3.7 Summary

In this chapter, a state space analysis for modelling and identification of linear time-invariant processes in terms of stable and unstable FOPTD, PIPTD and higher order process models is addressed. Using a relay feedback experiment, a set of explicit expressions for identification of each unknown parameters of a class of time delay processes is deduced in terms of limit cycle and its slope information. Thereafter, the effects of measurement noise over the limit cycle information are compensated using the FFT technique and Fourier series based curve fitting method. Based on identified process models, a set of tuning rules for feedforward and feedback controllers is designed using the ITAE and ITADE criterions. The proposed controllers have brought improved transient performances as compared to the method suggested in recent literature. Finally, well-known examples from literature are studied and the identified models using the proposed set of mathematical expressions are validated through simulations. The proposed set of explicit expressions is completely free from the simultaneous solution of a nonlinear set of mathematical equations. Moreover, the state space based explicit expressions have brought better identification accuracy therefore, the proposed identification algorithm is further extended for modelling and identification of stable and unstable SOPTD, integrating FOPTD processes with and without non-minimum phase behavior in the subsequent chapters.

# 4

# State Space Approach for Identification of Non-minimum Phase Processes with Time Delay

Contents

## 4.1 Introduction

Processes with non-minimum phase characteristics are one of the special class of industrial processes. Non-minimum phase process comprises of two different first order processes which brings the inverse response at the process output. To mention a few examples are water level in drum boiler, valve control system, telescope azimuth angle control system, DC-DC boost converters and some complex chemical processes. Consider a drum boiler where if the flow rate of cold water is raised, the volume of water at boiling unit and the overall liquid level will be decreased for a short span of time period. This is due to decrease in the level of temperature which ultimately effects the volume of water concentrated for the conversion of vapors. Secondly, the constant heat supply and constant production of steam, the liquid level at the boiling will start raising. Therefore, these two opposite characteristics when added together yields the non-minimum phase characteristics (see [77] for more details). Due to involvement of unstable zeros, control of such types of processes are difficult. A few researchers [31, 78, 79] have studied and utilized the time domain based identification algorithms for modelling and identification of such processes.

Using Laplace transform, Vivek and Chidambaram [3] have derived a set of analytical equations for the identification of SOPTD processes under symmetrical relay condition. Their methods yield a significant amount of error in the identified process model parameters due to consideration of frequency domain analysis. Soon after, Majhi [40] has proposed an ideal relay feedback experiment for modelling and identification of a class of time delay processes using state space approach. Their technique involves the simultaneous solution of a set of nonlinear equations for identification of unknown plants in terms of stable and unstable SOPTD, stable and unstable FOPTD process models with the proper guess of initial conditions. Thereafter, the author has suggested a method for calculation of time delay parameter of the assumed transfer function models using the second order derivative of limit cycle information in [40]. Padhy and Majhi [80] have derived a set of analytical expressions for the identification of non-minimum phase processes with time delay using an ideal relay. Their method involve the simultaneous solution of a set of nonlinear equations which suffer from the issue of initial guess of process model parameters for the convergence of parametric error during the process identification. Bajarangbali and Majhi [47] have proposed another set of nonlinear equations for the identification of a class of time delay processes with non-minimum phase behavior using an ideal relay with hysteresis which helps in minimization of effects of measurement noise during the identification.

Recently, Ghorai *et al.* [48] have proposed a set of analytical expressions for modelling and identification of a class of time delay processes using an asymmetrical relay feedback approach. Mehta and Majhi [81] proposed a set of mathematical expressions for the estimation of SOPTD process model parameters using limit cycle information with a prior estimation of process time delay.

In this chapter, a relay feedback scheme is proposed for modelling and identification of non-minimum phase time delay processes. Using the limit cycle information, attempts have been made to contribute a set of explicit expressions for an accurate identification of time delay processes in terms of non-minimum phase stable and unstable SOPTD models, non-minimum phase integrating FOPTD models. The proposed set of mathematical expressions for each unknown parameter of non-minimum phase process models are completely explicit which do not require any initial guess of process model parameters as compared to methods reported in literature. Furthermore, these explicit set of mathematical expressions are extended for identification of stable and unstable SOPTD models, integrating FOPTD models. When the process output is subjected to measurement noise, a clean limit cycle is retrieved using the Fourier series based curve fitting method and measured information is substituted in the derived set of mathematical expressions for the identification of time delay processes with/without non-minimum phase. Finally, the accuracy of the proposed set of mathematical expressions is verified through the consideration of well known examples from the literature.

## 4.2 Proposed Identification Scheme

Figure 4.1 shows a typical block diagram for relay based modelling and identification of a class of industrial processes. The two separate blocks each for an asymmetrical relay and unknown process are connected through a closed loop with a phase lag of $\pi$ radians. During the identification test, keeping the setpoint $R = 0$, the relay in feedback path helps in excitation of unknown process and the characteristics of unknown process are yielded in terms of sustained oscillatory responses. For non-minimum phase processes, the oscillatory responses show a point of non-smoothness due to presence of unstable zero in the process transfer function model with respect to processes without zeros as shown in Figure 4.2 and Figure 4.3. Based on process output and its first, second time derivatives, a set of mathematical expressions for the explicit representation of each unknown parameters of time delay processes with or without non-minimum phase are derived. Thereafter, the effects of measurement noise during the process identification are eradicated through a Fourier series based curve fitting

method where the important information from clean limit cycle and its subsequent derivatives are obtained from the fitted limit cycle data. Furthermore, the explicit set of mathematical expressions are extended for modelling of integrating processes with or without non-minimum phase.

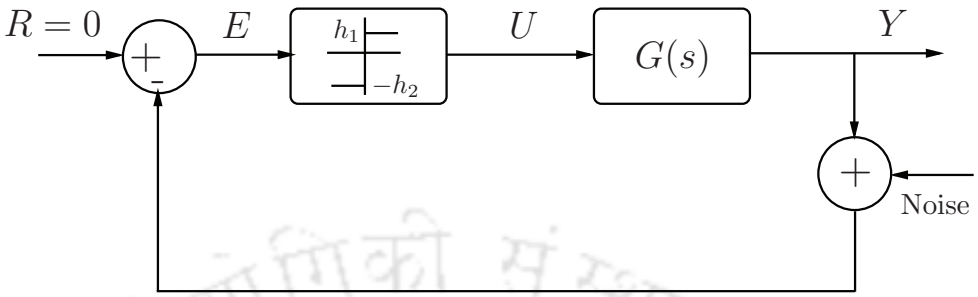


**Figure 4.1:** A schematic representation of relay feedback test

## 4.3 State Space Based Mathematical Expressions

In this section, a set of mathematical expressions for identification of non-minimum phase stable and unstable SOPTD process models are derived. Figure 4.2 shows a typical limit cycle for non-minimum phase SOPTD process where time instants $t_0$, $t_2$, $t_4$ refer to zero crossings, $t_1$, $t_3$ denote the

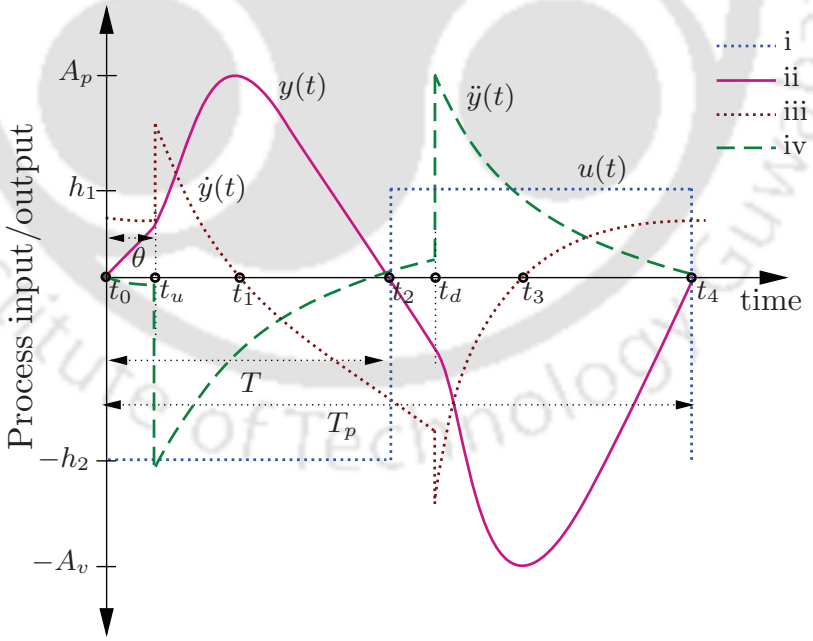


**Figure 4.2:** Plots for non-minimum phase SOPTD process: (i) relay output (ii) process output (iii) first derivative of process output (iv) second derivative of process output

time at which upper and lower peaks occur, $t_u$, $t_d$ signify the instant of abrupt change in the process

output, $T$ represents the time for which $y(t)$ remains greater than setpoint and $T_p$ describes the time period of limit cycle, respectively.

A general transfer function model for non-minimum phase SOPTD process is written as

$$G_m(s) = \frac{k(-\alpha_3 s + 1)e^{-\theta s}}{\alpha_2 s^2 + \alpha_1 s + \alpha_0} \tag{4.1}$$

where $k$, $\theta$, $\alpha_1, \alpha_2, \alpha_3$ denote the process model parameters, $\alpha_0 = \pm 1$ represents the non-minimum phase stable and unstable SOPTD process models. The Jordan canonical form representation of the above transfer function model is written as

$$\dot{\boldsymbol{x}}(t) = \underbrace{\begin{bmatrix} \lambda_1 & 0 \\ 0 & \lambda_2 \end{bmatrix}}_{\boldsymbol{J}} \boldsymbol{x}(t) + \underbrace{\begin{bmatrix} 1 \\ 1 \end{bmatrix}}_{\boldsymbol{B}} u(t-\theta) \tag{4.2}$$

$$y(t) = \underbrace{\begin{bmatrix} \pm\dfrac{k\lambda_1\lambda_2(\lambda_1+\lambda_3)}{\lambda_3(\lambda_1-\lambda_2)} & \mp\dfrac{k\lambda_1\lambda_2(\lambda_2+\lambda_3)}{\lambda_3(\lambda_1-\lambda_2)} \end{bmatrix}}_{\boldsymbol{C}} \boldsymbol{x}(t) \tag{4.3}$$

where $\lambda_1 = \dfrac{-\alpha_1 + \sqrt{\alpha_1^2 - 4\alpha_0\alpha_2}}{2\alpha_2}$, $\lambda_2 = \dfrac{-\alpha_1 - \sqrt{\alpha_1^2 - 4\alpha_0\alpha_2}}{2\alpha_2}$ are the eigen values of non-minimum phase SOPTD process model with $\alpha_1^2 - 4\alpha_0\alpha_2 \neq 0$, $\lambda_3 = -\dfrac{1}{\alpha_3}$.

For time range $t_0 \leq t < \theta$, the process output with $u(t-\theta) = h_1$ is written as

$$y(t) = -\boldsymbol{C}\boldsymbol{J}^{-1}\boldsymbol{B}h_1 + \boldsymbol{C}\boldsymbol{J}^{-1}[\boldsymbol{I} - \boldsymbol{e}^{\boldsymbol{J}T_p}]^{-1}[\boldsymbol{I} - \boldsymbol{e}^{\boldsymbol{J}T}]\boldsymbol{e}^{\boldsymbol{J}(t+T_p-T-\theta)}\boldsymbol{B}(h_1+h_2) \tag{4.4}$$

Similarly, the process output for time range $\theta \leq t < (t_2 + \theta)$ using $u(t-\theta) = -h_2$ is deduced as

$$y(t) = \boldsymbol{C}\boldsymbol{J}^{-1}\boldsymbol{B}h_2 - \boldsymbol{C}\boldsymbol{J}^{-1}[\boldsymbol{I} - \boldsymbol{e}^{\boldsymbol{J}T_p}]^{-1}[\boldsymbol{I} - \boldsymbol{e}^{\boldsymbol{J}(T_p-T)}]\boldsymbol{e}^{\boldsymbol{J}(t-\theta)}\boldsymbol{B}(h_1+h_2) \tag{4.5}$$

Finally, the process output for time range $(t_2 + \theta) \leq t < (t_4 + \theta)$ with $u(t-\theta) = h_1$ is derived as

$$y(t) = -\boldsymbol{C}\boldsymbol{J}^{-1}\boldsymbol{B}h_1 + \boldsymbol{C}\boldsymbol{J}^{-1}[\boldsymbol{I} - \boldsymbol{e}^{\boldsymbol{J}T_p}]^{-1}[\boldsymbol{I} - \boldsymbol{e}^{\boldsymbol{J}T}]\boldsymbol{e}^{\boldsymbol{J}(t-T-\theta)}\boldsymbol{B}(h_1+h_2) \tag{4.6}$$

Using the limit cycle and its slope information, a set of explicit expressions for each unknown parameters of non-minimum phase process models are deduced. Further, the derived set of explicit expressions are extended for the identification of non-minimum phase integrating FOPTD process,

stable and unstable SOPTD processes and integrating FOPTD process.

### 4.3.1 Non-minimum phase SOPTD process model

Substituting the $\boldsymbol{J}, \boldsymbol{B}, \boldsymbol{C}$ matrices in (4.5), the expression for process output is obtained as

$$y(t) = \mp kh_2(1 + \Lambda_1 V_1 e^{\lambda_1(t-\theta)} - \Lambda_2 V_2 e^{\lambda_2(t-\theta)}) \tag{4.7}$$

$$\text{where,} \quad \Lambda_1 = \frac{(h_1+h_2)(1-e^{\lambda_1(T_p-T)})}{h_2(1-e^{\lambda_1 T})},\ \Lambda_2 = \frac{(h_1+h_2)(1-e^{\lambda_2(T_p-T)})}{h_2(1-e^{\lambda_2 T})},$$

$$V_1 = \frac{\lambda_2(\lambda_1+\lambda_3)}{\lambda_3(\lambda_1-\lambda_2)},\ V_2 = \frac{\lambda_1(\lambda_2+\lambda_3)}{\lambda_3(\lambda_1-\lambda_2)}$$

The expressions for first and second time derivatives of (4.7) are written as

$$\dot{y}(t) = \mp kh_2\left(\Lambda_1 V_1 \lambda_1 e^{\lambda_1(t-\theta)} - \Lambda_2 V_2 \lambda_2 e^{\lambda_2(t-\theta)}\right) \tag{4.8}$$

$$\ddot{y}(t) = \mp kh_2\left(\Lambda_1 V_1 \lambda_1^2 e^{\lambda_1(t-\theta)} - \Lambda_2 V_2 \lambda_2^2 e^{\lambda_2(t-\theta)}\right) \tag{4.9}$$

Now the first and second time derivatives of process output at $t = t_2$ are written as

$$\dot{y}(t_2) = \mp kh_2\left(\Lambda_1 V_1 \lambda_1 e^{\lambda_1(t_2-\theta)} - \Lambda_2 V_2 \lambda_2 e^{\lambda_2(t_2-\theta)}\right) \tag{4.10}$$

$$\ddot{y}(t_2) = \mp kh_2\left(\Lambda_1 V_1 \lambda_1^2 e^{\lambda_1(t_2-\theta)} - \Lambda_2 V_2 \lambda_2^2 e^{\lambda_2(t_2-\theta)}\right) \tag{4.11}$$

The expression for $\Lambda_2 e^{\lambda_2(t_2-\theta)}$ is derived from $\ddot{y}(t_2)$ given in (4.11) as

$$\Lambda_2 e^{\lambda_2(t_2-\theta)} = \frac{1}{V_2\lambda_2^2}\left[\pm\frac{\ddot{y}(t_2)}{kh_2} + \Lambda_1 V_1 \lambda_1^2 e^{\lambda_1(t_2-\theta)}\right] \tag{4.12}$$

Substituting $\Lambda_2 e^{\lambda_2(t_2-\theta)}$ from (4.12) in (4.10) to yield the expression of $\Lambda_1 e^{\lambda_1(t_2-\theta)}$ as

$$\Lambda_1 e^{\lambda_1(t_2-\theta)} = \frac{\lambda_2}{V_1(\lambda_1\lambda_2 - \lambda_1^2)}\left[\pm\frac{\ddot{y}(t_2)}{kh_2\lambda_2} \mp \frac{\dot{y}(t_2)}{kh_2}\right] \tag{4.13}$$

Finally, the expression for $\Lambda_2 e^{\lambda_2(t_2-\theta)}$ is rewritten after the substitution of $\Lambda_1 e^{\lambda_1(t_2-\theta)}$ from (4.13) in (4.12) as

$$\Lambda_2 e^{\lambda_1(t_2-\theta)} = \frac{1}{V_2\lambda_2^2}\left[\pm\frac{\ddot{y}(t_2)}{kh_2} + \frac{\lambda_1^2\lambda_2}{(\lambda_1\lambda_2-\lambda_1^2)}\left(\mp\frac{\dot{y}(t_2)}{kh_2} \pm \frac{\ddot{y}(t_2)}{kh_2\lambda_2}\right)\right] \tag{4.14}$$

Now substituting the expressions of $\Lambda_1 e^{\lambda_1(t_2-\theta)}$, $\Lambda_2 e^{\lambda_2(t_2-\theta)}$ in (4.7) for $t = t_2$, we get

$$y(t_2) = \mp \left[ kh_2 \mp \dot{y}(t_2) \left( \frac{\lambda_1 + \lambda_2}{\lambda_1 \lambda_2} \right) \pm \frac{\ddot{y}(t_2)}{\lambda_1 \lambda_2} \right] \tag{4.15}$$

Repeating the above procedure, the expression for peak amplitude $y(t_1)$ occurring at $t = t_1$ is represented as

$$y(t_1) = \mp \left[ kh_2 \mp \dot{y}(t_1) \left( \frac{\lambda_1 + \lambda_2}{\lambda_1 \lambda_2} \right) \pm \frac{\ddot{y}(t_1)}{\lambda_1 \lambda_2} \right] \tag{4.16}$$

Solving (4.15) and (4.16) simultaneously, the expression for sum of eigen values $S = (\lambda_1 + \lambda_2)$ is obtained as

$$\lambda_1 + \lambda_2 = \frac{\mp y(t_1)\, \ddot{y}(t_2) - kh_2 \ddot{y}(t_2) \pm \ddot{y}(t_1)\, y(t_2) + \ddot{y}(t_1)\, kh_2}{\pm \dot{y}(t_1)\, y(t_2) + \dot{y}(t_1)\, kh_2 \mp \dot{y}(t_2)\, y(t_1) - \dot{y}(t_2)\, kh_2} \tag{4.17}$$

Substituting the sum of eigen values in any two expressions of $y(t_1)$ and $y(t_2)$ given in (4.15) and (4.16), the product of eigen values $P = \lambda_1 \lambda_2$ is derived as

$$\lambda_1 \lambda_2 = \frac{\mp \left[ \dot{y}(t_1)\, \ddot{y}(t_2) - \dot{y}(t_2)\, \ddot{y}(t_1) \right]}{\pm \dot{y}(t_1)\, y(t_2) + \dot{y}(t_1)\, kh_2 \mp \dot{y}(t_2)\, y(t_1) - \dot{y}(t_2)\, kh_2} \tag{4.18}$$

Now, one of the unknown parameter of non-minimum phase stable and unstable SOPTD process models is obtained in terms of sum of eigen values as

$$\alpha_1 = -\alpha_2(\lambda_1 + \lambda_2) \tag{4.19}$$

The expressions for another unknown parameter of non-minimum phase stable and unstable SOPTD process models ($\alpha_2$) are derived in terms of product of eigen values as

$$\alpha_2 = -\frac{1}{\lambda_1 \lambda_2} \quad \text{for stable model} \tag{4.20}$$

$$\alpha_2 = \frac{1}{\lambda_1 \lambda_2} \quad \text{for unstable model} \tag{4.21}$$

The steady state gain of process model is derived from ratios of process output area to process input area over the time period as

$$k = \frac{\int_0^{T_p} y(t)dt}{\int_0^{T_p} u(t)dt} \tag{4.22}$$

Moreover, the process time delay for non-minimum phase SOPTD process model is derived from the process output by measuring the distance between the initial relay switching instant and point of

non-smoothness in process output due to presence of unstable zero. Finally, the remaining unknown parameter ($\alpha_3$) in non-minimum phase SOPTD process model is derived using the expression of process peak time ($t_1$) as

$$e^{(\lambda_1-\lambda_2)(t_1-\theta)} = \frac{\Lambda_2(\lambda_2+\lambda_3)}{\Lambda_1(\lambda_1+\lambda_3)} \tag{4.23}$$

Therefore, the expression for $\alpha_3$ is derived from $\lambda_3$ as

$$\alpha_3 = -\frac{1}{\lambda_3} = -\frac{\Lambda_1 e^{(\lambda_1-\lambda_2)(t_1-\theta)} - \Lambda_2}{\lambda_2\Lambda_2 - \lambda_1\Lambda_1 e^{(\lambda_1-\lambda_2)(t_1-\theta)}} \tag{4.24}$$

### 4.3.2 Non-minimum phase integrating FOPTD process model

The transfer function model for non-minimum phase integrating FOPTD process is written from (4.1) with the substitution of $\alpha_0 = 0$ and $\alpha_1 = 1$ as

$$G_m(s) = \frac{k(-\alpha_3 s+1)e^{-\theta s}}{s(\alpha_2 s+1)} \tag{4.25}$$

where $k$, $\theta$, $\alpha_2$ and $\alpha_3$ are the process governing parameters.

When one of the eigen value tends to zero *i.e.,* $\lambda_1 \to 0$ such that $k/\lambda_1$ is finite, the non-minimum phase SOPTD process model becomes a non-minimum phase integrating FOPTD process model with $\lambda_2 = -1/\alpha_2$ and $\lambda_3 = -1/\alpha_3$.

The expression for process output for time range $\theta \le t < (t_1+\theta)$ as

$$y(t) = -kh_2\left[-\frac{T_p}{4} + \frac{(T_p-T)(h_1+h_2)}{T_p h_2}\left(t-\theta-\alpha_3+\frac{3(T_p-2T)}{8}\right) - \alpha_2\left(1-\frac{(\alpha_2+\alpha_3)}{\alpha_2}\Lambda_2 e^{-\frac{t-\theta}{\alpha_2}}\right)\right] \tag{4.26}$$

From (4.26), the expressions for limit cycle and its slope at $t = t_1$ are written as

$$\begin{aligned} y(t_1) = &-kh_2\left[-\frac{T_p}{4} + \frac{(T_p-T)(h_1+h_2)}{T_p h_2}\left(t_1-\theta-\alpha_3+\frac{3(T_p-2T)}{8}\right)\right. \\ &\left. - \alpha_2\left(1-\frac{(\alpha_2+\alpha_3)}{\alpha_2}\Lambda_2 e^{-\frac{t_1-\theta}{\alpha_2}}\right)\right] \end{aligned} \tag{4.27}$$

$$\dot{y}(t_1) = -kh_2\left[\frac{(T_p-T)(h_1+h_2)}{T_p h_2} - \frac{(\alpha_2+\alpha_3)}{\alpha_2}\Lambda_2 e^{-\frac{t_1-\theta}{\alpha_2}}\right] \tag{4.28}$$

Similarly, the expressions for limit cycle and its slope at $t = t_2$ are written from (4.26) as

$$y(t_2) = -kh_2\left[-\frac{T_p}{4}+\frac{(T_p-T)(h_1+h_2)}{T_p h_2}\left(t_2-\theta-\alpha_3+\frac{3(T_p-2T)}{8}\right)\right.$$
$$\left.-\alpha_2\left(1-\frac{(\alpha_2+\alpha_3)}{\alpha_2}\Lambda_2 e^{-\frac{t_2-\theta}{\alpha_2}}\right)\right] \tag{4.29}$$

$$\dot{y}(t_2) = -kh_2\left[\frac{(T_p-T)(h_1+h_2)}{T_p h_2}-\frac{(\alpha_2+\alpha_3)}{\alpha_2}\Lambda_2 e^{-\frac{t_2-\theta}{\alpha_2}}\right] \tag{4.30}$$

Solving (4.27) and (4.28), (4.29) and (4.30), the expressions for $y(t_1)$ and $y(t_2)$ are derived in simplified form as

$$y(t_1) = -kh_2\left[-\frac{T_p}{4}+\frac{(T_p-T)(h_1+h_2)}{T_p h_2}\left(t_1-\theta-\alpha_3+\frac{3(T_p-2T)}{T_p}\right)\right.$$
$$\left.-\alpha_2\left(1-\frac{(T_p-T)(h_1+h_2)}{T_p h_2}\right)\right] \tag{4.31}$$

$$y(t_2) = -kh_2\left[-\frac{T_p}{4}+\frac{(T_p-T)(h_1+h_2)}{T_p h_2}\left(t_2-\theta-\alpha_3+\frac{3(T_p-2T)}{8}\right)\right.$$
$$\left.-\alpha_2\left(1-\frac{\dot{y}(t_2)}{kh_2}-\frac{(T_p-T)(h_1+h_2)}{T_p h_2}\right)\right] \tag{4.32}$$

From the simultaneous solution of two equations (4.31) and (4.32), the explicit expressions for two unknown parameters ($\alpha_2$, $\alpha_3$) of non-minimum phase integrating FOPTD process model are derived. Finally, the process steady state gain is calculated from ratios of process output area to process input area over the time period using (4.22) and process time delay is measured from the distance between the initial relay switching instant at zero crossings and point of non-smoothness at the process output as shown in Figure 4.2.

### 4.3.3 SOPTD process model

Figure 4.3 shows a typical limit cycle for stable SOPTD process where $t_0$, $t_2$, $t_4$ represent time instants of zero crossings, $t_1$, $t_3$ refer to peak instants in upper and lower direction and $T, T_p$ signify the time for which $y(t)$ remains greater than setpoint and the time period of limit cycle, respectively. A general transfer function model for SOPTD process is written from the non-minimum phase SOPTD

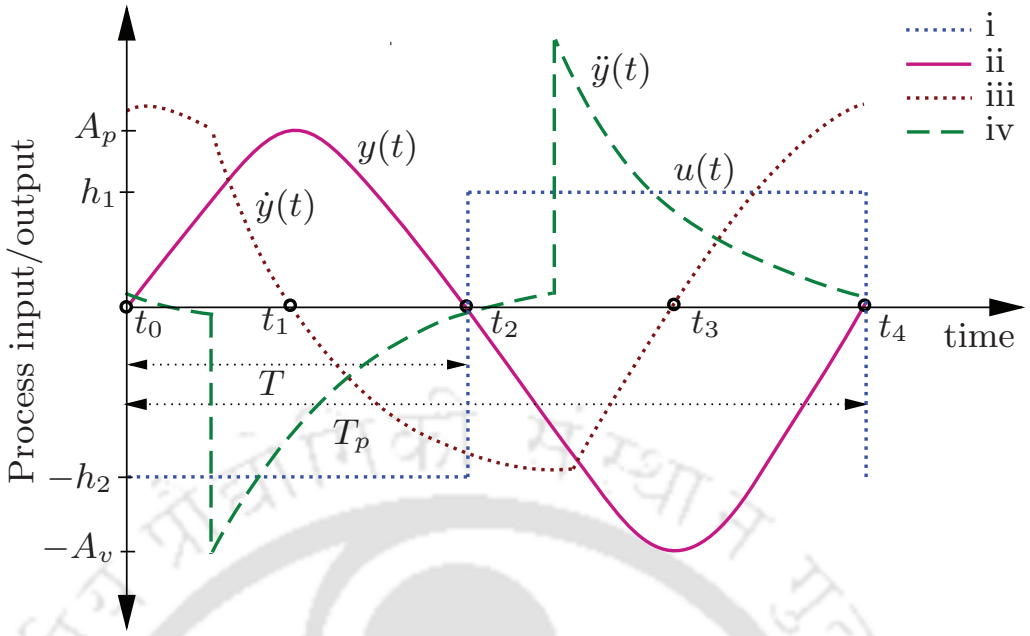


**Figure 4.3:** Plots for SOPTD process: (i) relay output (ii) process output (iii) first derivative of process output (iv) second derivative of process output

process model with the substitution of $\alpha_3 = 0$ in (4.1) as

$$G_m(s) = \frac{ke^{-\theta s}}{\alpha_2 s^2 + \alpha_1 s + \alpha_0} \tag{4.33}$$

where $k$, $\theta$, $\alpha_1, \alpha_2$ represent the process model parameters, $\alpha_0 = \pm 1$ denotes the stable and unstable SOPTD process models.

Substituting the $\boldsymbol{J}, \boldsymbol{B}, \boldsymbol{C}$ matrices in (4.5), the process output expression for the time range $\theta \leq t < (t_2 + \theta)$ is written as

$$y(t) = \mp k h_2 (1 + \Lambda_1 V_3 e^{\lambda_1 (t-\theta)} - \Lambda_2 V_4 e^{\lambda_2 (t-\theta)}) \tag{4.34}$$

$$\text{where,} \quad \Lambda_1 = \frac{(h_1 + h_2)(1 - e^{\lambda_1 (T_p - T)})}{h_2 (1 - e^{\lambda_1 T_p})}, \; \Lambda_2 = \frac{(h_1 + h_2)(1 - e^{\lambda_2 (T_p - T)})}{h_2 (1 - e^{\lambda_2 T_p})},$$

$$V_3 = \frac{\lambda_2}{(\lambda_1 - \lambda_2)}, \; V_4 = \frac{\lambda_1}{(\lambda_1 - \lambda_2)}$$

The first and second time derivatives of (4.34) yield the following expressions as

$$\dot{y}(t) = \mp k h_2 \left( \Lambda_1 V_3 \lambda_1 e^{\lambda_1 (t-\theta)} - \Lambda_2 V_4 \lambda_2 e^{\lambda_2 (t-\theta)} \right) \tag{4.35}$$

$$\ddot{y}(t) = \mp kh_2 \left( \Lambda_1 V_3 \lambda_1^2 e^{\lambda_1 (t-\theta)} - \Lambda_2 V_4 \lambda_2^2 e^{\lambda_2 (t-\theta)} \right) \tag{4.36}$$

Now the expressions for first and second time derivatives of process output at $t = t_2$ are written as

$$\dot{y}(t_2) = \mp kh_2 \left( \Lambda_1 V_3 \lambda_1 e^{\lambda_1 (t_2-\theta)} - \Lambda_2 V_4 \lambda_2 e^{\lambda_2 (t_2-\theta)} \right) \tag{4.37}$$

$$\ddot{y}(t_2) = \mp kh_2 \left( \Lambda_1 V_3 \lambda_1^2 e^{\lambda_1 (t_2-\theta)} - \Lambda_2 V_4 \lambda_2^2 e^{\lambda_2 (t_2-\theta)} \right) \tag{4.38}$$

The expression for $\Lambda_2 e^{\lambda_2 (t_2-\theta)}$ is derived from $\ddot{y}(t = t_2)$ given in (4.38) as

$$\Lambda_2 e^{\lambda_2 (t_2-\theta)} = \frac{1}{V_4 \lambda_2^2} \left[ \pm \frac{\ddot{y}(t_2)}{kh_2} + \Lambda_1 V_3 \lambda_1^2 e^{\lambda_1 (t_2-\theta)} \right] \tag{4.39}$$

Substituting $\Lambda_2 e^{\lambda_2 (t_2-\theta)}$ from (4.39) in (4.37) to yield the expression of $\Lambda_1 e^{\lambda_1 (t_2-\theta)}$ as

$$\Lambda_1 e^{\lambda_1 (t_2-\theta)} = \frac{\lambda_2}{V_3 (\lambda_1 \lambda_2 - \lambda_1^2)} \left[ \pm \frac{\ddot{y}(T)}{kh_2 \lambda_2} \mp \frac{\dot{y}(t_2)}{kh_2} \right] \tag{4.40}$$

Finally, the expression for $\Lambda_2 e^{\lambda_2 (t_2-\theta)}$ is obtained from (4.39) after the substitution of $\Lambda_1 e^{\lambda_1 (t_2-\theta)}$ from (4.40) as

$$\Lambda_2 e^{\lambda_2 (t_2-\theta)} = \frac{1}{V_4 \lambda_2^2} \left[ \pm \frac{\ddot{y}(t_2)}{kh_2} + \frac{\lambda_1^2 \lambda_2}{(\lambda_1 \lambda_2 - \lambda_1^2)} \left( \mp \frac{\dot{y}(t_2)}{kh_2} \pm \frac{\ddot{y}(t_2)}{kh_2 \lambda_2} \right) \right] \tag{4.41}$$

Now substituting $\Lambda_1 e^{\lambda_1 (t_2-\theta)}$, $\Lambda_2 e^{\lambda_2 (t_2-\theta)}$ in the expression of process output at $t = t_2$, we get

$$y(t_2) = \mp \left[ kh_2 \mp \dot{y}(t_2) \frac{\lambda_1 + \lambda_2}{\lambda_1 \lambda_2} \pm \frac{\ddot{y}(t_2)}{\lambda_1 \lambda_2} \right] \tag{4.42}$$

Repeating the above procedure, the expression for peak amplitude $y(t_1)$ occurring at $t = t_1$ is derived in terms of $\dot{y}(t_1)$ and $\ddot{y}(t_1)$ as

$$y(t_1) = \mp \left[ kh_2 \mp \dot{y}(t_1) \frac{\lambda_1 + \lambda_2}{\lambda_1 \lambda_2} \pm \frac{\ddot{y}(t_1)}{\lambda_1 \lambda_2} \right] \tag{4.43}$$

The expressions of $y(t_1)$ and $y(t_2)$ are solved simultaneously to obtain the sum of eigen values $S = (\lambda_1 + \lambda_2)$ as

$$\lambda_1 + \lambda_2 = \frac{\mp y(t_1)\, \ddot{y}(t_2) - kh_2 \ddot{y}(t_2) \pm \ddot{y}(t_1)\, y(t_2) + \ddot{y}(t_1)\, kh_2}{\pm \dot{y}(t_1)\, y(t_2) + \dot{y}(t_1)\, kh_2 \mp \dot{y}(t_2)\, y(t_1) - \dot{y}(t_2)\, kh_2} \tag{4.44}$$

Further substituting the sum of eigen values in any of two expressions of $y(t_1)$ and $y(t_2)$, the product of eigen values $P = \lambda_1\lambda_2$ is obtained as

$$\lambda_1\lambda_2 = \frac{\mp\left[\dot{y}\left(t_1\right)\ddot{y}\left(t_2\right) - \dot{y}\left(t_2\right)\ddot{y}\left(t_1\right)\right]}{\pm\dot{y}\left(t_1\right)y\left(t_2\right) + \dot{y}\left(t_1\right)kh_2 \mp \dot{y}\left(t_2\right)y\left(t_1\right) - \dot{y}\left(t_2\right)kh_2} \tag{4.45}$$

Using sum of eigen values, expression for $\alpha_1$ is derived for stable/unstable SOPTD process models as

$$\alpha_1 = -\alpha_2(\lambda_1 + \lambda_2) \tag{4.46}$$

The remaining unknown parameter ($\alpha_2$) of stable and unstable SOPTD process models is derived from product of eigen values as

$$\alpha_2 = -\frac{1}{\lambda_1\lambda_2} \qquad \text{for stable model} \tag{4.47}$$

$$\alpha_2 = \frac{1}{\lambda_1\lambda_2} \qquad \text{for unstable model} \tag{4.48}$$

The steady state gain of process model is derived using (4.22) whereas the process time delay for SOPTD process model is obtained from (4.23) with the substitution of $\lambda_3 = -\infty$ as

$$\theta = t_1 - \frac{1}{\lambda_1 - \lambda_2}\ln\left(\frac{\Lambda_2}{\Lambda_1}\right) \tag{4.49}$$

### 4.3.4 Integrating FOPTD process model

In this section, an explicit set of mathematical expressions for modelling and identification of an integrating FOPTD model is discussed. A general transfer function model for integrating FOPTD process is written from (4.33) with the substitution of $\alpha_0 = 0$ and $\alpha_1 = 1$ as

$$G_m(s) = \frac{ke^{-\theta s}}{s(\alpha_2 s + 1)} \tag{4.50}$$

where $k$, $\theta$ and $\alpha_2$ are the process model parameters. When one of eigen value tends to zero *i.e.*, $\lambda_1 \to 0$ such that $k/\lambda_1$ is finite, the SOPTD process model reduces to an integrating FOPTD process model dynamics with $\lambda_2 = -1/\alpha_2$. The expression of process output for time range $\theta \le t < (t_1 + \theta)$ is written as

$$y(t) = -kh_2\left[-\frac{T_p}{4} + \frac{(T_p - T)(h_1 + h_2)}{T_p h_2}\left(t - \theta + \frac{3(T_p - 2T)}{8}\right) - \alpha_2\left(1 - \Lambda_2 e^{-\frac{t-\theta}{T_p}}\right)\right] \tag{4.51}$$

From (4.51), the expressions for limit cycle and its slope are represented at $t = t_1$ as

$$y(t_1) = -kh_2\left[-\frac{T_p}{4} + \frac{(T_p - T)(h_1 + h_2)}{T_p h_2}\left(t_1 - \theta + \frac{3(T_p - 2T)}{8}\right) - \alpha_2\left(1 - \Lambda_2 e^{-\frac{t_1-\theta}{\alpha_2}}\right)\right] \tag{4.52}$$

$$\dot{y}(t_1) = -kh_2\left[\frac{(T_p - T)(h_1 + h_2)}{T_p h_2} - \Lambda_2 e^{-\frac{t_1-\theta}{\alpha_2}}\right] \tag{4.53}$$

Similarly, the expressions for limit cycle and its slope are written at $t = t_2$ using (4.51) as

$$y(t_2) = -kh_2\left[-\frac{T_p}{4} + \frac{(T_p - T)(h_1 + h_2)}{T_p h_2}\left(t_2 - \theta + \frac{3(T_p - 2T)}{8}\right) - \alpha_2\left(1 - \Lambda_2 e^{-\frac{t_2-\theta}{\alpha_2}}\right)\right] \tag{4.54}$$

$$\dot{y}(t_2) = -kh_2\left[\frac{(T_p - T)(h_1 + h_2)}{T_p h_2} - \Lambda_2 e^{-\frac{t_2-\theta}{\alpha_2}}\right] \tag{4.55}$$

Solving (4.52) and (4.53), (4.54) and (4.55), the expressions for $y(t_1)$ and $y(t_2)$ are derived in simplified form as

$$\begin{aligned} y(t_1) = -kh_2\Bigg[&-\frac{T_p}{4} + \frac{(T_p - T)(h_1 + h_2)}{T_p h_2}\left(t_1 - \theta + \frac{3(T_p - 2T)}{T_p}\right) \\ &- \alpha_2\left(1 - \frac{(T_p - T)(h_1 + h_2)}{T_p h_2}\right)\Bigg] \end{aligned} \tag{4.56}$$

$$\begin{aligned} y(t_2) = -kh_2\Bigg[&-\frac{T_p}{4} + \frac{(T_p - T)(h_1 + h_2)}{T_p h_2}\left(t_2 - \theta + \frac{3(T_p - 2T)}{8}\right) \\ &- \alpha_2\left(1 - \frac{\dot{y}(t_2)}{kh_2} - \frac{(T_p - T)(h_1 + h_2)}{T_p h_2}\right)\Bigg] \end{aligned} \tag{4.57}$$

From the simultaneous solution of two equations (4.56) and (4.57), the explicit expressions for two unknown parameters $(\alpha_2, \theta)$ of integrating FOPTD process model are derived. Using (4.22), the steady state gain $(k)$ is derived from ratios of areas under the process output to process input.

**Remark 4.1** *For the existence of sustained oscillations in unstable SOPTD and FOPTD processes, the second time derivative of limit cycle at $t = t_2$ for SOPTD process and the first time derivative of limit cycle at $t = t_2$ for FOPTD process should be less than zero. This leads to a limitation on relay settings. For non-minimum phase unstable SOPTD process, the condition for existence of limit cycle is derived as*

$$\theta\lambda_1 \leq \ln\left(\frac{h_1 + h_2}{h_2}\right) + \ln\left(\frac{\lambda_2}{\lambda_2 - \lambda_1}\right) + \ln\left(\frac{\lambda_1 + \lambda_3}{\lambda_3}\right) \tag{4.58}$$

*Substituting $\lambda_3 = -\infty$ in (4.58), the condition for existence of limit cycle in unstable SOPTD process is deduced as*

$$\theta\lambda_1 \leq \ln\left(\frac{h_1 + h_2}{h_2}\right) + \ln\left(\frac{\lambda_2}{\lambda_2 - \lambda_1}\right) \tag{4.59}$$

*For unstable FOPTD process, the limit cycle existence condition is obtained from (4.59) after the substitution of $\lambda_2 = -\infty$ as*

$$\theta\lambda_1 \leq \ln\left(\frac{h_1 + h_2}{h_2}\right) \tag{4.60}$$

## 4.4 Results and Discussion

This section presents six well-known examples from literature for the validation of the proposed relay based identification scheme and the derived set of mathematical expressions. Thereafter, the identification error between estimated models and actual process is evaluated using integral of absolute error (IAE) criterion.

### 4.4.1 Example 1: Non-minimum phase stable SOPTD process

Consider a non-minimum phase stable SOPTD process widely studied in the literature by Bajarangabali and Majhi [47] as $G_1(s) = \dfrac{(-s+1)e^{-s}}{10s^2 + 7s + 1}$. During the identification test, a biased relay with amplitudes ($h_1 = 1$ and $h_2 = -1.2$) is fedback to yield an asymmetrical limit cycle at the process output. Firstly, the process steady state gain is derived using (4.22) as $k = 1.0$ and the process time delay is evaluated from the limit cycle as $\theta = (t_u - t_0) = 1.0001$. The parameters measured from the limit cycle and its slope are $t_1 = 2.4040$, $t_2 = 5.3899$, $t_4 = 11.5065$, $y(t_1) = 0.3636$, $\dot{y}(t_1) = 0$, $\ddot{y}(t_1) = -0.1565$, $y(t_2) = 0$, $\dot{y}(t_2) = -0.1697$ and $\ddot{y}(t_2) = -1.2079 \times 10^{-3}$. Subsequently, the explicit expressions given in (4.19) and (4.20) are utilized to estimate the two unknown parameters of non-minimum phase SOPTD process model as $\alpha_2 = 10.0$, $\alpha_1 = 7.0060$, respectively. Substituting the limit cycle information and process model parameters $\alpha_1, \alpha_2$ in (4.24), a remaining unknown parameter of non-minimum phase stable SOPTD process model is derived as $\alpha_3 = 1.0007$ with a minimal amount of IAE tabulated in Table 4.1. The robustness of the proposed method is tested through the addition of Gaussian distributed random noise at the process output. Using the Fourier series based curve fitting method, a clean limit cycle is recovered and yielded limit cycle information is substituted in the derived set of mathematical expressions for estimation of non-minimum phase SOPTD process

models in presence of measurement noise. In Figure 4.4, comparisons between estimated models and true process are demonstrated through step response plots where the proposed method brings better accuracy in both identified models with or without noise.

**Table 4.1:** Comparison of identified process models with/without noise for Example 1

| SNR (dB) | $k$ | $\alpha_1$ | $\alpha_2$ | $\alpha_3$ | $\theta$ | IAE |
|---|---|---|---|---|---|---|
| 0 | 1.0 | 7.0060 | 10.0 | 1.0007 | 1.0001 | 0.0003 |
| 10 | 1.0201 | 7.1025 | 9.9532 | 0.9836 | 1.1020 | 0.0143 |
| 15 | 0.9892 | 6.8921 | 10.1321 | 1.0120 | 0.9953 | 0.0054 |

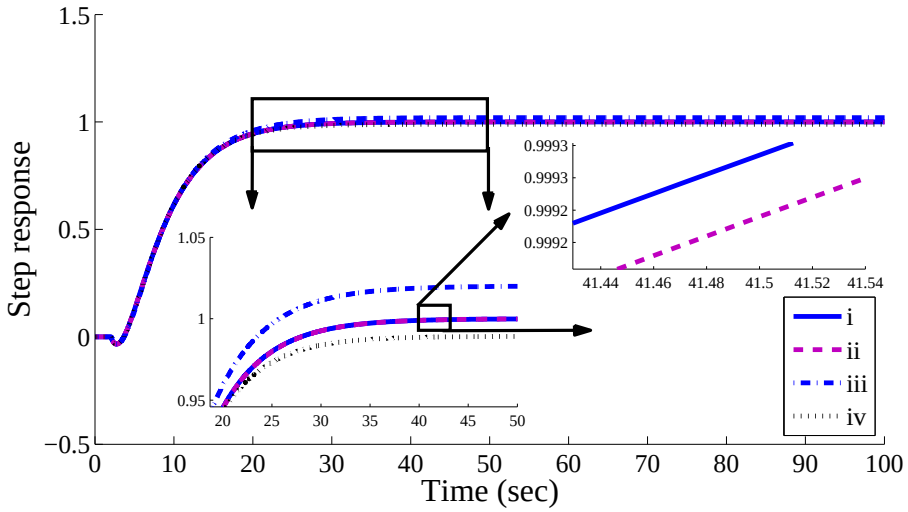


**Figure 4.4:** Step response plots for Example 1: (i) actual process (ii) proposed model without noise (iii) proposed model with 10dB noise (iv) proposed model with 15dB noise

### 4.4.2 Example 2: Non-minimum phase unstable SOPTD process

Let us consider a non-minimum phase unstable SOPTD process as $G_2(s) = \dfrac{(-0.2s+1)e^{-0.5s}}{s^2+1.5s-1}$. For an unstable process dynamics, an asymmetrical relay with amplitudes ($h_1 = 1$ and $h_2 = -1.2$) is considered for the generation of sustained oscillations. Similar to Example 1, the process steady state gain is derived from (4.22) as $k = 1.0$ and the process time delay is measured from limit cycle as $\theta = 0.50001$, respectively. Thereafter, the parameters measured from the process output and its slope are $t_1 = 1.3436$, $t_2 = 3.2719$, $t_4 = 9.9413$, $y(t_1) = 0.6292$, $\dot{y}(t_1) = 0$, $\ddot{y}(t_1) = -0.5715$, $y(t_2) = 0$, $\dot{y}(t_2) = -0.5938$ and $\ddot{y}(t_2) = -0.3089$. Subsequently, the explicit expressions deduced in (4.19) and (4.21) are utilized for estimation of two unknown parameters of non-minimum phase

unstable SOPTD process model as $\alpha_2 = 0.9988$, $\alpha_1 = 1.5012$, respectively. Thereafter, the remaining unknown parameter of process model is derived using (4.24) as $\alpha_3 = 0.2003$. Furthermore, the effects of measurement noise during the identification are minimized using the Fourier series based curve fitting method. Again, the recovered limit cycle information is substituted in the derived set of explicit expressions for the estimation of process model parameters. The closeness between the identified models with/without noise and actual process is compared through IAE in Table 4.2.

**Table 4.2:** Comparison of identified process models with/without noise for Example 2

| SNR (dB) | $k$ | $\alpha_1$ | $\alpha_2$ | $\alpha_3$ | $\theta$ | IAE |
|---|---|---|---|---|---|---|
| 0 | 1.0 | 1.5012 | 0.9988 | 0.2003 | 0.50001 | 0.0001 |
| 10 | 0.9876 | 1.4823 | 1.0131 | 0.1923 | 0.4831 | 0.0080 |
| 15 | 1.005 | 1.5210 | 0.9881 | 0.2011 | 0.5023 | 0.0036 |

### 4.4.3 Example 3: Non-minimum phase integrating FOPTD process

Consider a non-minimum phase integrating FOPTD process studied by Padhy and Majhi [80] as $G_3(s) = \dfrac{(-s+1)e^{-3s}}{s(2s+1)}$. During the identification test, a symmetrical relay ($h = \pm 1$) helps in the generation of sustained oscillations at the process output. The process steady state gain is derived from ratios of process output area to process input area using (4.22) as $k = 1.0$ and the process time delay is evaluated using the process output information as $\theta = (t_u - t_0) = 3.0$. The important limit cycle parameters are measured as $t_1 = 3.6203$, $t_2 = 7.9117$, $t_4 = 17.4064$, $y(t_1) = 3.0306$ and $\dot{y}(t_2) = -1.0596$. Substituting the limit cycle information, the unknown parameters of process model are obtained from the simultaneous solution of (4.31) and (4.32) as $\alpha_2 = 1.9998$, $\alpha_3 = 1.0005$. The robustness of the proposed method is examined in presence of measurement noise through the addition of Gaussian distributed noise to obtain the noisy limit cycles with 10dB and 15dB SNR, respectively. Further, a clean limit cycle is derived using the Fourier series based curve fitting method and the

**Table 4.3:** Comparison of identified process models with/without noise for Example 3

| SNR (dB) | $k$ | $\alpha_2$ | $\alpha_3$ | $\theta$ | IAE |
|---|---|---|---|---|---|
| 0 | 1.0 | 1.9998 | 1.0005 | 3.0 | 0.00001 |
| 10 | 0.9862 | 1.9692 | 0.9892 | 2.8925 | 0.0064 |
| 15 | 0.9962 | 0.9892 | 0.9902 | 3.010 | 0.0010 |

unknown process model parameters are obtained from the explicit set of mathematical expressions.

The comparisons between the identified models with/without noise and actual process are drawn to show the efficacy of proposed identification method in Table 4.3.

### 4.4.4 Example 4: Stable SOPTD process

Consider the stable SOPTD process studied by Liu and Gao [9] as $G_4(s) = \dfrac{e^{-2s}}{10s^2 + 11s + 1}$. During identification test, a relay with amplitudes ($h_1 = 1$, $h_2 = -1.2$) induces an asymmetrical limit cycle at the process output. Measurements made on the basis of a single relay test yields the limit cycle parameters as $t_1 = 2.4538$, $t_2 = 4.8942$, $t_4 = 10.5550$, $y(t_1) = 0.1940$, $\dot{y}(t_1) = 0$, $\ddot{y}(t_1) = -0.1395$, $y(t_2) = 0$, $\dot{y}(t_2) = -0.1079$ and $\ddot{y}(t_2) = -1.3698 \times 10^{-3}$, respectively. One of the crucial parameter of process model *i.e.,* steady state gain, $k$ is obtained from (4.22). Substituting the limit cycle parameters in the deduced set of mathematical expressions (4.46) and (4.47), the two unknown parameters ($\alpha_1$, $\alpha_2$) of stable SOPTD process model are evaluated as 11.0020 and 10.0, respectively. Now the remaining unknown parameter ($\theta$) of stable SOPTD process model is derived using (4.49) as $\theta = 2.0010$. Moreover, the robustness of the proposed identification scheme is demonstrated in presence of measurement noise through the addition of Gaussian distributed random signal with 10 dB SNR and 15dB SNR at the process output. Furthermore, the limit cycle is reconstructed using Fourier series based curve fitting

**Table 4.4:** Comparison of identified process models for Example 4

| Methods | Identified models | IAE |
|---|---|---|
| Proposed model | $\dfrac{1.0e^{-2.0010s}}{10.0s^2 + 11.0020s + 1}$ | 0.0002 |
| Bajarangbali *et al.* [8] model | $\dfrac{0.9923e^{-2.0s}}{10.0036s^2 + 10.9102s + 1}$ | 0.0016 |
| Liu *et al.* [9] model | $\dfrac{1.0122e^{-2.0037s}}{10.0368s^2 + 11.1098s + 1}$ | 0.0029 |
| Shen *et al.* [21] model | $\dfrac{0.998e^{-2.0s}}{9.54216s^2 + 10.184s + 1}$ | 0.0385 |

**Table 4.5:** Comparison of identified process models with/without noise for Example 4

| SNR (dB) | $k$ | $\alpha_1$ | $\alpha_2$ | $\theta$ | IAE |
|---|---|---|---|---|---|
| 0 | 1.0 | 11.0020 | 10.0 | 2.0010 | 0.0002 |
| 10 | 1.030 | 10.8602 | 9.8230 | 1.9632 | 0.0254 |
| 15 | 0.9956 | 11.1201 | 9.9621 | 2.1010 | 0.01969 |

technique and the yielded process output data is substituted in the derived set of explicit expressions

for the identification of SOPTD model. The effects of the parametric error in the estimated process model parameters is compared with the models reported in literature and measurement noise in Table 4.4 and Table 4.5.

### 4.4.5 Example 5: Unstable SOPTD process

Consider an unstable SOPTD process studied in literature by Bajarangbali *et al.* [8], Liu and Gao [2], Vivek and Chidambaram [3] as $G_5(s) = \dfrac{e^{-0.5s}}{s^2 + 1.5s - 1}$. A relay with amplitudes ($h_1 = 1, h_2 = -1.2$) is fedback to induce the sustained oscillations at the process output. The steady state gain of process model is obtained from (4.22) as $k = 1.0$. From the limit cycle information, the measured parameters are obtained as $t_1 = 1.0227$, $t_2 = 2.3257$, $t_4 = 5.7366$, $y(t_1) = 0.4257$, $\dot{y}(t_1) = 0$, $\ddot{y}(t_1) = -0.7749$, $y(t_2) = 0$, $\dot{y}(t_2) = -0.5713$ and $\ddot{y}(t_2) = -0.3428$, respectively. Substituting the measured parameters and further solving the explicit expressions (4.46) and (4.48), the two unknown parameters of unstable SOPTD process model ($\alpha_1$, $\alpha_2$) are estimated as 1.5020 and 1.0, respectively. Moreover, the process time delay is derived as $\theta = 0.5001$ after the substitution of $\alpha_1$, $\alpha_2$ in (4.49). Thereafter, the effects of measurement noise over the identification of process model parameters are studied through the addition of Gaussian distributed random signal at the process output. Subsequently, the important information is measured from the reconstructed limit cycle and its slope information as shown in Figure 4.5, Figure 4.6, Figure 4.7 and further substituted in the derived set of mathematical expressions for estimation of unstable SOPTD process model parameters. The parametric error in the identified

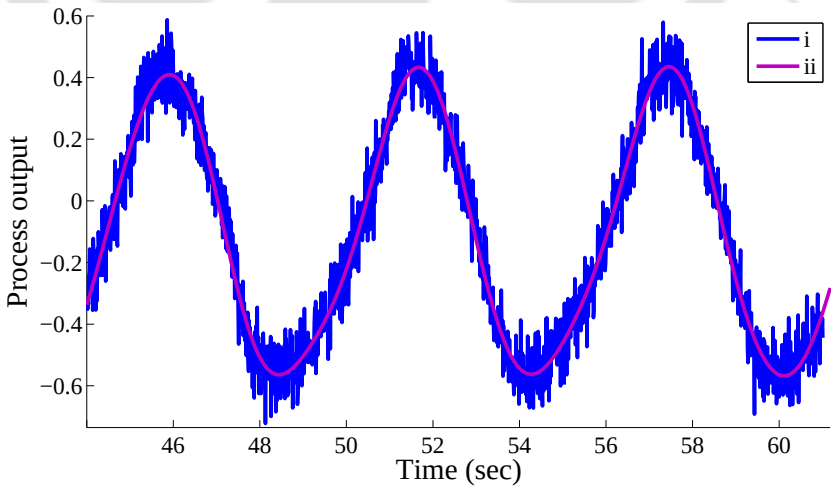


**Figure 4.5:** Plots for reconstruction of limit cycle using curve fitting method in Example 5: (i) noisy data (ii) fitted data

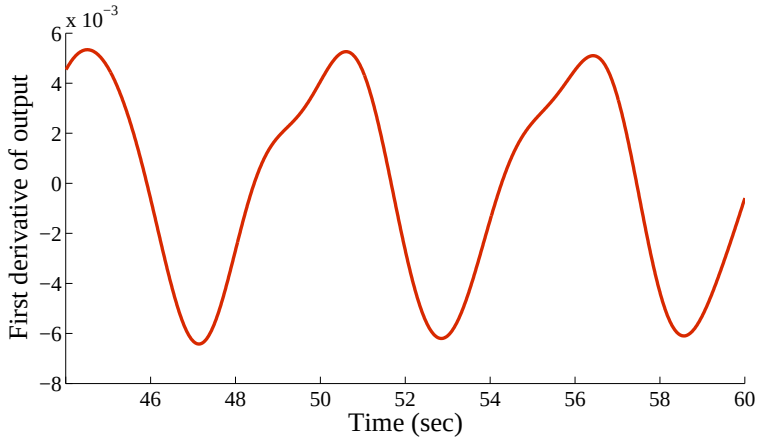


**Figure 4.6:** First derivative of reconstructed limit cycle data for Example 5

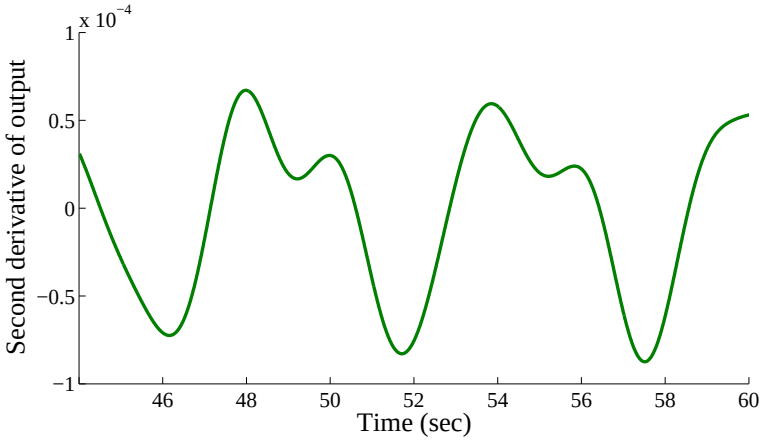


**Figure 4.7:** Second derivative of reconstructed limit cycle data for Example 5

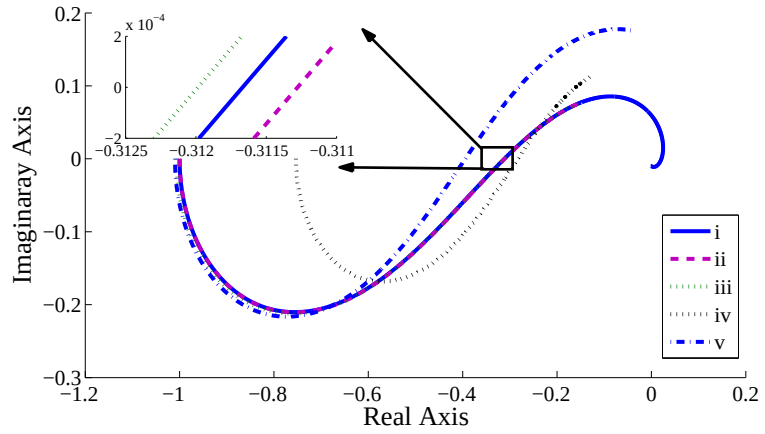


**Figure 4.8:** Nyquist plots for Example 5: (i) actual process (ii) proposed model (iii) Bajarangbali *et al.* [8] suggested model (iv) model proposed by Vivek and Chidambaram [3] (v) Liu and Gao [9] suggested model

and actual process dynamics is compared through Nyquist plots in Figure 4.8 and tabulated in Table 4.6 and Table 4.7 wherein the identified process models yield better identification accuracy over the models reported in literature.

**Table 4.6:** Comparison of identified process models for Example 5

| Methods | Identified models | IAE |
|---|---|---|
| Proposed model | $\frac{1.0e^{-0.5001s}}{1.0s^2+1.5020s-1}$ | 0.0006 |
| Bajarangbali *et al.* [8] model | $\frac{1.0069e^{-0.50s}}{1.0190s^2+1.5095s-1}$ | 0.0034 |
| Vivek and Chidambaram [3] model | $\frac{0.7534e^{-1.0412s}}{(2.1642s-1)}$ | 0.3499 |
| Liu and Gao [9] model | $\frac{1.0097e^{-1.36s}}{(2.74s-1)}$ | 0.2159 |

**Table 4.7:** Comparison of identified process models with/without noise for Example 5

| SNR (dB) | $k$ | $\alpha_1$ | $\alpha_2$ | $\theta$ | IAE |
|---|---|---|---|---|---|
| 0 | 1.0 | 1.5020 | 1.0 | 0.5001 | 0.0006 |
| 10 | 0.9805 | 1.5312 | 0.9826 | 0.4995 | 0.0269 |
| 15 | 1.01 | 1.4920 | 0.9926 | 0.4923 | 0.0140 |

### 4.4.6 Example 6: Integrating FOPTD process

Let us consider an integrating FOPTD process studied by Majhi [40] as $G_6(s) = \frac{e^{-1.5s}}{s(5s+1)}$. During relay based identification, an asymmetrical relay with amplitudes ($h_1 = 1$, $h_2 = -1.2$) brings a limit cycle at the process output. The steady state gain of process model is derived using (4.22) as $k = 1.0$. Measurements made on a single relay test yield the limit cycle parameters as $t_1 = 3.9732$, $t_2 = 8.6467$, $t_4 = 19.0238$ and $y(t_1) = 1.9647$. Using (4.56) and (4.57), the two unknown parameters of integrating FOPTD process are derived as $\theta = 1.5006$ and $\alpha_2 = 5.004$, respectively. To show the effects of measurement noise during the process identification, a Gaussian distributed random signal is added at the process output. Further, the recovered limit cycle information is substituted in the derived set of mathematical expressions for the estimation of integrating FOPTD process model parameters. Finally, comparison of identification error in the estimated process model with/without noise is tabulated in Table 4.8.

**Table 4.8:** Comparison of identified process models with/without noise for Example 6

| SNR (dB) | $k$ | $\alpha_2$ | $\theta$ | IAE |
|---|---|---|---|---|
| 0 | 1.0 | 5.004 | 1.5006 | 0.0001 |
| 10 | 0.9823 | 5.1216 | 1.4982 | 0.0096 |
| 15 | 1.012 | 4.9894 | 1.5026 | 0.0041 |

## 4.5 Summary

In this chapter, a relay feedback scheme for modelling and identification of a class of non-minimum phase processes with time delay is investigated. Using a relay feedback experiment, the important information from sustained oscillatory responses is collected and further substituted in the derived set of explicit expressions for the identification of plant dynamics in terms of non-minimum phase stable and unstable SOPTD process models. Thereafter, a set of mathematical expressions for the identification of non-minimum phase integrating FOPTD, stable and unstable SOPTD, integrating FOPTD processes is derived. The robustness of the proposed identification method is demonstrated through the addition of measurement noise at the process output and thereafter a Fourier series based fitted limit cycle information is substituted in the derived set of mathematical expressions for the identification of time delay process models in presence of measurement noise. Simulations of well-known examples from literature have verified the accuracy of proposed set of explicit expressions for the identification of a class of time delay processes. The comparisons between the identified process models with/without noise are drawn graphically through frequency response plots. Moreover, the proposed set of explicit expressions is completely free from the solution of nonlinear equations therefore a generalized set of mathematical expressions is derived in subsequent chapter.

# 5

# A Modified Relay Feedback Experiment for Identification of Time Delay Processes

Contents

With the rapid development of science and technology, relay feedback approach has emerged as an important tool for identification and autotuning of controllers in various industries. Since the last three decades, relay feedback approach has been widely implemented in on-off control systems, relay (bang-bang) servomechanisms, variable structure control, DC-DC converters, relay auto-tuners, sigma-delta modulators etc. (see [14] for more details). In real time environment, the processes under control are sensitive to external disturbances therefore, there is always a need of an accurate process model in the design of model based controllers for achieving the desired performances. Being a time efficient method, the relay feedback experiment plays a vital role in modelling and identification of industrial processes. Whenever, the controller fails to yield better response, the relay is turned on to update the model parameters and thereafter tuning parameters of controller are derived on the basis of identified process model.

Extensive works using the relay feedback technique have been reported by Majhi and Atherton [39], Wang *et al.* [31], Panda and Yu [24], Boiko [29], Liu and Gao [2] in the development of analytical expressions required for plant identification. In previous chapters, during the relay feedback test, the sustained oscillatory responses at the process output are obtained while keeping the setpoint zero. Such relay feedback methods faces difficulty during its hardware validation. To circumvent this issue, a setpoint with small amplitude is applied to bring the forced response at the process output and thereafter, a relay is turned on to yield the sustained oscillatory responses around the setpoint. Also in some industrial plants the control variables may not always permit negative relay settings. Therefore, earlier methods reported in literature suffer difficulty in the generation of sustained oscillation in the real-time level control system because of the non-negative absolute scale of physical parameter, *i.e.* the height of a liquid level column does not go below zero in real sense. Whereas, temperature and pressure may have variations from negative to positive and in real-time plants, those may show oscillations while considering negative relay settings. Using the conventional relay feedback experiment, Majhi [82] proposed the state space based analytical expressions for modelling and identification of a class of non-minimum phase processes with time delay. The important information from process output is extracted and substituted in the derived set of mathematical expressions for the identification of a class of time delay processes in terms of FOPTD and SOPTD process models with/without unstable zero. Their generalized set of nonlinear expressions are confined to an accurate estimation of two unknown parameters with an appropriate initial guess of unknown process model parameters. Thereafter, Liu

and Gao [83] studied the transfer function models considered by Majhi [82] and proposed an improved frequency domain approach for estimation of three unknown parameters of the generalized process model using a recursive least square method. However, their method is time consuming and lacks the explicit representation of each unknown parameters in the assumed transfer function models. Liu *et al.* [2] have contributed four identification algorithms using a biased and unbiased relay feedback waveforms for identification of stable/unstable FOPTD processes using frequency and time domain approaches. Out of the four algorithms, two were proposed to bring simplicity in the calculation and rest two algorithms were developed to achieve an enhanced accuracy in parameter estimation in higher order processes. Recently, Liu *et al.* [49] in their survey article, presented various process identification methods under load disturbance situations studied in literature based on relay and step tests. The authors have also explained the methodologies proposed in literature regarding the identification of multi-variable and nonlinear processes. Bajarangbali *et al.* [8] derived a nonlinear set of mathematical expressions for modelling and identification of second order time delay models using an ideal relay with hysteresis. However, the authors proposed the analytical expressions for second order processes with repeated roots through an approximation.

In this chapter, we have attempted to propose a modified relay feedback test for modelling and identification of time delay processes. While considering non-zero setpoint, a modified relay feedback experiment is conducted to induce sustained oscillations in a class of time delay processes around the setpoint. From the modified relay feedback responses, a generalized set of explicit expressions for the identification of industrial processes in terms of FOPTD models with/without zeros, SOPTD models with/without zeros is deduced. To show the robustness of the proposed identification scheme, a clean limit cycle is reconstructed using the Fourier series based curve fitting method. Finally, efficacy of the proposed relay based identification scheme and algorithms is demonstrated through Nyquist plots.

## 5.1 Proposed Identification Scheme

Figure 5.1 represents the block diagram for a modified relay feedback experiment where a biased relay is fedback to unknown plant for the generation of sustained oscillations around the setpoint. During the experiment, the process attempts to respond the user defined setpoint. After reaching the optimum value, the biased relay in the feedback loop helps the process in achieving the desired output around the user defined reference input through the generation of process responses in terms of limit

cycle as shown in Figure 5.2. The biased relay also helps in the minimization of static load disturbance and measurement noise during the identification test with the proper choice of relay amplitudes and hysteresis band. Using proposed set of mathematical expressions, attempts have been made to model the unknown plants in terms of first order plus time delay (FOPTD), first order plus time delay with zero (FOPTDZ), second order plus time delay with repeated poles (SOPTD), second order plus time delay with repeated poles and zero (SOPTDZ) models using limit cycle and its slope information. The

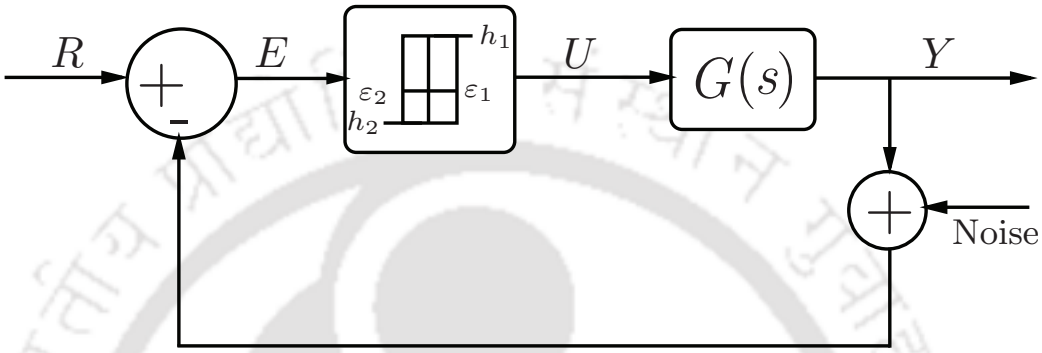


**Figure 5.1:** Proposed relay feedback experiment for process identification

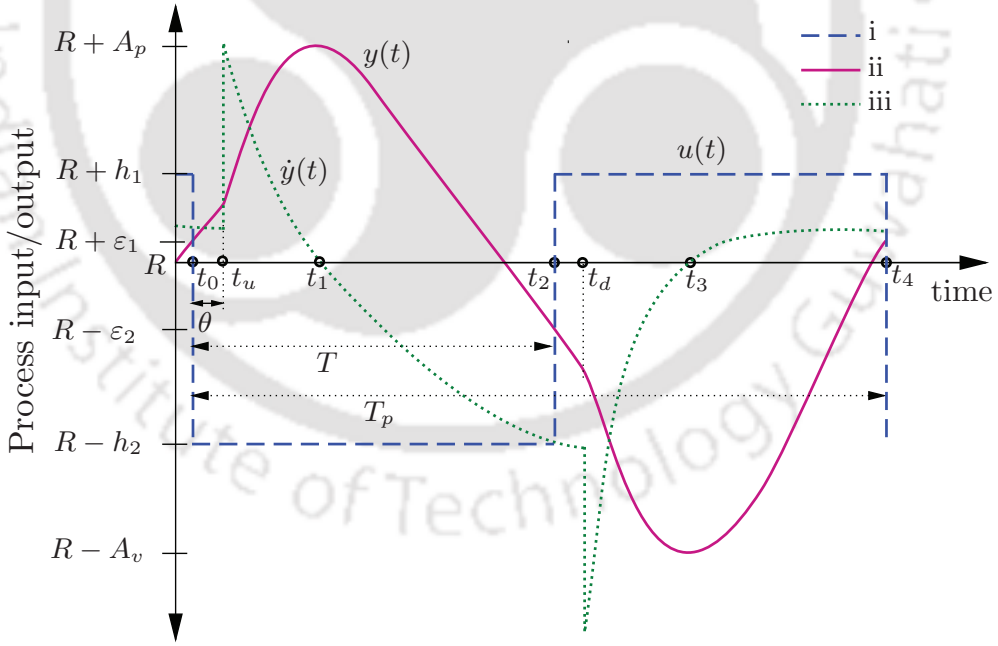


**Figure 5.2:** Plots for non-minimum phase SOPTD process: (i) relay output (ii) process output (iii) first derivative of process output

parameters $h_1$, $h_2$, $\varepsilon_1$ and $\varepsilon_2$ indicated in Figure 5.2 are relay settings as amplitudes and hysteresis width. The period for which process output remains greater than setpoint ($R$), time period, peak

amplitudes of the limit cycle, time at which upper and lower peak occurs are denoted by $t_2$, $t_4$, $A_p$, $A_v$, $t_1$ and $t_3$, respectively. The time instants at which actual switching of relay takes place is denoted by $t_0$, $t_2$ and $t_4$.

## 5.2 State Space Based Mathematical Expressions

Let the general transfer function model for a class of time delay processes with left or right half plane zero ($\vartheta = \pm 1$) be represented as

$$G_m(s) = \frac{k(\vartheta\alpha_z s + 1)e^{-\theta s}}{(\alpha_p s + 1)^n} \tag{5.1}$$

where, $k$, $\theta$, $\alpha_p$, $\alpha_z$ and $n$ are the process model parameters, respectively. Using the state space analysis, the assumed transfer function model is expressed in terms of state and output equations as

$$\begin{aligned} \dot{\boldsymbol{x}}(t) &= \boldsymbol{J}\boldsymbol{x}(t) + \boldsymbol{B}u(t-\theta) \\ y(t) &= \boldsymbol{C}\boldsymbol{x}(t) \end{aligned} \tag{5.2}$$

where $\boldsymbol{x}(t) \in \mathbb{R}^n$ is the process state vector, $u(t) \in \mathbb{R}$ represents process input, $y(t)$ defines the process output, $\boldsymbol{J} \in \mathbb{R}^{n\times n}$ denotes the system matrix, $\boldsymbol{B} \in \mathbb{R}^{n\times 1}$ is a column vector known as input distribution matrix, $\boldsymbol{C} \in \mathbb{R}^{1\times n}$ is a row vector defined as the output matrix. Now, the constant matrices and vectors associated with the state and output equations for the general transfer function model (5.1) are expressed as

$$\begin{aligned} \boldsymbol{J} &= \begin{bmatrix} \lambda_1 & 1 & 0 & \cdot & \cdot & \cdot & 0 \\ 0 & \lambda_1 & \cdot & \cdot & \cdot & \cdot & \cdot \\ 0 & \cdot & \cdot & \cdot & \cdot & \cdot & \cdot \\ \cdot & \cdot & \cdot & \cdot & \cdot & \cdot & 1 \\ 0 & \cdot & \cdot & \cdot & 0 & \lambda_1 \end{bmatrix} \quad \boldsymbol{B} = \begin{bmatrix} 0 \\ \cdot \\ \cdot \\ \cdot \\ 1 \end{bmatrix} \\ \boldsymbol{C} &= k(-\lambda_1)^n \begin{bmatrix} \left(1 + \dfrac{\lambda_1}{\lambda_2}\right) & \dfrac{1}{\lambda_2} & 0 & \cdot & \cdot & \cdot & 0 \end{bmatrix} \end{aligned} \tag{5.3}$$

where $\lambda_1 = -1/\alpha_p$ represents the eigen value of $n^{th}$ order process model and $\lambda_2 = 1/(\vartheta\alpha_z)$.

From the solution of the state space equation, the process output for time range $t_0 \leq t < \theta$ is written

around the setpoint $R$ as

$$y(t) = -\boldsymbol{CJ}^{-1}\boldsymbol{B}h_1 + \boldsymbol{CJ}^{-1}\left[\boldsymbol{I} - \boldsymbol{e}^{\boldsymbol{J}T_p}\right]^{-1}\left[\boldsymbol{I} - \boldsymbol{e}^{\boldsymbol{J}T}\right]\boldsymbol{e}^{\boldsymbol{J}(t+T_p-T-\theta)}\boldsymbol{B}(h_1+h_2) \tag{5.4}$$

Similarly, the process output for time range $\theta \leq t < (t_2+\theta)$ is written around the reference input $R$ as

$$y(t) = \boldsymbol{CJ}^{-1}\boldsymbol{B}h_2 - \boldsymbol{CJ}^{-1}\left[\boldsymbol{I} - \boldsymbol{e}^{\boldsymbol{J}T_p}\right]^{-1}\left[\boldsymbol{I} - \boldsymbol{e}^{\boldsymbol{J}(T_p-T)}\right]\boldsymbol{e}^{\boldsymbol{J}(t-\theta)}\boldsymbol{B}(h_1+h_2) \tag{5.5}$$

Finally, the expression of process output for time range $(t_2+\theta) \leq t < (t_4+\theta)$ is derived around the setpoint $R$ as

$$y(t) = -\boldsymbol{CJ}^{-1}\boldsymbol{B}h_1 + \boldsymbol{CJ}^{-1}\left[\boldsymbol{I} - \boldsymbol{e}^{\boldsymbol{J}T_p}\right]^{-1}\left[\boldsymbol{I} - \boldsymbol{e}^{\boldsymbol{J}T}\right]\boldsymbol{e}^{\boldsymbol{J}(t-T-\theta)}\boldsymbol{B}(h_1+h_2) \tag{5.6}$$

Moreover, the process output using the symmetrical relay is derived from the above expressions with the substitution of $h_1 = h_2 = h$ and $T_p = 2T$. Therefore, the process output for the time span $t_0 \leq t < \theta$ is written around the setpoint $(R)$ as

$$y(t) = -\boldsymbol{CJ}^{-1}\boldsymbol{B}h + 2\boldsymbol{CJ}^{-1}\left[\boldsymbol{I} + \boldsymbol{e}^{\boldsymbol{J}T}\right]^{-1}\boldsymbol{e}^{\boldsymbol{J}(t+T-\theta)}\boldsymbol{B}h \tag{5.7}$$

and $\theta \leq t < (t_2+\theta)$ as

$$y(t) = \boldsymbol{CJ}^{-1}\boldsymbol{B}h - 2\boldsymbol{CJ}^{-1}\left[\boldsymbol{I} + \boldsymbol{e}^{\boldsymbol{J}T}\right]^{-1}\boldsymbol{e}^{\boldsymbol{J}(t-\theta)}\boldsymbol{B}h \tag{5.8}$$

### 5.2.1 FOPTD process model

The general transfer function model for FOPTD process is represented from (5.1) with the substitution of $\alpha_z = 0$, $n = 1$ as

$$G_m(s) = \frac{ke^{-\theta s}}{\alpha_p s + 1} \tag{5.9}$$

where, $k$, $\theta$, $\alpha_p$ are the process gain, time delay and time constant, respectively.

Using the solution of the state space equation, the expression of process output is written for time range $t_0 \leq t < \theta$ as

$$y(t) = Ce^{J(t-t_0)}x(t_0) + CJ^{-1}\left(e^{J(t-\theta)} - 1\right)Bh_1 \tag{5.10}$$

Substituting the governing parameters of the FOPTD process model $J = -1/\alpha_p$, $B = k/\alpha_p$ and $C = 1$ in the first time derivative of (5.10) at $t = t_0$ and $t = t_1$, we get

$$\theta = -\alpha_p \ln\left[\frac{\dot{y}(t_1)}{\dot{y}(t_0)}\right] \tag{5.11}$$

Thus, the expression for process steady state gain ($k$) is determined from the substitution of $e^{J\theta}$ from (5.11) in the expression of peak amplitude

$$y(t_1) = \varepsilon e^{J\theta} + CJ^{-1}(e^{J\theta} - 1)Bh_1 \tag{5.12}$$

as

$$kh_1 = -\left[\frac{y(t_1)\dot{y}(t_0) - \varepsilon\dot{y}(t_1)}{\dot{y}(t_1) - \dot{y}(t_0)}\right] \tag{5.13}$$

The expression of process output for time range $t \in (t_1, t_2)$ is derived using the solution of state space equation as

$$y(t) = Ce^{J(t-t_0)}x(t_0) + CJ^{-1}[(h_1 + h_2)e^{J(t-t_1)} - h_1e^{Jt} - h_1]B \tag{5.14}$$

Now, the first time derivative of (5.14) at $t = t_2$ is written as

$$\dot{y}(t_2) = \left[-\frac{\varepsilon}{\alpha_p} + \frac{k}{\alpha_p}\left(-(h_1 + h_2)e^{-J(t_1-t_0)} + h_1\right)\right]e^{J\tau} \tag{5.15}$$

Simplifying (5.15), the explicit expression for process time constant ($\alpha_p$) of FOPTD process model is derived as

$$\alpha_p = -T\left[\ln\left(\frac{\dot{y}(t_1)\dot{y}(t_2)(kh_1 - \varepsilon)}{\dot{y}(t_0)\left(\dot{y}(t_1)(kh_1 - \varepsilon) - k(h_1 + h_2)\dot{y}(t_0)\right)}\right)\right]^{-1} \tag{5.16}$$

### 5.2.2 FOPTD process model with zero

The general transfer function model for non-minimum/minimum phase FOPTD process is represented from (5.1) with the substitution of $n = 1$ as

$$G_m(s) = \frac{k(\vartheta\alpha_z s + 1)e^{-\theta s}}{\alpha_p s + 1} \tag{5.17}$$

where, $k$, $\theta$, $\alpha_z$, $\alpha_p$ are the process model parameters, respectively.

The process output and its first time derivative can be written for a time range $\theta \leq t < (t_2 + \theta)$ after the substitution of governing parameters $J, B, C$ in (5.8) as

$$y(t) = kh\left[\frac{2(\alpha_p - \vartheta\alpha_z)}{\alpha_p\left(1 + e^{-\frac{T}{\alpha_p}}\right)}e^{-\frac{(t-\theta)}{\alpha_p}} - 1\right] \tag{5.18}$$

$$\dot{y}(t) = -kh \left[ \frac{2(\alpha_p - \vartheta\alpha_z)}{\alpha_p^2 \left(1 + e^{-\frac{T}{\alpha_p}}\right)} e^{-\frac{(t-\theta)}{\alpha_p}} \right] \tag{5.19}$$

The expressions for process output and its slope at $t = t_1$ and $t = t_2$ are written from (5.8) as

$$y(t_1) = kh \left[ \frac{2(\alpha_p - \vartheta\alpha_z)}{\alpha_p \left(1 + e^{-\frac{T}{\alpha_p}}\right)} e^{-\frac{(t_1-\theta)}{\alpha_p}} - 1 \right] \tag{5.20}$$

$$\dot{y}(t_1) = -kh \left[ \frac{2(\alpha_p - \vartheta\alpha_z)}{\alpha_p^2 \left(1 + e^{-\frac{T}{\alpha_p}}\right)} e^{-\frac{(t_1-\theta)}{\alpha_p}} \right] \tag{5.21}$$

$$\dot{y}(t_2) = -kh \left[ \frac{2(\alpha_p - \vartheta\alpha_z)}{\alpha_p^2 \left(1 + e^{-\frac{T}{\alpha_p}}\right)} e^{-\frac{(t_2-\theta)}{\alpha_p}} \right] \tag{5.22}$$

Now, the process time constant ($\alpha_p$) is derived using the expressions of $y(t_1)$, $\dot{y}(t_1)$, $\dot{y}(t_2)$ as

$$\alpha_p = \frac{y(t_1)}{\dot{y}(t_2) - \dot{y}(t_1)} \tag{5.23}$$

Similarly, the expression for steady state gain ($k$) is obtained from the simultaneous solution of $y(t_1)$, $\dot{y}(t_1)$, $\dot{y}(t_2)$ given in (5.20), (5.21), (5.22) as

$$k = \frac{y(t_1)\dot{y}(t_2)}{h(\dot{y}(t_1) - \dot{y}(t_2))} \tag{5.24}$$

The process time delay ($\theta$) is derived from the ratio of $\dot{y}(t_1)$ and $\dot{y}(t_2)$ as

$$\theta = t_2 - \alpha_p \ln \left[ \frac{\dot{y}(t_1)}{\dot{y}(t_2)} \right] \tag{5.25}$$

Finally, the remaining unknown parameter ($\alpha_z$) in FOPTDZ transfer function model is derived from the expression of $\dot{y}(t_1)$, $\dot{y}(t_2)$ as

$$\alpha_z = \frac{\alpha_p \left[ \dot{y}(t_2) - 0.5\dot{y}(t_1) \left(1 + e^{-\frac{T}{\alpha_p}}\right) \right]}{\vartheta \dot{y}(t_2)} \tag{5.26}$$

### 5.2.3 SOPTD process model with repeated poles

Similarly the second order transfer function model with repeated poles is represented as

$$G_m(s) = \frac{ke^{-\theta s}}{(\alpha_p s + 1)^2} \tag{5.27}$$

The scalar matrices for SOPTD process model with repeated poles are written as

$$\boldsymbol{J} = \begin{bmatrix} -\frac{1}{\alpha_p} & 1 \\ 0 & -\frac{1}{\alpha_p} \end{bmatrix} \quad \boldsymbol{B} = \begin{bmatrix} 0 \\ 1 \end{bmatrix} \quad \boldsymbol{C} = \frac{k}{\alpha_p^2} \begin{bmatrix} 1 & 0 \end{bmatrix}$$

Further the expressions for process output $y(t)$ and its first slope $\dot{y}(t)$ are obtained in (5.28) and (5.29) after substituting the matrices $\boldsymbol{J}, \boldsymbol{B}, \boldsymbol{C}$ in (5.5) as

$$y(t) = kh_2 \left[ \left( \frac{(t-\theta+\alpha_p)\left(1-e^{-\frac{(T_p-T)}{\alpha_p}}\right)}{\alpha_p\left(1-e^{-\frac{T_p}{\alpha_p}}\right)} - \frac{\left(T_p\left(1-e^{-\frac{T}{\alpha_p}}\right) - T\left(1-e^{-\frac{T_p}{\alpha_p}}\right)\right)e^{-\frac{(T_p-T)}{\alpha_p}}}{\alpha_p\left(1-e^{-\frac{T_p}{\alpha_p}}\right)^2} \right) \frac{(h_1+h_2)e^{-\frac{t-\theta}{\alpha_p}}}{h_2} - 1 \right] \tag{5.28}$$

$$\dot{y}(t) = k \left[ \frac{\left(1-e^{-\frac{(T_p-T)}{\alpha_p}}\right)}{\alpha_p\left(1-e^{-\frac{T_p}{\alpha_p}}\right)} - \frac{(t-\theta+\alpha_p)\left(1-e^{-\frac{(T_p-T)}{\alpha_p}}\right)}{\alpha_p^2\left(1-e^{-\frac{T_p}{\alpha_p}}\right)} + \frac{\left(T_p\left(1-e^{-\frac{T}{\alpha_p}}\right) - \tau\left(1-e^{-\frac{T_p}{\alpha_p}}\right)\right)e^{-\frac{(T_p-T)}{\alpha_p}}}{\alpha_p^2\left(1-e^{-\frac{T_p}{\alpha_p}}\right)^2} \right] (h_1+h_2)e^{-\frac{t-\theta}{\alpha_p}} \tag{5.29}$$

Firstly, the time delay ($\theta$) of SOPTD process model is measured from distance between initial relay switching instant and the abrupt change shown by second time derivative of process output as suggested by Majhi [40]. From (5.28) and (5.29), the process output and its slope at $t = \theta$ is written as

$$y(\theta) = kh_2(\gamma_1 - 1) \tag{5.30}$$

$$\dot{y}(\theta) = kh_2\left(\gamma_2 - \frac{\gamma_1}{\alpha_p}\right) \tag{5.31}$$

where

$$\gamma_1 = \frac{(h_1+h_2)}{h_2}\left[\frac{\left(1-e^{-\frac{(T_p-T)}{\alpha_p}}\right)}{\left(1-e^{-\frac{T_p}{\alpha_p}}\right)} - \frac{\left(T_p\left(1-e^{-\frac{T}{\alpha_p}}\right)-T\left(1-e^{-\frac{T_p}{\alpha_p}}\right)\right)e^{-\frac{(T_p-T)}{\alpha_p}}}{\alpha_p\left(1-e^{-\frac{T_p}{\alpha_p}}\right)^2}\right]$$

$$\gamma_2 = \left[\frac{(h_1+h_2)\left(1-e^{-\frac{(T_p-T)}{\alpha_p}}\right)}{h_2\alpha_p\left(1-e^{-\frac{T_p}{\alpha_p}}\right)}\right]$$

The expression for peak time is derived as

$$t_1 = \theta - \frac{T\mathrm{e}^{-\frac{(T_p-T)}{\alpha_p}} + \alpha_p\mathrm{e}^{-\frac{T_p}{\alpha_p}} - T\mathrm{e}^{-\frac{(2T_p-T)}{\alpha_p}} - \alpha_p\mathrm{e}^{-\frac{(T_p-T)}{\alpha_p}}}{1-\mathrm{e}^{-\frac{(T_p-T)}{\alpha_p}} - \mathrm{e}^{-\frac{T_p}{\alpha_p}} + \mathrm{e}^{-\frac{(2T_p-T)}{\alpha_p}}} \tag{5.32}$$

From the expression of peak time, the ratio of $\gamma_1$ and $\gamma_2$ is derived as $\gamma_1/\gamma_2 = (\alpha_p - t_1 + \theta)$. Now the expressions of $y(t_2)$ and $\dot{y}(t_2)$ from (5.28) and (5.29) are written in simplified form using $\gamma_1$ and $\gamma_2$ as

$$e^{-\frac{(t_2-\theta)}{\alpha_p}} = \frac{kh_2 + y(t_2)}{(\gamma_1+\gamma_2(t_2-\theta))kh_2} \tag{5.33}$$

$$\dot{y}(t_2) = (kh_2 + y(t_2))\left[\left(\frac{\gamma_2}{\gamma_1+\gamma_2(\alpha_p-\theta)}\right) - \frac{1}{\alpha_p}\right] \tag{5.34}$$

Substituting the expression of $\gamma_1$ and $\gamma_2$ *i.e.*, $(\gamma_1 = \gamma_2(\alpha_p - t_1 + \theta))$ in (5.34) which on further simplification yields the steady state gain as

$$k = \frac{\dot{y}(t_2)\,{\alpha_p}^2 - y(t_2)\,t_1 - \dot{y}(t_2)\,t_1\alpha_p + \dot{y}(t_2)\,t_2\alpha_p + y(t_2)\,t_2}{h_2(t_1-t_2)} \tag{5.35}$$

Substituting the $\gamma_1$, $\gamma_2$ and $k$ in (5.31), another explicit expression for process time constant is derived from the solution of quadratic equation $a\alpha_p^2 + b\alpha_p + c = 0$ as

$$\alpha_p = \frac{-b \pm \sqrt{b^2-4ac}}{2a} \tag{5.36}$$

where

$$a = \dot{y}(\theta)\,t_1 - \dot{y}(\theta)\,t_2 - \dot{y}(t_2)\,t_1 + \dot{y}(t_2)\,\theta$$

$$b = -\dot{y}(\theta)\,t_1^2 + \dot{y}(t_2)\,t_2\theta + \dot{y}(\theta)\,\theta t_1 + \dot{y}(t_2)\,t_1^2 + \dot{y}(\theta)\,t_1t_2 - \dot{y}(\theta)\,\theta t_2 - \dot{y}(t_2)\,t_1\theta - \dot{y}(t_2)\,t_2t_1$$

$$c = -y(\theta)\,\theta t_2 + y(t_2)\,t_2\theta + t_2t_1y(\theta) - y(t_2)\,t_2t_1 - y(t_2)\,t_1\theta + y(\theta)\,\theta t_1 - t_1^2y(\theta) + y(t_2)\,t_1^2$$

### 5.2.4 SOPTD process model with repeated poles and zero

The general transfer function model for non-minimum/minimum phase SOPTD process is represented from (5.1) with the substitution of $n = 2$ as

$$G_m(s) = \frac{k(\vartheta\alpha_z s + 1)e^{-\theta s}}{(\alpha_p s + 1)^2} \tag{5.37}$$

where, $k$, $\theta$, $\alpha_z$, $\alpha_p$ are the process model parameters, respectively.

Similar to previous case, the expressions for process output and its first time derivative after substituting $\boldsymbol{J}, \boldsymbol{B}, \boldsymbol{C}$ matrices in (5.8) for a time range $\theta \leq t < (t_2 + \theta)$ are written as

$$y(t) = kh\Bigg[2\Bigg(\frac{(\alpha_p - \vartheta\alpha_z)(t-\theta) + \alpha_p^2}{\alpha_p^2\left(1 + e^{-\frac{T}{\alpha_p}}\right)} - \frac{T(\alpha_p - \vartheta\alpha_z)e^{-\frac{T}{\alpha_p}}}{\alpha_p^2\left(1 + e^{-\frac{T}{\alpha_p}}\right)^2}\Bigg)e^{-\frac{t-\theta}{\alpha_p}} - 1\Bigg] \tag{5.38}$$

$$\dot{y}(t) = kh\Bigg[\frac{2(\alpha_p - \vartheta\alpha_z)}{\alpha_p^2\left(1 + e^{-\frac{T}{\alpha_p}}\right)} + \frac{2}{\alpha_p}\Bigg(\frac{T\left(\alpha_p - \vartheta\alpha_z\right)e^{-\frac{T}{\alpha_p}}}{\alpha_p^2\left(1 + e^{-\frac{T}{\alpha_p}}\right)^2} - \frac{(\alpha_p - \vartheta\alpha_z)(t-\theta) + \alpha_p^2}{\alpha_p^2\left(1 + e^{-\frac{T}{\alpha_p}}\right)}\Bigg)\Bigg]e^{-\frac{t-\theta}{\alpha_p}} \tag{5.39}$$

where $t_1$ is the peak time and $t_2 = T$ denotes the period for which limit cycle amplitude remains greater than setpoint value ($R$). The two unknown parameters ($\alpha_z$, $\alpha_p$) of SOPTDZ process model are derived from the expressions of $y(\theta)$, $\dot{y}(\theta)$, $\dot{y}(t_2)$. Finally, the steady state gain ($k$) of SOPTD process model with repeated poles and zero is calculated using the integral method as

$$k = \frac{\int_0^T y(t)dt}{\int_0^T u(t)dt} \tag{5.40}$$

Utilizing (5.38) and (5.39), the process output and its slope at $t = t_u$ is written as

$$y(t_u) = kh\underbrace{\Bigg[\frac{2}{\left(1 + e^{-\frac{T}{\alpha_p}}\right)} - \frac{2T(\alpha_p - \vartheta\alpha_z)e^{-\frac{T}{\alpha_p}}}{\alpha_p^2\left(1 + e^{-\frac{T}{\alpha_p}}\right)^2} - 1\Bigg]}_{\beta_1} \tag{5.41}$$

$$\dot{y}(t_u) = kh\Bigg[\underbrace{\frac{2(\alpha_p - \vartheta\alpha_z)}{\alpha_p^2\left(1+e^{-\frac{T}{\alpha_p}}\right)}}_{\beta_2} - \frac{\beta_1}{\alpha_p}\Bigg] \tag{5.42}$$

where $\beta_1$ is derived from (5.41) as $\beta_1 = \dfrac{kh + y(t_u)}{kh}$. Now the expressions of $y(t_2)$ and $\dot{y}(t_2)$ from (5.38) and (5.39) are simplified in terms of $\beta_1$ and $\beta_2$ as

$$e^{-\frac{(T-\theta)}{\alpha_p}} = \frac{1}{\beta_1 + \beta_2(T-\theta)} \tag{5.43}$$

$$\dot{y}(t_2) = kh\left[\left(\frac{\beta_2}{\beta_1 + \beta_2(T-\theta)}\right) - \frac{1}{\alpha_p}\right] \tag{5.44}$$

Substituting the expression of $\alpha_p$ from (5.42) in (5.44) to yield a simplified expression of $\dot{y}(t_2)$ as

$$\dot{y}(t_2) = kh\left[\frac{\beta_2}{\beta_1 + \beta_2(T-\theta)} - \frac{\beta_2}{\beta_1} + \frac{\dot{y}(t_u)}{kh\beta_1}\right] \tag{5.45}$$

Simplifying (5.45), a quadratic equation in terms of $\xi$ is obtained as

$$\xi^2 + \beta_3\xi + \frac{\beta_3}{(T-t_u)} = 0 \tag{5.46}$$

which on further simplification yields the roots of $\xi$ as

$$\xi = \frac{1}{2}\left[-\beta_3 \pm \sqrt{\beta_3^2 - \frac{4\beta_3}{T-t_u}}\right] \tag{5.47}$$

where $\xi = \dfrac{\beta_2}{\beta_1}$, $\beta_3 = \dfrac{kh[\dot{y}(t_2) - \dot{y}(\theta)] + \dot{y}(t_2)y(\theta)}{kh[kh + y(\theta)]}$.

The explicit representation of one of the unknown parameter ($\alpha_p$) of SOPTDZ process model is derived from the expression of $\beta_1$ as

$$\frac{2}{\left(1+e^{-\frac{T}{\alpha_p}}\right)} - \beta_1 = \frac{2T(\alpha_p - \vartheta\alpha_z)e^{-\frac{T}{\alpha_p}}}{\alpha_p^2\left(1+e^{-\frac{T}{\alpha_p}}\right)^2} \tag{5.48}$$

$$\frac{2 - \beta_1\left(1+e^{-\frac{T}{\alpha_p}}\right)}{Te^{-\frac{T}{\alpha_p}}} = \frac{2(\alpha_p - \vartheta\alpha_z)}{\alpha_p^2\left(1+e^{-\frac{T}{\alpha_p}}\right)} = \beta_1\xi \tag{5.49}$$

$$\Longrightarrow \alpha_p = -\frac{T}{\ln\left[\frac{2-\beta_1}{\beta_1(1+T\xi)}\right]} \tag{5.50}$$

Now the explicit expression for $\alpha_z$ can be derived from the expression of $\beta_2$ given in (5.42) as,

$$\frac{2(\alpha_p - \vartheta\alpha_z)}{\alpha_p^2\left(1+e^{-\frac{T}{\alpha_p}}\right)} = \beta_2 = \beta_1\xi \tag{5.51}$$

$$\Longrightarrow \alpha_z = \frac{2\alpha_p - \beta_1\xi\alpha_p^2\left(1+e^{-\frac{T}{\alpha_p}}\right)}{2\vartheta} \tag{5.52}$$

Moreover, the expression for $\alpha_z$ can also be obtained for SOPTDZ process model using the peak time of process output as

$$\vartheta\,\alpha_z = \frac{\alpha_p\left(Te^{-\frac{T}{\alpha_p}} - (t_1-\theta)\left(1+e^{-\frac{T}{\alpha_p}}\right)\right)}{Te^{-\frac{T}{\alpha_p}} - (t_1-\theta-\alpha_p)\left(1+e^{-\frac{T}{\alpha_p}}\right)} \tag{5.53}$$

**Remark 5.1** *Due to consideration of setpoint (R) and modified relay settings, the necessary condition for existence of limit cycle depend on lower and upper bounds of relay amplitudes and setpoint values. For a step signal with* 0% *to* 100% *as input signal range, the upper half of limit cycle (or repsonse greater than R) is obtained when* $kh_1 > R$ *and vice-versa for lower half of limit cycle i.e.* $kh_2 < R$*. Therefore the lower and upper bounds for a relay block with* 0% *to* 100% *amplitude range in terms of process gain and setpoint is written as* $(h_2 < R/k < h_1)$*. For existence of sustained oscillations/limit cycle, this condition has to be satisfied by the assumed transfer function models (5.1) under the proposed relay feedback scheme.*

## 5.3 Results and Discussion

From literature, four examples are illustrated to validate the proposed relay feedback experiment for parameter estimation of a class of time delay processes using the derived set of mathematical expressions. The symmetrical and asymmetrical relays with or without hysteresis band are utilized for the identification of various time delay processes. The process identification using the proposed relay based identification scheme can be erroneous while taking into account of measurement errors induced due to presence of noisy sensors at the process output. Therefore, the actual process output and its first time derivative are recovered from Fourier series based curve fitting method.

### 5.3.1 Example 1: FOPTD process

Consider a stable FOPTD process studied in literature by Vijayan and Panda [6], Jeng *et al.* [5] as $G_1(s) = \dfrac{e^{-1.5s}}{s+1}$. During identification, an asymmetrical relay with hysteresis ($\varepsilon = \pm 0.55$) yields a biased limit cycle at the process output around the setpoint $R = 2$. The process output and its slope information are extracted as $\dot{y}(t_1) = 1.6768$, $t_2 = 3.2842$, $y(t_2) = -0.55$, $\dot{y}(t_0) = 1.4508$, $\dot{y}(t_1) = 0.3234$ and $\dot{y}(t_2) = -0.4502$. Substituting the measured information in explicit expressions (5.11), (5.13) and (5.16), three unknown parameters of FOPTD process model are obtained. Thereafter, the parametric error between actual process and identified models using proposed method is elaborated in Table 5.1. The robustness of proposed identification technique towards noise is demonstrated by considering additive white Gaussian noise with 10% and 20% NSR at the process output. Further, utilizing the Fourier series based curve fitting method, a clean process output is retrieved. Finally, the yielded limit cycle information is substituted in the derived set of mathematical expressions for estimation of unknown process model parameters.

**Table 5.1:** Comparison of identified process models for Example 1

| NSR % | $k$ | $\alpha_1$ | $\theta$ | IAE |
|---|---|---|---|---|
| 0 | 1.0000 | 0.9999 | 1.5008 | 0.0004 |
| 10 | 1.0394 | 1.1003 | 1.4509 | 0.0253 |
| 20 | 1.0452 | 1.0606 | 1.4830 | 0.0370 |

### 5.3.2 Example 2: SOPTD process with repeated poles

Let us consider the SOPTD process with repeated poles studied in literature by Vivek and Chidambaram [10] as $G_2(s) = \dfrac{e^{-0.5s}}{(20s+1)^2}$. During identification, a biased relay with amplitudes ($h_1 = 4$, $h_2 = 1$, $\varepsilon = \pm 0.3$) is fedback to bring the sustained oscillations around the setpoint ($R = 2$). Measurements made on a relay test yield the limit cycle information as $t_1 = 8.8184$, $T = 43.5285$, $y(t_1) = 0.3216$, $\dot{y}(t_1) = -0.30$, $\dot{y}(t_2) = -0.0223$, respectively. The process time delay is measured as $\theta = 0.5005$ and the remaining two unknown parameters are derived after substituting the measured limit cycle information in (5.35) and (5.36) as $\alpha_p = 20.0013$ and $k = 0.9938$. Furthermore, the parameters calculated using describing function method are $k = 1.0$, $\alpha_p = 20.4803$ and $\theta = 0.5813$. Using curve fitting method, a clean limit cycle data and its slope are recovered as shown in Figure 5.3 and Figure 5.4. Further the recovered limit cycle information is substituted in the derived set of

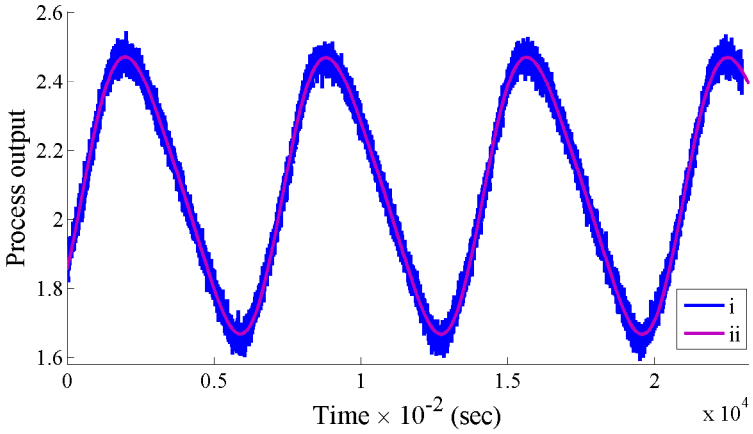


**Figure 5.3:** Plots for Example 2: (i) noisy data (ii) fitted data

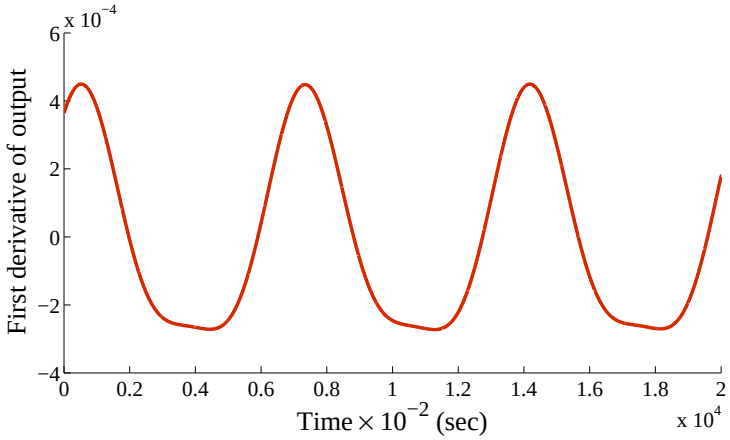


**Figure 5.4:** First derivative of reconstructed limit cycle data for Example 2

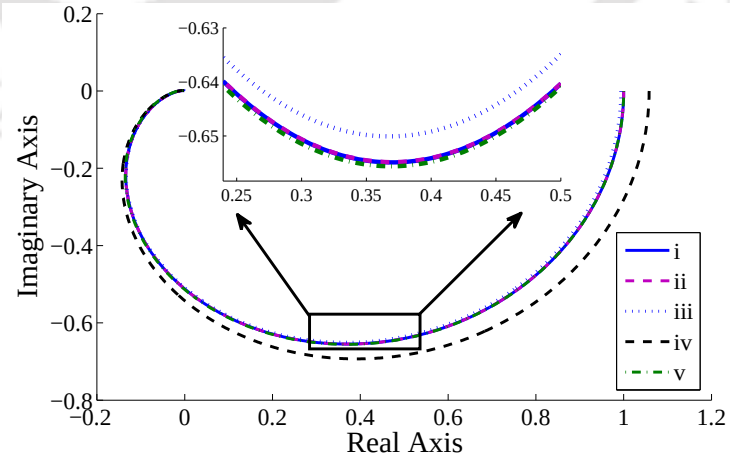


**Figure 5.5:** Nyquist plots for Example 2: (i) actual process (ii) proposed model without noise (iii) proposed model with noise (SNR = 20dB) (iv) model proposed by Vivek and Chidambaram [10] without noise (v) proposed model by DF method without noise

mathematical expressions for the estimation of SOPTD process model parameters as shown in Table 5.2. Finally, the identification error between the proposed models and the models suggested in literature are compared through Nyquist plots in Figure 5.5.

**Table 5.2:** Comparison of identified process models for Example 2

| Methods | Identified models | IAE |
|---|---|---|
| Proposed SOPTD model without noise | $\frac{0.9938e^{-0.5005s}}{(20.0013s+1)^2}$ | 0.0005 |
| Proposed SOPTD model with 20dB noise | $\frac{0.9932e^{-0.4718s}}{(20.2210s+1)^2}$ | 0.0108 |
| Model by Vivek and Chidambaram [10] without noise | $\frac{1.058e^{-0.551s}}{(20.81s+1)^2}$ | 0.0158 |
| Model by DF method without noise | $\frac{1.0e^{-0.5813s}}{(20.4803s+1)^2}$ | 0.0209 |

### 5.3.3 Example 3: Non-minimum phase FOPTD process

Consider a non-minimum phase stable FOPTD process as $G_3(s) = \frac{(-s+1)e^{-s}}{2s+1}$. An ideal relay ($h = 2$) is fedback to above process for the generation of limit cycle around the setpoint ($R = 1$). From the limit cycle information, the measured parameters $y(t_1) = 1.3930$, $\dot{y}(t_1) = -1.1962$, $\dot{y}(t_2) = -0.5001$, $T = 2.7460$ are substituted in (5.23), (5.24), (5.25) and (5.26) to evaluate all the four unknown parameters ($k$, $\alpha_z$, $\alpha_p$, $\theta$) of non-minimum phase stable FOPTD process model as (1.0007, 0.9989, 2.0011, 1.0008). While, those obtained using describing function method are (1.0, 1.4550, 1.2817, 1.0), respectively. Thereafter, the measurement noise with SNR = 20dB is added at the process output to study the robustness of the proposed method. Thereafter, a fitted limit cycle

**Table 5.3:** Comparison of identified process models for Example 3

| Methods | Identified models | IAE |
|---|---|---|
| Proposed FOPTDZ model without noise | $\frac{1.0007(-0.9989s+1)e^{-1.0008s}}{(2.0011s+1)}$ | 0.0005 |
| Proposed FOPTDZ model with 20dB noise | $\frac{1.0251(-0.9821s+1)e^{-1.0812s}}{(2.0402s+1)}$ | 0.0591 |
| Model by DF method without noise | $\frac{1.0(-1.4550s+1)e^{-1.0s}}{(1.2817s+1)}$ | 0.2889 |

information is substituted in the derived set of analytical expressions for the estimation of unknown

process model parameters. Finally, the comparisons between estimated and true process dynamics is tabulated in Table 5.3 which illustrates that the proposed model obtained through explicit expressions has better accuracy compared to describing function method.

### 5.3.4 Example 4: Higher order process

Consider a higher order process studied by Liu and Gao [83] as $G_4(s) = \dfrac{1}{(s+1)^5}$. During relay based identification test, a symmetrical limit cycle is yielded at the process output around the setpoint ($R = 1$) using relay settings ($h = 2$). The limit cycle parameters from a relay feedback test are measured as $\theta = 1.7320$, $t_1 = 2.1322$, $T = 4.3389$, $y(t_p) = 0.4495$, $\dot{y}(t_1) = 0.101$ and $\dot{y}(t_2) = -0.47$, respectively. One of the crucial parameter of non-minimum phase SOPTD process model *i.e.,* steady state gain $k = 1.0$ is obtained from (5.40) and time delay ($\theta$) from the process output waveform. Thereafter, the two unknown process model parameters of SOPTDZ process ($\alpha_p$, $\alpha_z$) are derived after the substitution of limit cycle information in (5.50), (5.52) or (5.53) as (1.7973, 0.6782). Again, the two unknown process model parameters of SOPTD process with repeated poles ($\alpha_p$, $k$) are estimated from (5.35), (5.36) as (1.7973, 1.0062), respectively. The parametric error in estimated process model parameters due to presence of measurement noise is derived using integral of squared error (ISE) criterion followed by comparisons between estimated models and actual process dynamics in Table 5.4.

**Table 5.4:** Comparison of identified process models for Example 4

| Methods | Identified models | ISE |
|---|---|---|
| Proposed SOPTDZ model without noise | $\dfrac{1.0(-0.6782s+1)e^{-1.2836s}}{(1.7973s+1)^2}$ | 0.0037 |
| Proposed SOPTDZ model with noise | $\dfrac{1.0(-0.6512s+1)e^{-1.7836s}}{(1.7783s+1)^2}$ | 0.0214 |
| Proposed SOPTD model without noise | $\dfrac{1.0062e^{-1.7320s}}{(1.7973s+1)^2}$ | 0.0008 |
| Proposed SOPTD model with noise | $\dfrac{1.0e^{-1.8361s}}{(1.7783s+1)^2}$ | 0.0013 |
| Model by Liu and Gao [83] without noise | $\dfrac{1.0076e^{-1.7557s}}{(1.8174s+1)^2}$ | 0.0011 |
| Model by DF method without noise | $\dfrac{1.0e^{-1.75803s}}{(1.8703s+1)^2}$ | 0.0024 |

## 5.4 Summary

In this chapter, a modified relay feedback experiment is proposed for the generation of sustained oscillatory responses in a class of time delay processes. Using the state space approach, a generalized set of explicit expressions for modelling and identification of a class of time delay processes is derived in terms of relay settings and limit cycle information. The proposed set of explicit expressions is completely free from the simultaneous solution of nonlinear equations. When the process output is subjected to measurement noise, a Fourier series based curve fitting method yields a clean limit cycle information which is further substituted in the derived set of mathematical expressions for estimation of process model parameters in presence of measurement noise. Extensive simulation results are included to show the validation of proposed identification scheme and its superiority over the other relevant methods reported in literature. Finally, to show the practical validation of the proposed relay feedback scheme and the derived set of mathematical expressions, the experimental set-ups of level control system, coupled tanks system are considered in subsequent chapter.

# 6

# Experimental Case Studies


Contents

## 6.1 Applications to Level Control System

In this section, a liquid level control system by YOKOGAWA is considered as an industrial plant. Using the important information yielded during the relay feedback experiment, the liquid level control system is modelled in terms of various time delay transfer function models. The physical description, working, identification and model validation of level control system are discussed in subsequent subsections.

### 6.1.1 Physical description and working

The experimental set-up of level control system comprises of an overhead storage tank having one inlet pneumatic control valve from reservoir to tank through pump and two outlet valves, known as manual valve (MV) and outlet valve (OV) which is another pneumatic control valve as shown in Figure 6.1. Both the pneumatic control valves are used to control the storage tank water level, controlled by a field control station (FCS), while manual valve helps in supplying water for continuous consumption as shown in Figure 6.2. Out of the remaining two outlets, one of a manual control valve is needed to discharge the liquid with a constant flow rate and another control valve is kept in fully closed position throughout the period of identification. FCS with YOKOGAWA [84] is considered for both controller and relay operation. The high speed data communication link between FCS and engineering station as well as with human interface station (HIS) is provided by VLnet. For continuous consumption of water, storage tank needs to maintain a minimum height of water level. During identification, the relay acts as a controller and maintain the level of the storage tank through sequential opening and closing of control valve. This operation yields the sustained oscillations/limit cycle at the plant output around the user defined setpoint value as shown in Figure 6.3.

### 6.1.2 Identification tests and model validation

In process control, the level control system is typically modelled in terms of first order transfer function form as

$$\dot{h}^l(t) = \frac{1}{A_l}(q_{in} - q_{out}) \tag{6.1}$$

where the tank parameters $h^l$, $q_{in}$, $q_{out}$, $A_l$ represents the liquid level, controlled flow, outflow and cross-sectional area. Due to presence of nonlinearity in control valve, the overall dynamics of level control system is linearized and further modelled in terms of second order process transfer function

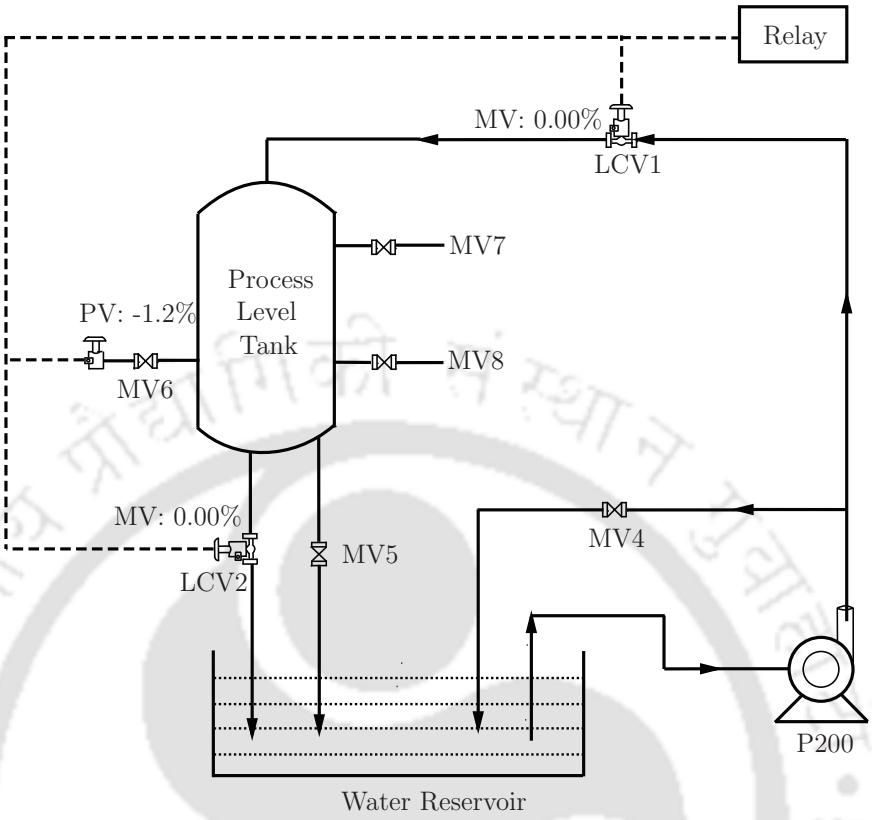


**Figure 6.1:** Physical layout of YOKOGAWA level control system

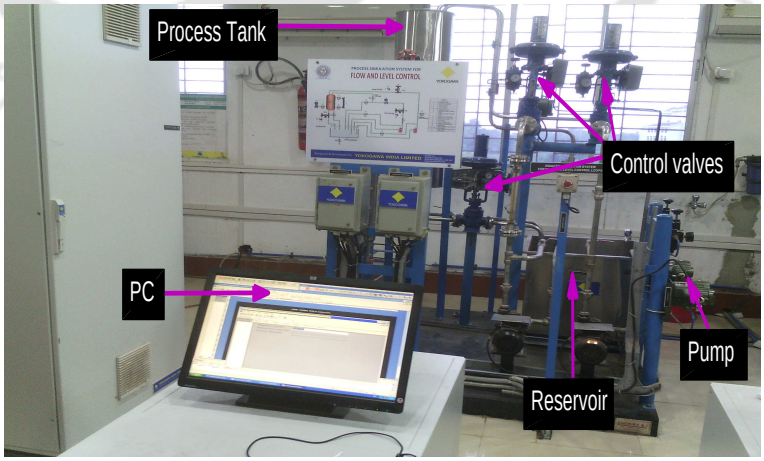


**Figure 6.2:** Experimental set-up of YOKOGAWA level control system

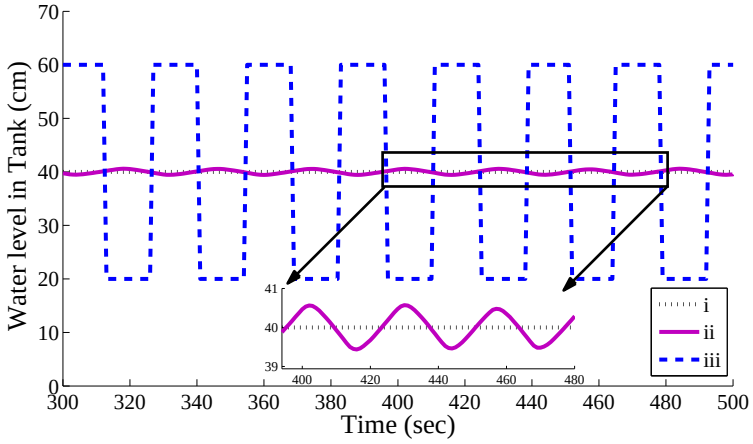


**Figure 6.3:** Plots for level control system responses: (i) setpoint $R = 40\%$ (ii) plant output (iii) relay output

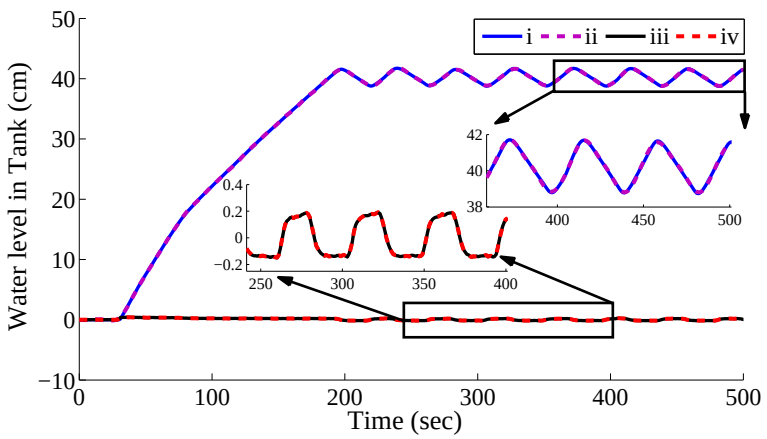


**Figure 6.4:** Plots for recovery of level control system responses: (i) plant output (ii) recovered plant output (iii) first derivative of plant output (iv) first derivative of recovered plant output

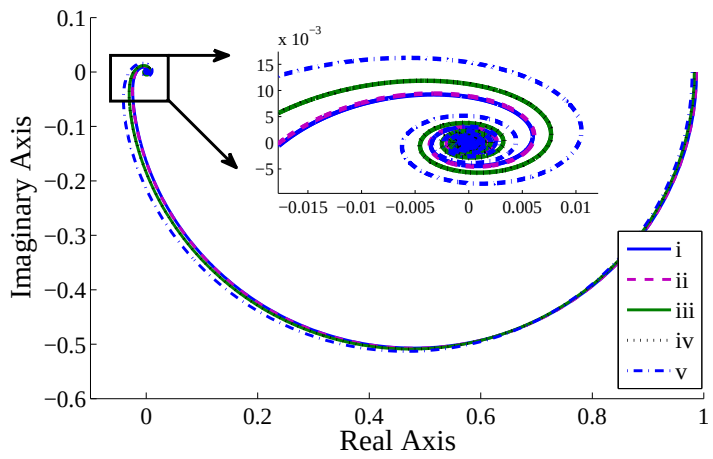


**Figure 6.5:** Nyquist plots for level control system: (i) proposed FOPTD model by SS method (ii) proposed FOPTDZ model by SS method (iii) proposed FOPTD model by FD method (iv) proposed FOPTDZ model by FD method (v) FOPTD model by ZN method

**Table 6.1:** Comparison of the identified process models for level control system

| Methods | Identified models |
|---|---|
| Proposed FOPTD model by SS method | $\frac{0.9870e^{-6.9695s}}{(249.5575s+1)}$ |
| Proposed FOPTDZ model by SS method | $\frac{0.9870(-0.12859s+1)e^{-6.9695s}}{(249.5575s+1)}$ |
| FOPTD model by FD method | $\frac{0.9830e^{-7.3773s}}{(204.8544s+1)}$ |
| FOPTDZ model by FD method | $\frac{0.9830(-0.1773s+1)e^{-7.2000s}}{(205.0056s+1)}$ |
| FOPTD model by Ziegler Nichols (ZN) Method | $\frac{0.9790e^{-8.4127s}}{(169.6874s+1)}$ |
| Proposed SOPTDZ model by SS method | $\frac{0.9830(-0.1773s+1)e^{-4.0726s}}{(30.5645s+1)^2}$ |
| Proposed Non-minimum phase SOPTD model by SS method | $\frac{1.0(-3.0041s+1)e^{-7.2840s}}{2238.5519s^2+234.1679s+1}$ |
| SOPTDZ model by FD method | $\frac{0.9830(-0.0424s+1)e^{-1.3800s}}{(30.1911s+1)^2}$ |

models. For identification, symmetrical relay with hysteresis band ($h_1 = 60$, $h_2 = 20$ and $\varepsilon = \pm 0.5$) and asymmetrical relay with hysteresis width ($h_1 = 75$, $h_2 = 15$ and $\varepsilon = \pm 0.5$) are fedback to level control system to induce sustained oscillations around a setpoint $R = 40\%$ which can be observed from Figure 6.3, Figure 6.4. Using the Fourier series based curve fitting method, a clean limit cycle is recovered as shown in Figure 6.4. After few cycles, limit cycle information is obtained from symmetrical relay test as $T_p = 21.2510$, $y(t_1) = 0.4442$, $\dot{y}(t_0) = 0.0737$, $\dot{y}(t_1) = 0.0715$, $\dot{y}(t_2) = -0.0922$ and substituted in the derived set of mathematical expressions which yields the FOPTD process model parameters as $k = 0.9870$, $\alpha_1 = 249.5575$ and $\theta = 6.9695$, respectively. Similarly the measurements from the asymmetrical oscillations are collected in the form of process output and its slope information as $T = 23.0042$, $y(t_1) = 1.709$, $\dot{y}(t_0) = 0.1821$, $\dot{y}(t_1) = 0.1754$ and $\dot{y}(t_2) = -0.132$. Thereafter, the frequency domain (FD) and state space (SS) based mathematical expressions derived in previous Chapters 2-5 are utilized for modelling and identification of level control system in terms of FOPTD, SOPTD and non-minimum phase transfer function models. Finally, the comparison between the identified plant models with the models deduced using the well known methods reported in literature are tabulated in Table 6.1. The ultimate frequency of identified process model lies close to operating point in Figure 6.5 as compared to ZN method.

## 6.2 Applications to Coupled Tanks System

In this section, the relay based identification schemes discussed in Chapters 2-5 are utilized for frequency domain and state space based modelling and identification of coupled tanks system by FEEDBACK Instruments [85]. The physical description, working, identification tests and validation of coupled tanks system are well elaborated in subsequent subsections.

### 6.2.1 Physical description and working

Figure 6.6, Figure 6.7 represent the block diagrams of proposed relay feedback experiments for the identification of single tank (Tank 1) and two coupled tanks (Tank 2). The experimental set-up of coupled tanks system by FEEDBACK Instruments consists of four tanks placed on two parallel facing structure with a fifth reservoir tank at the bottom as shown in Figure 6.8. The two submersible pumps are placed in the reservoir which pump the water as per the demand of each tanks. The water flows through the experimental set-up is configured using the manual valves (MVA, MVB, MV1, MV2....). These valves helps in realization of dynamic coupling effects during the analysis of multivariable systems. Furthermore, the coupled tanks system is equipped with Power Supply Unit

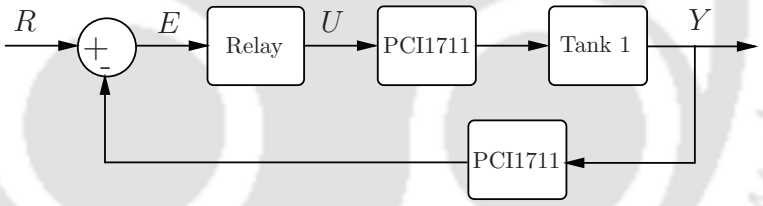


**Figure 6.6:** Block diagram representation of relay feedback experiment for Tank 1

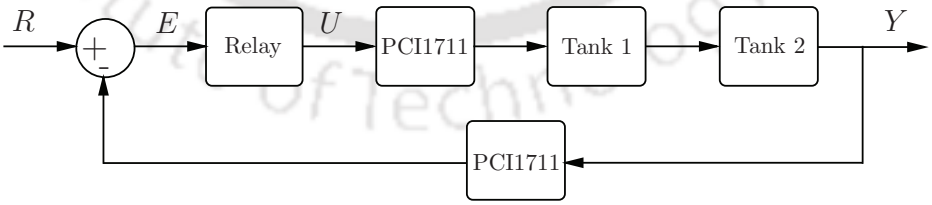


**Figure 6.7:** Block diagram representation of relay feedback experiment for Tank 2

and Power Amplifier (PSUPA), the Cable Connecter Box. The PSUPA units helps in the amplification of pressure sensor signals with respect to water level and forwarded to PCI1711 Digital to Analog (DAC) card for generation of effective output in response to coupled tanks system. Moreover, the

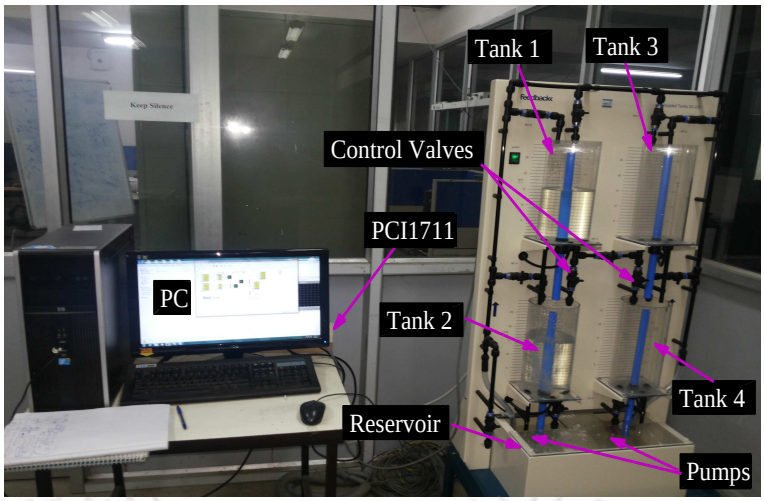


**Figure 6.8:** Experimental set-up of coupled tanks system by FEEDBACK Instruments

physical specifications of coupled tanks system are given from [85] as

- Cross-sectional area of tanks $(A) = 0.1389m^2$.
- Tank outlet area $(a_{i=1,..4}) = 5.027 \times 10^{-5}m^2$.
- Pump control voltage constant $\eta = 0.0024m^3/V.s$.

Now the physical modelling of single and two coupled tanks model is carried out using the mass balance equation. Therefore, a nonlinear model for coupled tanks system is described in [85] as

$$\frac{dh_1^l}{dt} = -\frac{a_1}{A}\sqrt{2gh_1^l(t)} + \eta u(t) \tag{6.2}$$

$$\frac{dh_2^l}{dt} = \frac{a_1}{A}\sqrt{2gh_1^l(t)} - \frac{a_2}{A}\sqrt{2gh_2^l(t)} \tag{6.3}$$

where the water level in each tanks 1 and 2 is represented as $h_1^l, h_2^l$, the outlet areas of each tanks is denoted as $a_1, a_2$, cross-sectional area of the tanks is represented as $A$, gravitational constant is denoted by $g$, the constant relating the control voltage with water flow from the pump is represented by $\eta$. Using linearisation, the nonlinear models for single and two tanks of coupled tanks system are represented in linear transfer function form. Considering the initial working points, expressions for water levels in each tanks are written as

$$\frac{a_1}{A}\sqrt{2gh_{1i}^l} = \eta u_i(t) \tag{6.4}$$

Further on simplification, the expressions for initial conditions are represented as

$$h_{1i}^{l} = \frac{1}{2g}\left(\frac{\eta u_0 A}{a_1}\right)^2 \tag{6.5}$$

$$\frac{a_1}{A}\sqrt{2gh_{1i}^{l}} = \frac{a_2}{A}\sqrt{2gh_{2i}^{l}} \tag{6.6}$$

$$h_{2i}^{l} = h_{1i}^{l}\left(\frac{a_1}{a_2}\right)^2 \tag{6.7}$$

From linearisation, we get

$$\frac{d\Delta h_1^l(t)}{dt} = \frac{d}{dh_1^l}\left(-\frac{a_1}{A}\sqrt{2gh_1^l(t)}\right)\Delta h_1^l(t) + \eta\Delta u(t) \tag{6.8}$$

$$\frac{d\Delta h_2^l(t)}{dt} = \frac{d}{dh_1^l}\left(\frac{a_1}{A}\sqrt{2gh_1^l(t)}\right)\Delta h_1^l(t) + \frac{d}{dh_2^l}\left(-\frac{a_2}{A}\sqrt{2gh_2^l(t)}\right)\Delta h_2^l(t) \tag{6.9}$$

Substituting the initial conditions of water levels in each tanks in above expressions, the single and two coupled tanks are represented in first and second order models, respectively. The resulted transfer function models are written as

$$\frac{H_1^l(s)}{U(s)} = \frac{\eta}{s + \left(\frac{a_1}{A}\right)^2 \frac{g}{\eta u_0}} \tag{6.10}$$

$$\frac{H_2^l(s)}{H_1^l(s)} = \frac{\left(\frac{a_1}{A}\right)^2 \frac{g}{\eta u_0}}{s + \left(\frac{a_2}{A}\right)^2 \frac{g}{\eta u_0}} \tag{6.11}$$

$$\frac{H_2^l(s)}{U(s)} = \frac{\left(\frac{a_1}{A}\right)^2 \frac{g}{u_0}}{\left(s + \left(\frac{a_2}{A}\right)^2 \frac{g}{\eta u_0}\right)\left(s + \left(\frac{a_1}{A}\right)^2 \frac{g}{\eta u_0}\right)} \tag{6.12}$$

### 6.2.2 Identification tests and model validation

A relay is connected to coupled tanks system through a negative feedback using the MATLAB/SIMULINK environment. During the relay based identification experiment, an asymmetrical relay with amplitudes ($h_1 = 25, h_2 = -15$), asymmetrical relay with hysteresis band ($h_1 = 25, h_2 = -15, \varepsilon = \pm 0.5$) are fedback to Tank 1 and Tank 2 of coupled tanks system for the generation of sustained oscillations around the setpoint $R = 10$ which can be seen from Figure 6.9 and Figure 6.12.

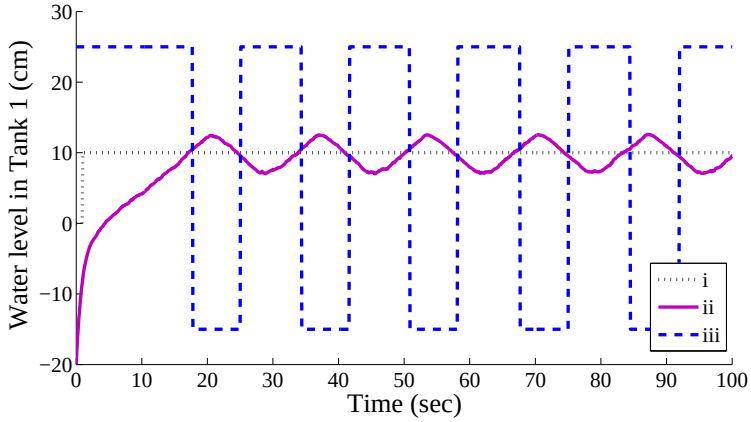


**Figure 6.9:** Plots for coupled tanks system responses: (i) setpoint (ii) Tank 1 output (iii) relay output

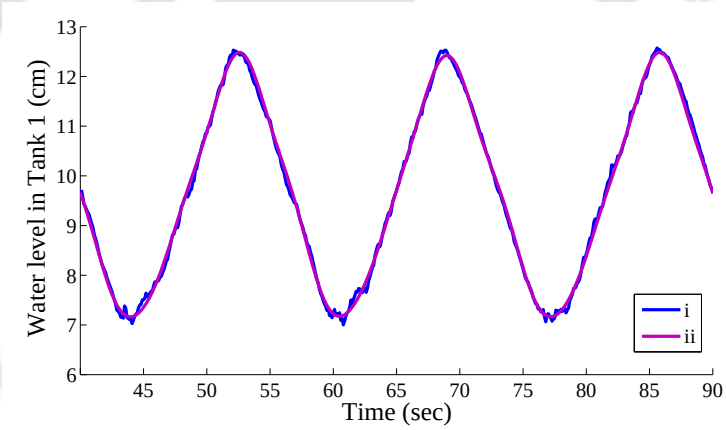


**Figure 6.10:** Plots for recovery of coupled tanks system responses using curve fitting method (i) Tank 1 output (ii) recovered Tank 1 output

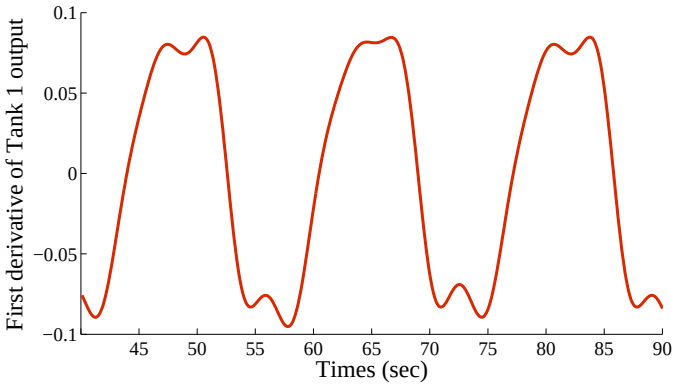


**Figure 6.11:** First derivative of recovered Tank 1 output of coupled tanks system

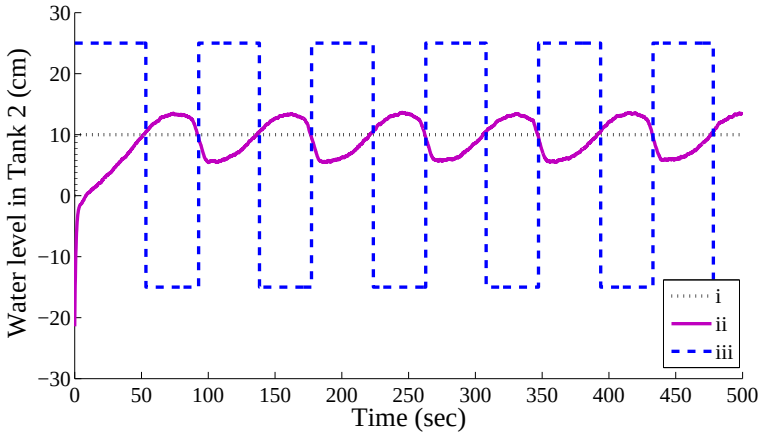


**Figure 6.12:** Plots for coupled tanks system responses: (i) setpoint (ii) Tank 2 output (iii) relay output

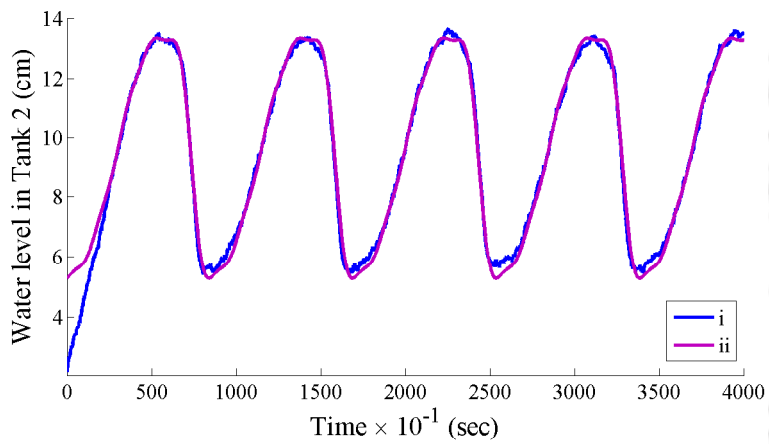


**Figure 6.13:** Plots for recovery of coupled tanks system responses using curve fitting method: (i) Tank 2 output (ii) recovered Tank 2 output

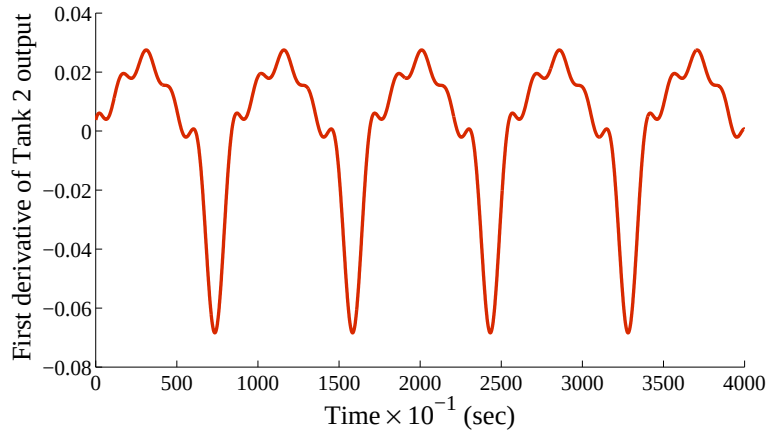


**Figure 6.14:** First derivative of recovered Tank 2 output of coupled tanks system

Further, the clean limit cycle data and its derivative are recovered using the curve fitting method as shown in Figure 6.10, Figure 6.11, Figure 6.13 and Figure 6.14. The fitted limit cycle information for Tank 1 is measured as $y(t_1) = 2.4826$, $t_1 = 3.6095$, $T = 7.4831$, $T_p = 16.4961$, $y(t_3) = 2.8276$ and for Tank 2 is $y(t_1) = 3.3359$, $t_1 = 21.5905$, $T = 40.6963$, $T_p = 84.9053$, $y(t_3) = 6.8805$. Using the frequency domain based identification algorithm, the yielded limit cycle information is substituted in the derived set of mathematical expressions for modelling and identification of single and two coupled tanks systems in terms of first and second order time delay models. Due to involvement of approximation in relay gain, the identified model may exhibit erroneous process model parameters. Therefore, the limit cycle information is further substituted in the state space based explicit expressions for the estimation of accurate process model parameters for each tanks of coupled tanks system. Finally, the comparison between the identified process models using the state space approach and frequency domain based identification algorithms are drawn in Table 6.2.

**Table 6.2:** Comparison of identified process models for Tank 1 and Tank 2 of coupled tanks system

| **Methods** | $k$ | $\alpha_1$ | $\sqrt{\alpha_2}$ | $\theta$ |
|---|---|---|---|---|
| Proposed FOPTD | 3.0666 | 67.5890 | - | 3.2978 |
| Proposed SOPTD | 4.0260 | - | 95.2572 | 4.5210 |
| DF Method FOPTD | 3.0666 | 72.2800 | - | 3.6971 |
| DF Method SOPTD | 4.0260 | - | 91.1206 | 4.3050 |

## 6.3 Summary

In this chapter, attempts have been made to validate the proposed identification algorithms on two well known process control applications. Therefore, the relay feedback configurations discussed in previous Chapters 2-5 are utilized for the generation of sustained oscillatory responses in the experimental set-ups of level control system and coupled tanks system. Using the Fourier series based curve fitting method, the clean limit cycle data is recovered and the resulted plant models are derived using the set of mathematical expressions for FOPTD, SOPTD and non-minimum phase models. Finally, the efficacy of the proposed identification schemes for both the experiments are demonstrated through the comparison between the identified models from frequency and state space based mathematical expressions.

# 7

# Conclusions and Future Work

Contents

## 7.1 Concluding remarks

Most of the works in this thesis are focussed on the relay based process modelling and identification of a class of time delay processes. In this thesis, several new results are investigated to bring better accuracy in the estimation of process model parameters and improved transient performances. Briefly, the results are summarized as follows:

**I. Frequency Domain Approach for Identification of Time Delay Processes**

In this chapter, we have investigated the frequency domain based identification algorithms. An asymmetrical relay is considered for excitation of unknown plants associated with various industrial applications. Thereafter, important information from the sustained oscillatory responses or limit cycle is utilized in the derivation of mathematical expressions for the identification of a class of relay feedback processes in terms of stable and unstable FOPTD, stable and unstable SOPTD, SOPTD with repeated poles, integrating FOPTD, PIPTD, non-minimum phase stable and unstable FOPTD, non-minimum phase SOPTD with repeated poles, non-minimum phase integrating FOPTD models. The models identified in this chapter exhibit the parametric errors due to consideration of an approximation in the derivation of equivalent gain of an asymmetrical relay. Moreover, the effects of measurement noise during the process identification are rectified using the Fourier series based curve fitting method. Simulations of well known examples are demonstrated through the comparisons between Nyquist plots.

**II. State Space Approach for Identification and Control of Time Delay Processes**

Due to use of approximation in the derivation of equivalent gain of an asymmetrical relay, the frequency domain method brings the erroneous process model parameters and hence led to inaccurate design of controller parameters. Therefore, a state space approach is utilized for an accurate modelling and identification of a class of time delay processes under relay feedback control. From the relay feedback responses, a generalized set of explicit expressions for stable/unstable FOPTD and PIPTD process models are deduced. The proposed set of expressions yield better accuracy in the identification of time delay processes. Subsequently, the effect of measurement noise during the relay based identification experiment is minimized using a FFT technique. Finally, identified models using the proposed set of mathematical expressions yield better accuracy which have further been utilized in the design of model based controllers. Thereafter, a set of controller tuning parameters are designed

using the balanced tuning rules which have yielded improved transient performances.

**III. State Space Approach for Identification of Non-minimum Phase Processes with Time Delay**

It has been observed in Chapter 3 that the state space based identification method brings better accuracy in the estimation of process model parameters. Therefore, the relay feedback experiment is further extended for the modelling and identification of processes exhibiting the non-minimum phase and time delay characteristics. From the limit cycle and its slope information, a set of explicit expressions for the identification of non-minimum phase stable and unstable SOPTD processes is derived. Furthermore, these proposed set of explicit expressions are generalized for modelling and identification of non-minimum phase integrating FOPTD, stable and unstable SOPTD and integrating FOPTD processes. The effects of measurement noise at the process output are suppressed using the Fourier series based curve fitting method. Finally, the simulations of typical examples from literature have shown the better identification accuracy in the estimation of process model parameters.

**IV. A Modified Relay Feedback Experiment for Identification of Time Delay Processes**

In this chapter, a relay feedback experiment is proposed where a biased relay with non-zero setpoint is utilized for excitation of a class of time delay processes. Thereafter, a set of explicit expressions for modelling and estimation of $n^{th}$ order time delay processes is deduced using the limit cycle and its respective slope information. Finally, the efficacy of the proposed set of mathematical expressions is tested in the presence of measurement noise and the best fitted limit cycle data is recovered using Fourier series based curve fitting method which have brought better accuracy in the estimation of each unknown parameter of time delay processes with $n^{th}$ orders.

**V. Experimental Case Studies**

In this chapter, the relay based identification algorithms discussed in Chapters 2-5 are validated through practical applications. Firstly, an experimental set-up of the level control system by YOKOGAWA is considered for real-time implementation of relay feedback experiment. During the experiment, the water level in the tank is controlled by the sequential opening and closing of control valves through the relay. Thereafter, the derived set of explicit expressions is utilized for frequency do-

main and state space based modelling and identification of level control system in terms of FOPTD, SOPTD, non-minimum phase FOPTD and non-minimum phase SOPTD process models. Similarly, another experimental set-up of coupled tanks system by FEEDBACK Instruments is considered for identification of single and two coupled tanks in terms of FOPTD, SOPTD models. Finally, the models identified using the frequency domain and state space methods are compared through Nyquist plots.

## 7.2 Suggestions for further work

There are several ways in which the work in this thesis can be extended and further investigated. Some of them are enumerated as follows.

- In Chapter 2, the frequency domain based identification algorithms can be extended for identification of a class of stable, unstable and integrating processes in the presence of controllers to bring better accuracy in the estimation of process model parameters which also helps in avoiding the adverse effects of static load disturbances during the identification.

- In Chapter 3 and Chapter 4, the controllers can be designed for stable/unstable SOPTD, integrating FOPTD, non-minimum phase stable/unstable SOPTD and integrating FOPTD processes. However, it will be more interesting if the proposed analysis is extended to state space based identification of processes in the presence of controllers.

- The state feedback controllers can also be designed for the processes characterizing non-minimum phase behavior with time delay. The main challenge lies in the stability of internal dynamics in non-minimum phase processes. Moreover, the closed-loop stability is ensured by forcing all of the process state variables to follow their corresponding reference trajectories.

- In Chapter 5, the proposed relay feedback configuration can be utilized for identification of time delay processes with unstable, integrating and higher orders ($n \geq 3$).

- The thesis is restricted to single-input single-output linear time-invariant systems. However, all of the techniques used in the thesis can be readily extended to square multi-input multi-output linear, nonlinear, fractional order systems. Further extension to non-square systems is more challenging and appropriately left for future work.

# A

# Supplementary Materials

Contents

## A.1 Derivation of expression (2.3)

Consider a relay feedback compensation scheme where a nonlinear element (relay) helps in the generation of sustained oscillatory responses from a class of time delay processes. Based on the process output, the relay switches twice in one complete period of limit cycle as shown in Figure f-1. In frequency domain analysis, the input to a nonlinear element is assumed to be the sinusoidal signal

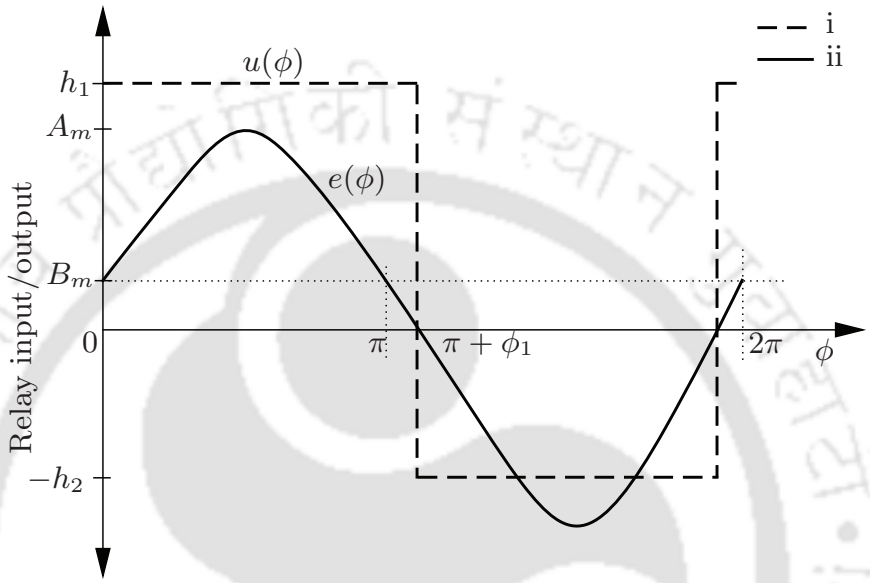


**Figure f-1:** Plots for SOPTD process: (i) relay output (ii) relay input

which can be described as

$$e(\phi) = A_m \sin(\phi) \tag{A-1}$$

where $A_m$ is an average of the peak amplitudes of a relay input signal and $\phi$ is frequency of the relay input signal. The relay output is described as

$$u(\phi) = \begin{cases} h_1 & 0 < \phi < \pi + \phi_1 \\ -h_2 & \pi + \phi_1 < \phi < 2\pi - \phi_1 \\ h_1 & 2\pi - \phi_1 < \phi < 2\pi \end{cases} \tag{A-2}$$

where

$$\phi_1 = \sin^{-1}\left(\frac{B_m}{A_m}\right) \tag{A-3}$$

Using the describing function method, the equivalent gain of a nonlinear element (relay) is obtained. Generally processes are assumed to exhibit low pass filter characteristics therefore, the equivalent gain of an asymmetrical relay is derived while considering the principal harmonic components available in the relay output signal. Therefore, the equivalent gain of relay is derived as

$$N(A_m, B_m) = \frac{1}{\pi A_m} \int_0^{2\pi} u(\phi) \left[\sin(\phi) + j\cos(\phi)\right] d\phi \tag{A-4}$$

or

$$N(A_m, B_m) = \frac{1}{\pi A_m} \left[ \int_0^{2\pi} u(\phi)\sin(\phi) d\phi + j \int_0^{2\pi} u(\phi)\cos(\phi) d\phi \right] \tag{A-5}$$

Let

$$\aleph_1 = \int_0^{2\pi} u(\phi)\sin(\phi) d\phi \tag{A-6}$$

and

$$\aleph_2 = \int_0^{2\pi} u(\phi)\cos(\phi) d\phi \tag{A-7}$$

in (A-5), the expression for $N(A_m, B_m)$ is rewritten as

$$N(A_m, B_m) = \frac{1}{\pi A_m} \left[\aleph_1 + j\aleph_2\right] \tag{A-8}$$

The solution of the constant $\aleph_1$ is obtained using (A-2) and (A-6) as

$$\aleph_1 = \int_0^{\pi+\phi_1} h_1 \sin(\phi) d\phi + \int_{\pi+\phi_1}^{2\pi-\phi_1} -h_2 \sin(\phi) d\phi + \int_{2\pi-\phi_1}^{2\pi} h_1 \sin(\phi) d\phi \tag{A-9}$$

Simplifying the above equation (A-9), we get

$$\aleph_1 = 2(h_1 + h_2)\cos(\phi_1) \tag{A-10}$$

Similarly, the expression for the remaining constant $\aleph_2$ is derived from (A-2) and (A-7) as

$$\aleph_2 = \int_0^{\pi+\phi_1} h_1 \cos(\phi) d\phi + \int_{\pi+\phi_1}^{2\pi-\phi_1} -h_2 \cos(\phi) d\phi + \int_{2\pi-\phi_1}^{2\pi} h_1 \cos(\phi) d\phi \tag{A-11}$$

Further on simplification, we get

$$\aleph_2 = 0 \tag{A-12}$$

Substituting the expressions of $\aleph_1$ from (A-10) and $\aleph_2$ from (A-12) in (A-8) to get the equivalent gain of an asymmetrical relay as

$$N(A_m, B_m) = \frac{2(h_1 + h_2)\cos(\phi_1)}{\pi A_m} \tag{A-13}$$

Finally, substituting the expression of $\cos(\phi_1)$ from (A-3), we get

$$N(A_m, B_m) = \frac{2(h_1 + h_2)}{\pi A_m}\sqrt{1 - \left(\frac{B_m}{A_m}\right)^2} \tag{A-14}$$

## A.2 Detailed derivation of the expressions (4.4), (4.5) and (4.6)

Figure f-2 shows a typical limit cycle for a non-minimum phase SOPTD process. Now the transfer

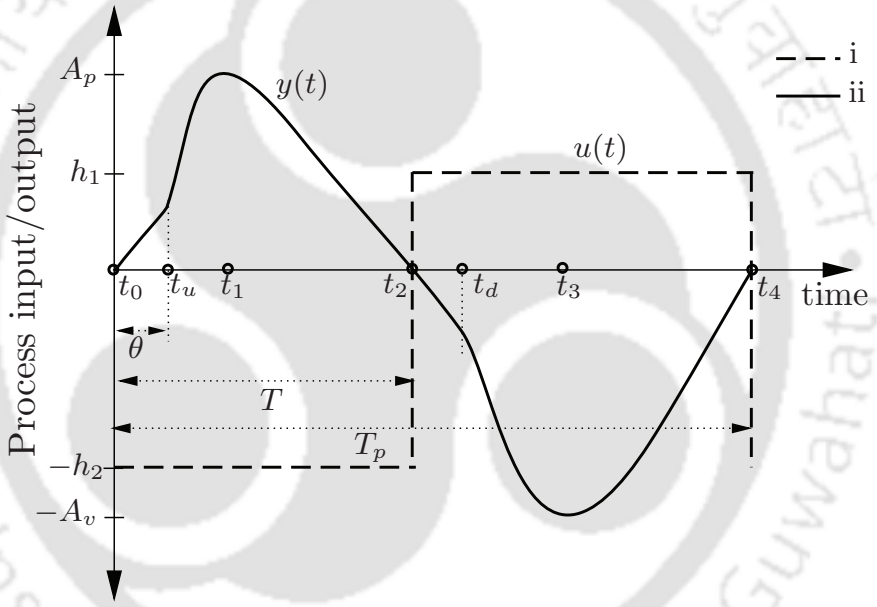


**Figure f-2:** Plots for non-minimum phase SOPTD process: (i) relay output (ii) process output

function model given in (4.1) is rewritten as

$$G_m(s) = \frac{Y(s)}{U(s)e^{-\theta s}} = \frac{-k\alpha_3(s + \lambda_3)}{\alpha_2\,(s - \lambda_1)\,(s - \lambda_2)} \tag{A-15}$$

The partial fractions of (A-15) are written as

$$\frac{Y(s)}{U(s)e^{-\theta s}} = \mu\left[\frac{(\lambda_1 + \lambda_3)}{(s - \lambda_1)} - \frac{(\lambda_2 + \lambda_3)}{(s - \lambda_2)}\right] \tag{A-16}$$

where

$$\mu = \frac{\pm k\lambda_1\lambda_2}{\lambda_3(\lambda_1 - \lambda_2)} \tag{A-17}$$

Representing (A-16) in the Jordan canonical form as

$$\dot{\boldsymbol{x}}(t) = \underbrace{\begin{bmatrix} \lambda_1 & 0 \\ 0 & \lambda_2 \end{bmatrix}}_{\boldsymbol{J}} \boldsymbol{x}(t) + \underbrace{\begin{bmatrix} 1 \\ 1 \end{bmatrix}}_{\boldsymbol{B}} u(t-\theta) \tag{A-18}$$

$$y(t) = \underbrace{\begin{bmatrix} \pm\dfrac{k\lambda_1\lambda_2(\lambda_1+\lambda_3)}{\lambda_3(\lambda_1-\lambda_2)} & \mp\dfrac{k\lambda_1\lambda_2(\lambda_2+\lambda_3)}{\lambda_3(\lambda_1-\lambda_2)} \end{bmatrix}}_{\boldsymbol{C}} \boldsymbol{x}(t) \tag{A-19}$$

From the solution of the state space equation, the process output is written as

$$y(t) = \boldsymbol{C}\boldsymbol{e}^{\boldsymbol{J}(t-t_0)}\boldsymbol{x}(t_0) + \boldsymbol{C}\int_{t_0}^{t} \boldsymbol{e}^{\boldsymbol{J}(t-\tau)}\boldsymbol{B}u(\tau-\theta)d\tau \tag{A-20}$$

The relay output serves as input to process dynamics, therefore the relay output or process input with time delay for one complete period is written as

$$u(t-\theta) = \begin{cases} h_1 & \text{if } t_0 < t < \theta \\ -h_2 & \text{if } \theta < t < (t_2+\theta) \\ h_1 & \text{if } (t_2+\theta) < t < (t_4+\theta) \end{cases} \tag{A-21}$$

The expression of process output for time range $t_0 \leq t < \theta$ is written using (A-20) as

$$y(t) = \boldsymbol{C}\boldsymbol{e}^{\boldsymbol{J}(t-t_0)}\boldsymbol{x}(t_0) + \boldsymbol{C}\boldsymbol{J}^{-1}(\boldsymbol{e}^{\boldsymbol{J}(t-t_0)} - \boldsymbol{I})\boldsymbol{B}h_1 \tag{A-22}$$

For time range $\theta \leq t < (t_2+\theta)$, the process output is derived using (A-20) as

$$y(t) = \boldsymbol{C}\boldsymbol{e}^{\boldsymbol{J}(t-\theta)}\boldsymbol{x}(\theta) - \boldsymbol{C}\boldsymbol{J}^{-1}(\boldsymbol{e}^{\boldsymbol{J}(t-\theta)} - \boldsymbol{I})\boldsymbol{B}h_2 \tag{A-23}$$

Finally, for time range $(t_2+\theta) \leq t < (t_4+\theta)$, the process output is deduced using (A-20) as

$$y(t) = \boldsymbol{C}\boldsymbol{e}^{\boldsymbol{J}(t-t_2-\theta)}\boldsymbol{x}(t_2+\theta) + \boldsymbol{C}\boldsymbol{J}^{-1}(\boldsymbol{e}^{\boldsymbol{J}(t-t_2-\theta)} - \boldsymbol{I})\boldsymbol{B}h_1 \tag{A-24}$$

For the existence of sustained oscillations, $\boldsymbol{x}(t_4) = \boldsymbol{x}(t_0)$ which yields an expression for $\boldsymbol{x}(t_0)$ as

$$\boldsymbol{x}(t_0) = \left[\boldsymbol{I} - \boldsymbol{e}^{\boldsymbol{J}T_p}\right]^{-1} \boldsymbol{J}^{-1} \left[(h_1 + h_2)\boldsymbol{e}^{\boldsymbol{J}(T_p - T - \theta)} + h_1 \boldsymbol{e}^{\boldsymbol{J}T_p} - (h_1 + h_2)\boldsymbol{e}^{\boldsymbol{J}(T_p - \theta)} - h_1 \boldsymbol{I}\right] \boldsymbol{B} \tag{A-25}$$

Substituting $\boldsymbol{x}(t_0)$ from (A-25) in the expression of $y(t)$ for time range $t_0 \leq t < \theta$, we get

$$y(t) = -\boldsymbol{C}\boldsymbol{J}^{-1}\boldsymbol{B}h_1 + \boldsymbol{C}\boldsymbol{J}^{-1}[\boldsymbol{I} - \boldsymbol{e}^{\boldsymbol{J}T_p}]^{-1}[\boldsymbol{I} - \boldsymbol{e}^{\boldsymbol{J}T}]\boldsymbol{e}^{\boldsymbol{J}(t + T_p - T - \theta)}\boldsymbol{B}(h_1 + h_2) \tag{A-26}$$

Similarly, the process output for time range $\theta \leq t < (t_2 + \theta)$ is written after the substitution of $\boldsymbol{x}(t_0)$ from (A-25) as

$$y(t) = \boldsymbol{C}\boldsymbol{J}^{-1}\boldsymbol{B}h_2 - \boldsymbol{C}\boldsymbol{J}^{-1}[\boldsymbol{I} - \boldsymbol{e}^{\boldsymbol{J}T_p}]^{-1}[\boldsymbol{I} - \boldsymbol{e}^{\boldsymbol{J}(T_p - T)}]\boldsymbol{e}^{\boldsymbol{J}(t - \theta)}\boldsymbol{B}(h_1 + h_2) \tag{A-27}$$

Finally, the expression of process output for time range $(t_2 + \theta) \leq t < (t_4 + \theta)$ is derived using $\boldsymbol{x}(t_0)$ from (A-25) as

$$y(t) = -\boldsymbol{C}\boldsymbol{J}^{-1}\boldsymbol{B}h_1 + \boldsymbol{C}\boldsymbol{J}^{-1}[\boldsymbol{I} - \boldsymbol{e}^{\boldsymbol{J}T_p}]^{-1}[\boldsymbol{I} - \boldsymbol{e}^{\boldsymbol{J}T}]\boldsymbol{e}^{\boldsymbol{J}(t - T - \theta)}\boldsymbol{B}(h_1 + h_2) \tag{A-28}$$

# Bibliography


[1] G. Fedele, "A new method to estimate a first-order plus time delay model from step response." *Journal of the Franklin Institute*, vol. 346, pp. 1–9, 2009.

[2] T. Liu and F. Gao, "Alternative identification algorithms for obtaining a first-order stable/unstable process model from a single relay feedback test," *Industrial & Engineering Chemistry Research*, vol. 47, no. 4, pp. 1140–1149, 2008.

[3] S. Vivek and M. Chidambaram, "Identification using single symmetrical relay feedback test," *Computers and Chemical Engineering*, vol. 29, no. 7, pp. 1625–1630, 2005.

[4] K. Srinivasan and M. Chidambaram, "Modified relay feedback method for improved system identification," *Computers and Chemical Engineering*, vol. 27, no. 5, pp. 727–732, 2003.

[5] J. C. Jeng, H. P. Huang, and F. Y. Lin, "Modified relay feedback approach for controller tuning based on assessment of gain and phase margins," *Industrial & Engineering Chemistry Research*, vol. 45, no. 12, pp. 4043–4051, 2006.

[6] V. Vijayan and R. C. Panda, "Design of a simple setpoint filter for minimizing overshoot for low order processes," *ISA Transactions*, vol. 51, no. 2, pp. 271–276, 2012.

[7] C. S. Jung, H. K. Song, and J. C. Hyun, "A direct synthesis tuning method of unstable first-order-plus-time-delay processes," *Journal of Process Control*, vol. 9, no. 3, pp. 265–269, 1999.

[8] R. Bajarangbali, S. Majhi, and S. Pandey, "Identification of FOPDT and SOPDT process dynamics using closed loop test." *ISA Transactions*, vol. 53, no. 4, pp. 1223–1231, 2014.

[9] T. Liu, F. Gao, and Y. Wang, "A systematic approach for on-line identification of second-order process model from relay feedback test," *AIChE Journal*, vol. 54, no. 6, pp. 1560–1578, 2008.

[10] S. Vivek and M. Chidambaram, "An improved relay autotuning of PID controllers for critically damped SOPDT systems," *Chemical Engineering Communications*, vol. 199, no. 11, pp. 1437–1462, 2012.

[11] K. J. Åström and P. Eykhoff, "System identification - a survey," *Automatica*, vol. 7, no. 2, pp. 123–162, 1971.

[12] L. Wang and W. R. Cluett, *From Plant Data to Process Control: Ideas for Process Identification and PID Design*, london ed. CRC Press, Taylor and Francis Group, 2000.

[13] W. L. Luyben, "Derivation of transfer functions for highly nonlinear distillation columns," *Industrial & Engineering Chemistry Research*, vol. 26, no. 12, pp. 2490–2495, 1987.

[14] Y.Z.Tsypkin, *Relay Control Systems*. Cambridge, U.K.: Cambridge Univ. Press, 1984.

[15] J. K. C. Chung and D. P. Atherton, "The determination of periodic modes in relay systems using the state space approach," *International Journal of Control*, vol. 4, pp. 105–126, 1966.

[16] R. Balasubramanian, "Stability of limit cycles in feedback systems containing a relay," *IEE Proceedings of Control Theory Appl*, vol. 128, pp. 24–29, 1981.

[17] S. Majhi and D. P. Atherton, "Stability of limit cycles in relay control systems," in *In Proceedings of the IFAC NOLCOS, Enschede, The Netherlands*, July 1998, pp. 59–94.

[18] J. Gonclaves, "Global stability of relay feedback systems," *IEEE Transactions on Automatic Control*, vol. 47(9), pp. 550–562, 2001.

[19] C. Lin, Q. G. Wang, and T. H. Lee, "Relay feedback: A complete analysis for first order systems," *Ind. Eng. Chem. Res.*, vol. 43, no. 26, pp. 8400–8402, 2004.

[20] J. T. Hawkins, "Automatic regulators for heating apparatus," *Trans. Amer. Soc. Mech. Eng.*, vol. 9, p. 432, 1887.

[21] S. H. Shen, J. S. Wu, and C. C. Yu, "Use of biased-relay feedback for system identification," *AIChE Journal*, vol. 42, no. 4, pp. 1174–1180, 1996.

[22] D. P. Atherton and S. Majhi, "Plant parameter identification under relay control," in *Proceedings of the 37th IEEE Conference on Decision and Control*, vol. 2, Tampa, Florida, December 1998, pp. 1272–1277.

[23] T. Thyagarajan and C. C. Yu, "Improved autotuning using the shape factor from relay feedback," *Industrial and Engineering Chemistry Research*, vol. 42, no. 20, pp. 4425–4440, 2003.

[24] R. Panda and C. C. Yu, "Analytical expressions for relay feedback responses," *Journal of Process Control*, vol. 13, no. 6, pp. 489–501, 2003.

[25] T. Lee, Q. Wang, and K. Tan, "A modified relay-based technique for improved critical point estimation in process control," *IEEE Transactions on Control Systems Technology*, vol. 3, no. 3, pp. 330–337, 1995.

[26] G. de Arruda and P. Barros, "Relay-based closed loop transfer function frequency points estimation," *Automatica*, vol. 39, no. 2, pp. 309–315, 2003.

[27] K. Tan, T. Lee, S. Huang, K. Chua, and R. Ferdous, "Improved critical point estimation using a preload relay," *Journal of Process Control*, vol. 16, no. 5, pp. 445–455, 2006.

[28] K. J. Åström, *Oscillations in Systems with Relay Feedback*, ser. The IMA Volumes in Mathematics and its Applications. Springer New York, 1995, vol. 74.

[29] I. Boiko, "Autotune identification via the locus of a perturbed relay system approach," *IEEE Transactions on Control Systems Technology*, vol. 16, no. 1, pp. 182–185, 2008.

[30] Q. G. Wang, H. Fung, and Y. Zhang, "Robust estimation of process frequency response from relay feedback," *ISA Transactions*, vol. 38, no. 1, pp. 3–9., 1999.

[31] Q. G. Wang, Y. Zhang, and X. Guo, "Robust closed-loop identification with application to auto-tuning," *Journal of Process Control*, vol. 11, no. 5, pp. 519–530, 2001.

[32] R. C. Panda and C. C. Yu, "Shape factor of relay response curves and its use in autotuning," *Journal of Process Control*, vol. 15, pp. 893–906, 2005.

[33] D. P. Atherton, "Relay autotuning: an overview and alternative approach," *Industrial & Engineering Chemistry Research*, vol. 45, pp. 4075–4080, 2006.

[34] I. Kaya and D. Atherton, "Parameter estimation from relay autotuning with asymmetric limit cycle data," *Journal of Process Control*, vol. 11, no. 4, pp. 429–439, 2001.

[35] P. K. Padhy and S. Majhi, "Relay based PI-PD design for stable and unstable FOPDT processes," *Computers and Chemical Engineering*, vol. 30, pp. 790–796, 2006.

[36] ——, "Improved automatic tuning of PID controller for stable processes," *ISA Transactions*, vol. 48, pp. 423–427, 2009.

[37] J. Lee, S. W. Sung, and T. F. Edgar, "Integrals of relay feedback responses for extracting process information," *AIChE Journal*, vol. 53, no. 9, pp. 2329–2338, 2007.

[38] M. Liu, Q. G. Wang, B. Huang, and C. C. Hang, "Improved identification of continuous-time delay processes from piecewise step tests." *Journal of Process Control*, vol. 17, pp. 51–57, 2006.

[39] S. Majhi and D. P. Atherton, "Autotuning and controller design for processes with small time delays," *IEE Proceedings-Control Theory and Applications*, vol. 146, no. 5, pp. 415–425, 1999.

[40] S. Majhi, "Relay based identification of processes with time delay," *Journal of Process Control*, vol. 17, pp. 93–101, 2007.

[41] J. Kim, J. Byeon, D. Chun, S. W. Sung, and J. Lee, "Relay feedback method for processes under noisy environments," *AIChE Journal*, vol. 56, pp. 560–562, 2010.

[42] R. C. Panda, V. Vijayan, V. Sujatha, P. Deepa, D. Manamali, and A. B. Mandal, "Parameter estimation of integrating and time delay processes using single relay feedback test," *ISA Transactions*, vol. 50, pp. 529–537, 2011.

[43] T. Liu and F. Gao, "A frequency domain step response identification method for continuous-time processes with time delay," *Journal of Process Control*, vol. 20, pp. 800–809, 2010.

[44] C. H. Jeon, Y. J. Cheon, J. S. Kim, J. Lee, and S. W. Sung, "Relay feedback methods combining sub-relays to reduce harmonics," *Journal of Process Control*, vol. 20, pp. 228–234, 2010.

[45] T. B. Šekara and M. R. Mataušek, "Relay-based critical point estimation of a process with the PID controller in the loop," *Automatica*, vol. 47, pp. 1084–1088, 2011.

[46] Bajarangbali and S. Majhi, "Relay based identification of systems," *International Journal of Scientific & Engineering Research*, vol. 3, no. 6, pp. 1–4, 2012.

[47] R. Bajarangbali and S. Majhi, "Identification of non-minimum phase processes with time delay in the presence of measurement noise," *ISA Transactions*, vol. 57, pp. 245–253, 2015.

[48] P. Ghorai, S. Majhi, and S. Pandey, "Modelling and identification of real time processes based on non-zero setpoint autotuning test," *Journal of Dynamic Systems, Measurement and Control*, vol. 139, no. 1, pp. 021 010–1–021 010–8, 2017.

[49] T. Liu, Q. G. Wang, and H. P. Huang, "A tutorial review on process identification from step or relay feedback test," *Journal of Process Control*, vol. 23, no. 10, pp. 1597–1623, 2013.

[50] K. J. Åström and T. Hägglund, "Automatic tuning of simple regulators with specifications on phase and amplitude margins," *Automatica*, vol. 20, no. 5, pp. 645–651, 1984.

[51] G. Cohen and G. Coon, "Theoretical consideration of retarded control," *Trans. ASME*, vol. 75, pp. 827–834, 1953.

[52] M. Yuwana and D. Seborg, "A new method for on-line controller tuning," *AIChE Journal*, vol. 28, p. 434, 1982.

[53] E. Bristol, "Pattern recognition: an alternative to parameter identification in adaptive control," *Automatica*, vol. 13, pp. 197–202, 1977.

[54] ——, "The design of industrially useful adaptive controllers," *ISA Trans.*, vol. 22 (3), pp. 17–25, 1983.

[55] B. Wittenmark and K. Åström, *Simple self-tuning controllers, in: H. Unbehauen (Ed.), Methods And Applications In Adaptive Control*. Springer, Berlin, 1980.

[56] P. Gawthrop, *Self-Tuning PI and PID Controllers: Proceeding Functions and Nonlinear Systems Design*. McGraw Hill, New York, 1982.

[57] Bajarangbali, "Identification of process dynamics using relay with hysteresis," Ph.D. dissertation, Indian Institute of Technology Guwahati, July 2014.

[58] D. P. Atherton, *Nonlinear Control Engineering*. Van Nostrand Reinhold, 1982.

[59] R. C. Chang, S. H. Shen, and C. C. Yu, "Derivation of transfer function from relay feedback systems," *Industrial & Engineering Chemistry Research*, vol. 31, no. 3, pp. 855–860, 1992.

[60] G. Marchetti, C. Scali, and D. R. Lewin, "Identification and control of open loop unstable processes by relay methods," *Automatica*, vol. 37, pp. 2049–2055, 2001.

[61] K. K. Tan, T. H. Lee, S. Huang, K. Y. Chua, and R. Ferdous, "Improved critical point estimation using a preload relay," *Journal of Process Control*, vol. 16, pp. 445–455, 2006.

[62] W. Ho, E. Feng, and O. Gan, "A novel relay auto-tuning technique for processes with integration," *Control Engineering Practice*, vol. 4, no. 7, pp. 923–928, 1996.

[63] W. Li, E. Eskinat, and W. L. Luyben, "An improved autotune identification method," *Industrial & Engineering Chemistry Research*, vol. 30, pp. 1530–1541, 1991.

[64] Q. G. Wang, C. C. Hang, and B. Zou, "Low-order modeling from relay feedback," *Industrial & Engineering Chemistry Research*, vol. 36, no. 2, pp. 375–381, 1997.

[65] Q. G. Wang, C. C. Hang, and Q. Bi, "A technique for frequency response identification from relay feedback," *IEEE Transactions on Control Systems Technology*, vol. 7, no. 1, pp. 122–128, Jan 1999.

[66] P. Ghorai, S. Majhi, and S. Pandey, "Dynamic model identification of a real-time simple level control system," *Journal of Control and Decision*, vol. 3, no. 4, pp. 248–266, 2016.

[67] MATLAB Curve fitting toolbox, The Mathworks Inc., 2013.

[68] S. Majhi and D. P. Atherton, "Online tuning of controllers for an unstable FOPDT process," *IEE Proceedings-Control Theory and Applications*, vol. 147, no. 4, pp. 421–427, 2000.

[69] W. K. Ho and W. Xu, "PID tuning for unstable processes based on gain and phase margin specifications," *IEE Proceedings Control Theory and Applications*, vol. 145, no. 5, pp. 392–396, 1998.

[70] I. Kaya, "Parameter estimation for integrating processes using relay feedback control under static load disturbances," *Industrial & Engineering Chemistry Research*, vol. 45, no. 13, pp. 4726–4731, 2006.

[71] I. Kaya and D. P. Atherton, "Exact parameter estimation from relay autotuning under static load disturbances," in *Proceedings of the American Control Conference*, Arlington, 2001, pp. 3274–3279.

[72] S. Majhi, "On-line PI control of stable processes," *Journal of Process Control*, vol. 15, no. 8, pp. 859–867, 2005.

[73] J. G. Proakis and D. G. Manolakis, *Digital signal processing 3rd ed.: principles, algorithms, and applications*. United States, US: Prentice-Hall International, Inc., 1996.

[74] P. Klán and R. Gorez, "Balanced tuning of PI controllers," *European Journal of Control*, vol. 6, pp. 541–550, 2000.

[75] T. Hägglund, "Automatic detection of sluggish control loops," *Control Engineering Practice*, vol. 7, no. 12, pp. 1505–1511, 1999.

[76] S. Skogestad, "Simple analytic rules for model reduction and PID controller tuning," *Journal of Process Control*, vol. 13, no. 4, pp. 291–309, 2003.

[77] G. Stephanopoulos, *Chemical Process Control-An Introduction to Theory and Practice*. Prentice Hall, 1983.

[78] Y. J. Huang and Y. J. Wang, "Robust PID controller design for non-minimum phase time delay systems," *ISA Transactions*, vol. 40, no. 1, pp. 31–39, 2001.

[79] C. Kravaris and P. Daoutidis, "Nonlinear state feedback control of second-order nonminimum-phase nonlinear systems," *Computers & Chemical Engineering*, vol. 14, no. 4, pp. 439–449, 1990.

[80] P. Padhy and S. Majhi, "Exact analysis for the identification of nonminimum phase processes," *Journal of the Franklin Institute*, vol. 348, no. 10, pp. 2734–2743, 2011.

[81] U. V. Mehta, "Relay feedback method for process modelling," Ph.D. dissertation, Indian Institute of Technology Guwahati, August 2011.

[82] S. Majhi, "Relay-based identification of a class of nonminimum phase SISO processes," *IEEE Transactions on Automatic Control*, vol. 52, no. 1, pp. 134–139, Jan 2007.

[83] T. Liu and F. Gao, "A generalized relay identification method for time delay and non-minimum phase processes," *Automatica*, vol. 45, no. 4, pp. 1072–1079, 2009.

[84] Y. Electric, *Technical Information: CENTUM CS3000 Integrated Production Control System (IPCS)TI 33Q01B10-01E*, 6th ed., Yokogawa Electric Corp., Tokyo, Japan, 2002.

[85] Feedback, *Coupled Tanks Control Experiments 33-041-S*, 02nd ed., Feedback Instruments Ltd., East Sussex, United Kingdom, 2013.